République Algérienne Démocratique et Populaire
Ministère de l'Enseignement Supérieur et de la Recherche Scientifique
UNIVERSITE FERHAT ABBAS – SETIF-1

Faculté des Sciences
Département d'Informatique

THESE

Présentée en vue de l'obtention du diplôme de Doctorat en Sciences

Knowledge Discovery in Big Data: Application to Arabic Handwriting Characters Recognition and Genomic

Domaine : Mathématiques et Informatique
Filière : Informatique
Spécialité : Systèmes d'Information et de Connaissances

Par :
Nasri Khaled

Directeur de Thèse :

Pr. MOUSSAOUI Abdelouahab	Professeur	Université Ferhat Abbas, Sétif-1

DEVANT LE JURY

Président :		
Pr. Abdelaziz Lakhfif	Professeur	Université Ferhat Abbas, Sétif-1
Examinateurs :		
Pr. Melkmi Kamel-Eddine	Professeur	Université Batna 2
Pr. SIAM Abderrahim	Professeur	Université Khenchela
Pr. Sabri Lyazid	Professeur	Université Bordj Bou Arreridj
Invité :		
Pr. Oussalah Mourad	Professeur	Université Oulu, Finlande

Février 2026

Dédicace à Mon Encadrant Professeur Moussaoui

Je tiens à exprimer ma profonde gratitude et à dédier ce travail à mon encadrant de thèse, le **Professeur Abdelouahab Moussaoui**, *pour sa patience exemplaire, sa rigueur scientifique et la qualité de son encadrement tout au long de ce parcours doctoral.*

Ses orientations pertinentes, son exigence méthodologique et sa disponibilité constante ont largement contribué à la maturation scientifique de ce travail. Par son sens critique et son engagement académique, il m'a appris la discipline de la recherche, la précision dans l'analyse et la persévérance face aux défis scientifiques.

Qu'il trouve ici l'expression de mon profond respect et de ma reconnaissance pour l'accompagnement, la confiance et le soutien qu'il m'a accordés.

Dédicace aux membres du jury

Je tiens à adresser mes sincères remerciements et à dédier ce travail aux membres du jury, qui ont accepté d'examiner cette thèse et d'en évaluer la qualité scientifique.

Leur expertise, leurs remarques pertinentes et leur regard critique ont contribué à l'amélioration de ce travail et à l'enrichissement de ma réflexion scientifique. Je leur suis profondément reconnaissant pour le temps consacré à l'analyse de ce manuscrit, ainsi que pour la rigueur et l'objectivité avec lesquelles ils ont conduit cette évaluation.

Qu'ils trouvent ici l'expression de mon respect et de ma gratitude pour l'honneur qu'ils m'ont fait en acceptant de participer à ce jury.

Dédicace à Ma famille

*À la mémoire de mes chers parents, **Lehmadi** et **Boutout Yamina**, dont l'amour, les sacrifices et la sagesse ont été la première lumière de mon chemin.*

Vous m'avez appris la patience, le courage et la dignité.

Même absents, vous demeurez présents dans chaque réussite, dans chaque pas accompli, et dans chaque rêve que je poursuis.

Que Dieu, dans Son infinie miséricorde, vous accorde Son pardon et vous ouvre les portes du Paradis.

*À mon épouse, **Sarra**,*

Compagnonne de vie, source de sérénité et de force, merci pour ton soutien indéfectible, ta compréhension et ton amour, qui ont rendu possible l'achèvement de ce travail.

*À mes chers enfants, **Yahia** et **Amira**,*

Qui donnent un sens à mes efforts et illuminent mon quotidien.

Vous êtes ma plus belle motivation et mon plus grand espoir.

*À la mémoire de mon frère **Adel** et de ma sœur **Lamia**,*

Dont le souvenir reste gravé dans mon cœur.

Que Dieu leur accorde Sa miséricorde et Sa paix éternelle.

*À mon frère **Fayçal**, à son épouse **Ilham**, et à leurs enfants **Noufel**, **Roukia**, **Anfel**, **Wissal** et **Djawad**, pour leur affection, leur présence et leur soutien.*

À ma sœur **Malika**, à son époux **Abdelkarim**, et à leurs enfants **Ines**, **Maya** et **Ilya**, pour leur amour fraternel et leur encouragement constant.

À ma sœur **Widad** et à son époux **Azedine**, pour leur bienveillance et leur soutien précieux.

À ma sœur **Amel**, à son époux **Moustafa**, et à leurs enfants **Adel**, **Arwa**, **Rawane** et **Royaa**, pour leur présence chaleureuse et leur affection sincère.

À ma sœur **Hadjer**, à son époux **Djalel**, et à leurs enfants **Lamia**, **Razane** et **Shahine**, pour leur soutien et leurs prières.

À mes oncles **Rabah**, **Rachide** et **Said**, pour leur encouragement, leur confiance et leur soutien moral.

Enfin, à toute ma famille, proche et lointaine, qui a toujours cru en moi et m'a accompagné par la pensée, la prière et l'amour.

Dédicace à mes amis et collègues

Je souhaite dédier ce travail à mes amis et collègues, Samir Belbal, Youcef Boulekhiout, Nouredine Mekroud, Lakhdar Goudjil, Azeddine Kemmoume, Bouzerzour Ismail, Fared Belhi, Nabil Berkane et Saleh Namoune, Seguiri Badredine.

En témoignage de mon amitié et de ma reconnaissance. Leur soutien moral, leurs échanges constructifs et leur esprit de collaboration ont été une source précieuse de motivation tout au long de ce parcours doctoral.

À travers les discussions scientifiques, les encouragements et les moments de partage, ils ont contribué, chacun à sa manière, à la réussite de ce travail. Qu'ils trouvent ici l'expression de mon estime et de mes sincères remerciements.

General Introduction

The advent of Big Data has transformed the way knowledge is generated, validated, and applied across scientific, medical, and technological domains. The exponential increase in data volume, velocity, and heterogeneity has outpaced traditional analytical methods, creating an urgent need for scalable architectures and intelligent algorithms capable of extracting actionable knowledge from large datasets. Within this paradigm, Knowledge Discovery in Big Data has emerged as a critical field, integrating distributed computing, advanced machine learning, and data mining to uncover meaningful patterns and support decision-making in real-world contexts.

Among the domains most profoundly impacted by Big Data is genomics, where high-throughput sequencing technologies continuously generate terabytes of complex and multidimensional biological data. Extracting knowledge from genomic data requires not only statistical and computational efficiency but also scalable methods that can manage data variety and quality challenges. Specialized techniques, such as normalization, dimensionality reduction, and batch-effect correction, have become essential steps in ensuring reliable discovery, whereas machine learning architectures enable the classification, prediction, and modeling of biological phenomena at scale. In particular, genomic variant calling the identification and characterization of genetic variations from sequencing data exemplifies the computational challenges inherent in processing population-scale datasets while maintaining high accuracy and reproducibility.

Concurrently, the rise of deep learning has reshaped the artificial intelligence landscape, demonstrating state-of-the-art performance in image analysis, speech recognition, and natural language processing. However, the application of very deep neural networks to Big Data ecosystems introduces scalability constraints that require parallelization and distributed training strategies. This is especially evident in domains such as genomics and medical imaging, where data repositories reach the terabyte and petabyte scale, and effective processing necessitates hybrid solutions combining GPUs, distributed frameworks, and multimodal data integration. Research on CNNs, Transformers, Capsule Networks, and attention mechanisms illustrates the ongoing efforts to balance accuracy, scalability, and computational feasibility while leveraging heterogeneous data sources.

Building upon these methodological foundations, this thesis extends the study of knowledge discovery through two complementary perspectives. First, we develop and evaluate a distributed deep learning pipeline for genomic variant calling that integrates multimodal sequencing data through hybrid Transformer-CNN architectures with attention-based fusion mechanisms. This pipeline addresses both the scalability challenge through Distributed Data Parallel training and the accuracy challenge through multimodal learning, demonstrating how modern deep learning can be adapted to production-grade genomics workflows. Second, we apply advanced deep learning to a real-world pattern recognition problem: Arabic handwriting recognition. Arabic script presents intrinsic challenges, such as cursiveness, diacritic sensitivity, and stylistic variability, which require architectures capable of capturing spatial hierarchies and contextual dependencies. To address these challenges, we developed and evaluated hybrid architectures, particularly Capsule-embedded Residual Networks, to enhance recognition accuracy while preserving scalability across diverse datasets.

Through this multidisciplinary exploration spanning Big Data methodologies, genomics, distributed computing, and pattern recognition, this thesis demonstrates how scalable knowledge discovery and deep learning innovation converge to address pressing challenges across domains, bridging theory and application to advance both computational science and domain-specific discovery.

Thesis Structure

Chapter 1: Theoretical Background of Big Data and Knowledge Discovery

This chapter establishes the theoretical and methodological foundations of Big Data analytics and introduces knowledge discovery processes, data mining techniques, and scalable frameworks for extracting knowledge. It provides the conceptual groundwork for understanding how distributed computing, parallelization strategies, and advanced machine learning enable effective knowledge extraction from massive, heterogeneous datasets.

Chapter 2: Knowledge Discovery in Big Genomic Data

This chapter investigates the methodological challenges and opportunities posed by large-scale genomic datasets, focusing on how deep learning models can be adapted for knowledge extraction in this context. Particular attention is given to scalability issues and the strategies of parallelization and distributed training required to handle high-throughput sequencing data. The biological complexity of genomic data, including sequence structure, alignment patterns, and variant characteristics, is examined to motivate specialized preprocessing and feature extraction approaches. Case studies in genomics and medical imaging are presented to demonstrate how domain-specific complexities, such as data heterogeneity, dimensionality, and quality, shape the design and adaptation of advanced learning architectures.

Chapter 3: Distributed Deep Learning Pipeline for Genomic Variant Calling

This chapter presents a comprehensive methodology for scalable variant calling from high-throughput sequencing data, addressing both computational efficiency and classification accuracy through distributed deep learning. The chapter details the complete pipeline architecture, from data preparation and multimodal feature extraction (sequence context and read pileup representations) to the hybrid Transformer-CNN model design with attention-based fusion. The distributed training strategy using Data

Parallel approaches across multiple GPUs is thoroughly examined, including gradient synchronization mechanisms and computational efficiency analysis. Multi-task learning for simultaneous variant type classification, genotype prediction, quality estimation, and artifact detection is presented, along with techniques for handling severe class imbalance through weighted loss functions. The evaluation methodology includes rigorous benchmarking against established baseline methods (GATK HaplotypeCaller and DeepVariant) using community-standard tools (hap.py) and Genome in a Bottle consortium data.

Chapter 4: Case Study in Knowledge Discovery: Arabic Handwriting Character Recognition

This chapter presents a real-world application of advanced architectures for Arabic script recognition, extending our published work on Capsule-embedded Residual Networks. The intrinsic challenges of Arabic handwriting including cursive connectivity, positional letter variations, diacritical marks, and significant inter-writer stylistic variability motivate the development of specialized neural architectures. The chapter details the hybrid Caps-ResNet architecture that embeds Capsule Networks within Residual Networks to capture both hierarchical feature representations and spatial relationships between character components. Experiments, dataset characteristics, model design, training strategies, and comprehensive performance evaluations demonstrate how domain-specific architectural innovations can address pattern recognition challenges in complex script systems while maintaining computational efficiency.

Abstract

The exponential growth of Big Data necessitates scalable knowledge discovery methodologies capable of handling massive, heterogeneous datasets. This dissertation explores distributed and parallel deep learning architectures across two critical application domains: genomics and Arabic handwriting recognition.

In genomics, a novel distributed pipeline for variant calling integrates multimodal sequencing data through a hybrid Transformer-CNN architecture with attention-based fusion. The system simultaneously processes DNA sequence context via transformer encoders and read alignment evidence through three-dimensional convolutional networks, enabling accurate genomic variant classification while achieving computational efficiency through Distributed Data Parallel (DDP) training across multiple GPUs. Multi-task learning addresses variant type classification, genotype prediction, quality score estimation, and artifact detection, while class-weighted loss functions handle severe data imbalance inherent in genomic datasets.

In Arabic handwriting recognition, a hybrid architecture embedding Capsule Networks within Residual Networks (Caps-ResNet) captures hierarchical features and spatial relationships essential for cursive script analysis. This specialized architecture overcomes unique challenges including ligature complexity, diacritical mark sensitivity, and significant stylistic variability across writing styles.

This multidisciplinary research demonstrates how hybrid architectures, multimodal fusion mechanisms, and distributed computing strategies enable robust, accurate, and computationally efficient knowledge extraction systems applicable to diverse scientific domains. The results contribute to the development of scalable deep learning solutions that bridge theoretical innovations with real-world applications in genomics and natural language processing.

Keywords: Big Data, Knowledge Discovery, Distributed Deep Learning, Genomic Variant Calling, Multimodal Learning, Transformer-CNN Architectures, Data Parallelism, Arabic Handwriting Recognition, Hybrid Neural Networks.

Résumé

La croissance exponentielle du Big Data nécessite des méthodologies d'extraction de connaissances évolutives capables de traiter des ensembles de données massifs et hétérogènes. Cette thèse explore les architectures d'apprentissage profond distribuées et parallèles à travers deux domaines d'application critiques : la génomique et la reconnaissance de l'écriture arabe manuscrite.

En génomique, un pipeline distribué novateur pour l'identification de variants intègre des données de séquençage multimodales à travers une architecture hybride Transformer-CNN avec fusion basée sur l'attention. Le système traite simultanément le contexte de séquence ADN via des encodeurs Transformers et les données d'alignement de lectures par des réseaux de convolution tridimensionnels, permettant une classification précise des variants génomiques tout en atteignant une efficacité computationnelle grâce à l'entraînement distribué en parallèle de données (DDP) sur plusieurs GPU. L'apprentissage multitâches adresse la classification des types de variants, la prédiction des génotypes, l'estimation des scores de qualité et la détection d'artefacts, tandis que les fonctions de perte pondérées par classe gèrent le déséquilibre sévère inhérent aux données génomiques.

En reconnaissance de l'écriture arabe manuscrite, une architecture hybride intégrant des réseaux capsule au sein de réseaux résiduels (Caps-ResNet) capture les caractéristiques hiérarchiques et les relations spatiales essentielles pour l'analyse des scripts cursifs. Cette architecture spécialisée surmonte les défis uniques incluant la complexité des ligatures, la sensibilité aux signes diacritiques et la variabilité stylistique importante entre différents styles d'écriture.

Cette recherche multidisciplinaire démontre comment les architectures hybrides, les mécanismes de fusion multimodale et les stratégies de calcul distribué permettent des systèmes d'extraction de connaissances robustes, précis et computationnellement efficaces, applicables à divers domaines scientifiques. Les résultats contribuent au développement de solutions d'apprentissage profond évolutives qui établissent un pont entre innovations théoriques et applications pratiques en génomique et traitement du langage naturel.

Mots-clés : Big Data, Extraction de Connaissances, Apprentissage Profond Distribué, Identification de Variants Génomiques, Apprentissage Multimodal, Architectures Transformer-CNN, Parallélisme de Données, Reconnaissance de l'Écriture Arabe, Réseaux de Neurones Hybrides.

الملخص

إنّ النمو المتسارع للبيانات الضخمة يفرض الحاجة إلى مناهج قابلة للتوسّع لاكتشاف المعرفة، قادرة على معالجة مجموعات بيانات ضخمة ومتغايرة. تتناول هذه الأطروحة البنى العميقة الموزّعة والمتوازية عبر مجالين تطبيقيين أساسيين: علم الجينوم والتعرّف على الخط العربي.

في مجال الجينوم، يتم اقتراح سلسلة معالجة موزّعة لاكتشاف المتغيّرات الجينية تعتمد على دمج بيانات تسلسل متعددة الأنماط باستخدام بنية هجينة تجمع بين المحوّلات (Transformers) والشبكات الالتفافية (CNN) مع آلية دمج قائمة على الانتباه. يعالج النظام سياق تسلسل الحمض النووي عبر مشفّرات المحوّلات، وأدلّة محاذاة القراءات عبر شبكات التفاف ثلاثية الأبعاد، مما يتيح تصنيفًا دقيقًا للمتغيّرات الجينية مع تحقيق كفاءة حسابية عالية بفضل التعلّم المتوازي الموزّع (DDP) على عدّة وحدات معالجة رسومية. كما تعتمد المنهجية على التعلّم متعدّد المهام لتصنيف نوع المتغيّر، والتنبؤ بالنمط الجيني، وتقدير درجة الجودة، والكشف عن الشوائب، مع استخدام دوال خسارة موزونة لمعالجة عدم توازن البيانات الحاد في الجينوم.

أما في مجال التعرّف على الخط العربي، فقد تم اعتماد بنية هجينة تدمج شبكات الكبسولة (Capsule Networks) داخل شبكات البواقي (Residual Networks)، قادرة على التقاط السمات الهرمية والعلاقات المكانية الضرورية لتحليل الخط المتصل. تتجاوز هذه البنية التحديات الخاصة بالخط العربي، مثل تعقيد الوصلات، وحساسية العلامات التشكيلية، والتنوّع الكبير في أساليب الكتابة.

تُبرز هذه الدراسة متعددة التخصّصات كيف تُمكّن البنى الهجينة، وآليات الدمج متعددة الأنماط، واستراتيجيات الحوسبة الموزّعة من بناء أنظمة قوية ودقيقة وفعّالة حسابيًا لاستخراج المعرفة، قابلة للتطبيق في مجالات علمية مختلفة. وتُسهم النتائج في تطوير حلول تعلّم عميق قابلة للتوسّع، تربط بين الابتكار النظري والتطبيقات الواقعية في علم الجينوم ومعالجة اللغة الطبيعية.

الكلمات المفتاحية:

البيانات الضخمة، اكتشاف المعرفة، التعلّم العميق الموزّع، اكتشاف المتغيّرات الجينية، التعلّم متعدد الأنماط، بنى Transformer-CNN، التوازي البياني، التعرّف على الخط العربي، الشبكات العصبية الهجينة.

Table of Contents

Chapter 1: Theoretical Background of Big Data and Knowledge Discovery

Chapter 2: Knowledge Discovery in Big Genomic Data

Chapter 3: Distributed Deep Learning Pipeline for Genomic Variant Calling

Chapter 4: Case Study in Knowledge Discovery: Arabic Handwriting Character Recognition

Chapter 1

Theoretical Background of Big Data and Knowledge Discovery

1. Introduction

The exponential growth in data volume, velocity, and variety, commonly referred to as "Big Data," necessitates advanced methodologies for extracting meaningful insights and recognizing complex patterns. This phenomenon, prevalent across diverse domains such as healthcare, finance, and scientific research, presents significant challenges and unparalleled opportunities for knowledge discovery. Effectively managing and analyzing such vast datasets requires novel architectures, techniques, algorithms, and analytical approaches to extract their value and hidden knowledge. This chapter delves into the methodological foundations underpinning knowledge extraction and pattern recognition within the Big Data paradigm, highlighting the essential understanding of both the data itself and its domain for effective analysis. Specifically, it addresses the challenges associated with data deluge, data opacity, and data hubris, which arise from the indiscriminate application of computational analyses to large datasets. Overcoming these challenges requires a holistic approach to data quality management and the development of adaptive solutions for knowledge discovery.

2. Foundations of Big Data

2.1 Definition

Big Data refers to extremely large, diverse, and high-velocity datasets that exceed the capabilities of traditional database systems for efficient capture, storage, management, and analysis. Characterized by the well-established ‘Vs’: volume, velocity, variety, and veracity. Big Data requires new computational frameworks and analytical paradigms to extract value, support decision-making, and enable discovery across domains. Beyond its scale, Big Data is transformative in that it demands novel epistemologies and infrastructures, shifting how knowledge is generated and applied in fields ranging from genomics to computer vision.

2.2 Characteristics

The descriptive framework of big data is often anchored in a set of core attributes, each representing a challenge domain of storage, processing, and analytic interpretation. The most widely referenced dimensions are Volume, Velocity, Variety, Veracity, and Value. Although these concepts are often summarized concisely, their operational manifestations can vary substantially across domains (Fig 1.1).

Figure 1.1 5 V's of Big Data

- **Volume**: Describes the massive scale of Big Data, which spans structured databases, unstructured images, and high-throughput genomic repositories. Unlike traditional datasets that are manageable on single servers, sequencing or imaging outputs often generate terabytes per experiment. In genomics, large cohort studies compound this scale across multiple modalities, creating non-linear storage and computational demands. The processing time frequently grows faster than the data size because of memory-intensive algorithms [1]. To better illustrate the scale at which Big Data operates**,** Table 1.1 summarizes the standard capacity measures, expressed in gigabyte (GB) equivalents, ranging from kilobytes to yottabytes, and highlights their relevance in typical Big Data contexts such as genomics, medical imaging, and global data repositories.

Unit	Equivalent in Bytes	Equivalent in GB	Typical Big Data Context Example
Kilobyte (KB)	10^3 bytes = 1,000 B	≈ 0.000001 GB	Log file entries, metadata
Megabyte (MB)	10^6 bytes = 1,000,000 B	≈ 0.001 GB	Small images, genomic FASTQ chunks
Gigabyte (GB)	10^9 bytes = 1,000,000,000 B	1 GB	A single whole-exome sequencing sample
Terabyte (TB)	10^{12} bytes = 1,000,000,000,000 B	1,000 GB	Large medical image archives, sequencing runs
Petabyte (PB)	10^{15} bytes = 1,000,000,000,000,000 B	1,000,000 GB	National biobanks (e.g., UK Biobank genomic data)
Exabyte (EB)	10^{18} bytes = 1,000,000,000,000,000,000 B	1,000,000,000 GB	Global healthcare or astronomy datasets
Zettabyte (ZB)	10^{21} bytes = 1,000,000,000,000,000,000,000 B	1,000,000,000,000 GB	Annual worldwide data creation
Yottabyte (YB)	10^{24} bytes = 1,000,000,000,000,000,000,000,000 B	1,000,000,000,000,000 GB	Hypothetical future data scales

Table 1.1 Big Data Standard Capacity Measures

- **Velocity**: Captures the speed at which data are produced and must be analyzed. Sensors, sequencers, and imaging systems generate outputs within seconds to hours, requiring timely integration into workflows. Clinical genomics often requires same-day analysis for decision-making, where latency directly impacts patient care. Similar dynamics exist in streaming applications, where relevance decays rapidly. Delays in handling fast-moving data reduce their practical value [2].
- **Variety**: Refers to the heterogeneity of Big Data, encompassing structured, semi-structured, and unstructured formats. Genomic pipelines, for instance, integrate raw sequencing reads, expression profiles, and clinical notes. In computer vision, textual reports may need to be combined with imaging data for a unified diagnosis of the disease. Managing such diversity requires hybrid analytical approaches across modalities, such as NLP and CV. This heterogeneity is both a challenge and a source of insight [3].
- **Veracity**: Highlights the uncertainty and unreliability of Big Data sources. Issues arise from noisy sensors, batch effects in experiments, missing values, and mislabeled images in training sets. In genomics, misalignments may inflate false-positive variants, and in vision, mislabeled data degrade model performance. Ensuring trust requires provenance tracking and adherence to rigorous metadata standards. Poor veracity undermines the reliability of the extracted patterns, even with advanced models [4].
- **Value**: Emphasizes the insights and benefits derived from the processed data. Large datasets are not inherently valuable unless they produce actionable results. In healthcare, a small dataset with validated biomarkers may be more impactful than terabytes of unfiltered log data. The definition of value depends on the context, whether economic, clinical, or scientific. Therefore, effective pipelines must align technical capacities with real-world objectives [5].

2.3 Ecosystems and Architectures

Big Data ecosystems are complex computational environments built to manage the enormous storage and processing requirements of modern data-intensive sciences (Fig 1.2). Instead of relying on a single high-performance machine, these ecosystems distribute workloads across clusters of commodity hardware. This distributed approach offers scalability, fault tolerance, and cost-effectiveness, making it the foundation of data-intensive disciplines such as genomics and computer vision, where datasets reach terabyte or even petabyte scales [6].

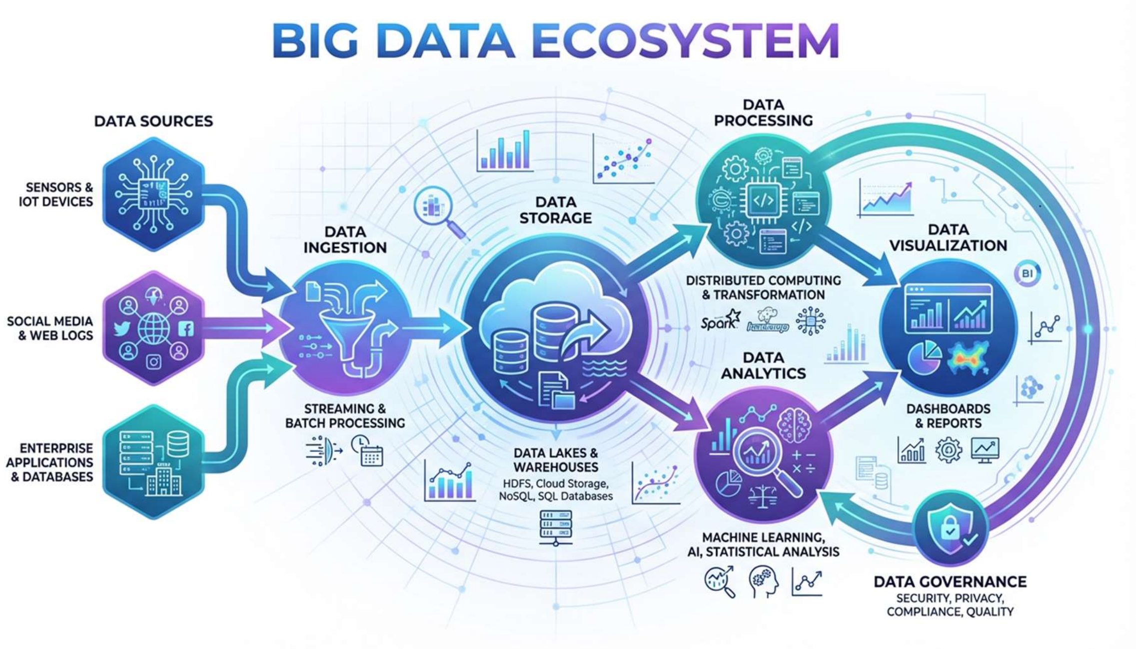

Figure 1.2 Big Data Ecosystem

2.3.1 Key Components of a Distributed Architecture

At the core of most Big Data ecosystems are two foundational technologies: The Hadoop Distributed File System (HDFS), which handles distributed storage, and Apache Spark, which provides large-scale computation. These technologies illustrate the principle of "storage-computation co-location," where the system seeks to process data as close as possible to where it is stored, minimizing costly data transfers across the network.

a) Hadoop Distributed File System (HDFS)

HDFS is the storage backbone of many Big Data frameworks and is designed to manage extremely large files, ranging from terabytes to petabytes, across thousands of nodes. Its design philosophy follows a "write once, read many times" model, which is particularly suitable for analytical workloads. HDFS provides three essential features that make it suitable for Big Data environments. Fault tolerance is achieved through block replication across multiple nodes, ensuring uninterrupted access, even if individual machines fail. For instance, genomic repositories often duplicate sequencing reads across different nodes to safeguard hardware failures. Scalability is supported by a horizontal scaling model, where the storage capacity can be expanded simply by adding more nodes to the cluster, offering a more cost-effective solution than vertically upgrading a single machine. Finally, high throughput is delivered by the HDFS design principle of moving computation to the data rather than transferring massive files across the network, thereby minimizing congestion and significantly accelerating batch analytics workflows [7].

The HDFS is designed on a master–slave architecture (Fig 1.3), where a central master node coordinates the distributed worker nodes. Its robustness stems from clear role separation and replication strategies that ensure fault tolerance and high throughput.

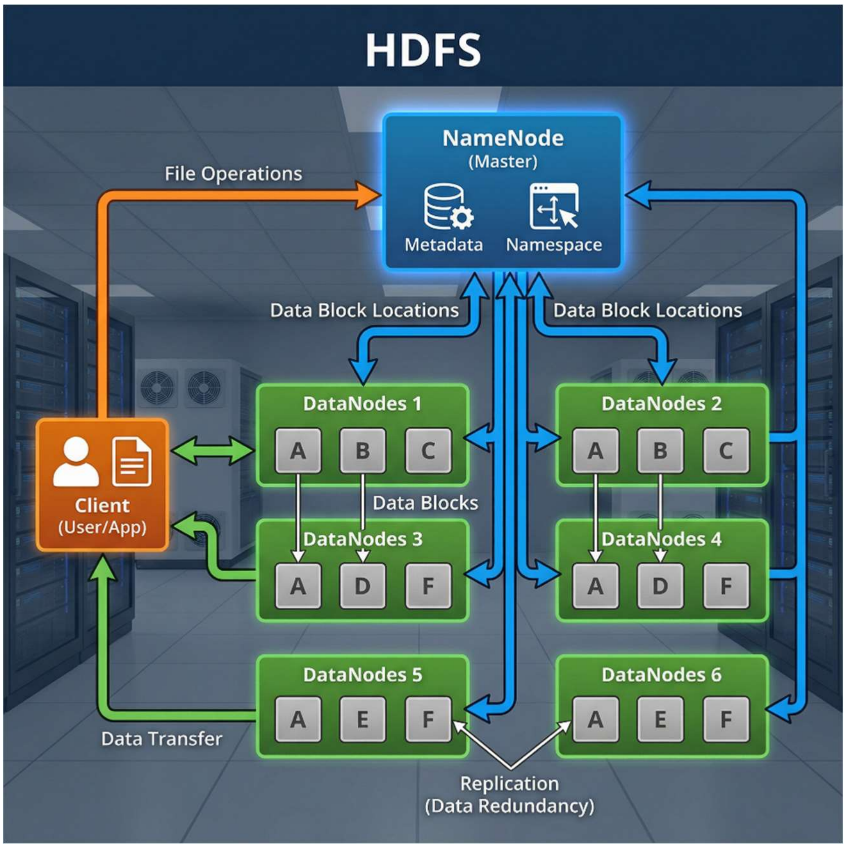

Figure 1.3 HDFS Architecture

- **The NameNode**: The master server manages the HDFS metadata and file system namespace. It tracks which blocks make up each file and which DataNodes store the blocks. It does not store any actual file data. Its critical role necessitates high-availability setups to prevent a single point of failure in the entire cluster.

- **DataNodes**: Worker servers are responsible for storing the actual data blocks on their local disks. They continuously communicate with the NameNode via heartbeats and block reports to verify their status. Their primary functions are to serve read/write requests from clients and replicate data blocks for fault tolerance, as instructed by the NameNode.

- **The Secondary NameNode**: A helper node that performs periodic checkpoints of the NameNode metadata to prevent edit logs from becoming excessively large. Contrary to its name, it is not a hot standby and cannot take over if the primary NameNode fails to function. Its role is to maintain metadata health, a function that is largely replaced by true high-availability setups in modern deployments.

- **The Block**: The fundamental unit of data storage in HDFS is typically 128 or 256MB in size. Files are split into these blocks, which are distributed across multiple DataNodes to enable parallel processing and large-scale storage of data. Each block is replicated multiple times across different nodes to ensure data durability and availability in the event of hardware failure.
- **The Client:** The interface for user or application interaction with HDFS. It first contacts the NameNode to retrieve metadata (such as block locations) for any file operation. It then communicates directly with the relevant DataNodes to read or write actual data. This design avoids making the NameNode a bottleneck during the data transfer.
- **Balancers and Checkpoint:** Auxiliary services for cluster maintenance. The Balancer redistributes data blocks across DataNodes to ensure that the storage capacity is evenly utilized, preventing hotspots. The Checkpoint Node (or function) periodically merges the namespace image of the NameNode with its edit logs to create a new checkpoint, simplifying the recovery process and reducing the startup time.

b) MapReduce

MapReduce is a programming paradigm introduced by Google [6] to enable the scalable and fault-tolerant processing of massive datasets across distributed clusters. It abstracts complex distributed computing into two high-level operations, Map and Reduce, allowing developers to focus on data transformations rather than low-level system details.

- **Map Phase*:*** The input dataset is divided into fixed-size splits, and each split is processed in parallel using map functions. The mapper transforms input key–value pairs (k_1, v_1) into intermediate pairs (k_2, v_2):

$$map\ (k1, v1) \rightarrow [\ (k2, v2)] \qquad \textbf{1.1}$$

- **Shuffle and Sort:** The framework automatically groups all intermediate values (v_2) by their keys (k_2), redistributing the data across nodes to ensure that all values for a key are processed together.
- **Reduce Phase:** The grouped values are then aggregated using the reduce function, which merges them into a smaller set of results.

$$reduce: (k2, [v2]) \rightarrow (k3, v3) \qquad \textbf{1.2}$$

Its impact was significant, as MapReduce enabled processing at the petabyte scale, distributing workloads across thousands of nodes while ensuring robust fault tolerance and reducing the complexity of cluster management. Nonetheless, its disk-based design introduces substantial I/O overhead, limiting performance for iterative tasks such as machine learning or graph analytics. The framework's reliance on only map and reduce primitives also restricts flexibility, requiring complementary tools for advanced querying. These shortcomings led to the emergence of more advanced engines, such as Apache Spark, which leverages in-memory computation and richer APIs. Today, Spark has largely supplanted MapReduce in Big Data pipelines, particularly in genomics and computer vision, where iterative and data-intensive analyses dominate [8].

c) Apache Spark

Apache Spark provides the computational engine for Big Data analysis. It is a unified analytics platform capable of handling diverse workloads ranging from SQL queries to machine learning pipelines, real-time data streams, and graph processing. Its design emphasizes speed, scalability, and ease of integration, making it one of the most widely adopted Big Data frameworks.

- **In-Memory Processing:** Unlike MapReduce, which writes intermediate results to disk, Spark retains data in memory across multiple iterations. This significantly accelerates iterative algorithms, such as clustering, logistic regression, and gradient descent, which are common in machine learning [8].
- **Unified Engine:** Spark integrates a wide range of libraries under a single framework, reducing the need for specialized tools. These include Spark SQL for structured queries, Spark Streaming for real-time analytics, MLlib for distributed machine learning, GraphX for graph processing, and SparkR and PySpark for statistical and Python-based data science workflows.
- **Fault Tolerance:** Spark employs Directed Acyclic Graphs (DAGs) to track the computation lineage. This ensures that if a node fails, the lost partitions can be recomputed automatically, allowing jobs to resume without requiring a full restart.
- **Cluster Management:** Spark can run in diverse environments, including YARN, Mesos, Kubernetes, or its standalone cluster manager, making it highly portable across on-premises and cloud infrastructures.
- **APIs and Language Support:** Spark provides high-level APIs in Scala, Java, Python, and R, allowing developers and data scientists from different backgrounds to use a unified framework without steep learning curves.
- **Integration with Storage Systems:** Spark can directly access data from HDFS, Apache Hive, HBase, Cassandra, Amazon S3, and other cloud-native data lakes, ensuring seamless interoperability across heterogeneous storage backends.

d) Core Resource Management: YARN

At the foundation of the Hadoop ecosystem lies **Y**et **A**nother **R**esource **N**egotiator (YARN), which manages the cluster resources and schedules jobs. YARN allocates CPU, memory, and storage across nodes, thereby ensuring the fair and efficient execution of multiple workloads. By decoupling resource management from application logic, YARN allows diverse engines, such as Spark, Hive, and MapReduce, to run concurrently on the same cluster [9].

e) Storage and Query Layers

storage and query layers form a crucial bridge between raw data and analytical applications. The storage layer reliably persists in massive and diverse datasets across distributed nodes with built-in fault tolerance and scalability. The query layer then provides efficient tools and abstractions for users to access and manipulate these data without handling the underlying complexity. Together, they enable performant and accessible data workflows, from batch processing to real-time queries.

- **HBase**: is a distributed, NoSQL column-oriented database built atop the Hadoop Distributed File System (HDFS) designed to provide low-latency, random real-time read and write access to massive datasets. This capability makes it exceptionally valuable in genomics, where researchers need to rapidly query specific genetic variants or retrieve specific patient metadata from enormous genome sequencing datasets without performing full-table scans.

- **Hive**: offers a data warehouse abstraction layer for big data, providing a familiar SQL-like interface called HiveQL for querying and managing large datasets stored in HDFS. It translates these SQL-like queries into underlying execution engines, such as MapReduce or Tez, thereby enabling data analysts and domain experts proficient in SQL to interact with and analyze petabytes of data without needing to write complex low-level code.

- **Apache Drill:** is an innovative, schema-free SQL query engine designed for interrogating a wide range of heterogeneous data sources, from HDFS and NoSQL stores to cloud storage and flat files, without requiring any upfront schema definitions. This flexibility is particularly powerful in biomedical contexts, as it allows for seamless integration and querying of diverse genomic, clinical, and experimental datasets, even when their structures are inconsistent or unknown beforehand.

- **Apache Pig:** is a high-level platform and scripting language (Pig Latin) for creating complex data transformation and ETL (Extract, Transform, Load) pipelines for large datasets. By compiling its scripts into sequences of MapReduce jobs, it significantly simplifies the process of cleaning, enriching, and preparing raw, unstructured data for subsequent analysis, making it an efficient tool for structuring complex genomic data.

f) Machine Learning and Analytics: Mahout and Spark MLlib

Machine learning has become a cornerstone of Big Data analytics, enabling the extraction of patterns and predictive insights from massive, heterogeneous datasets. Within the Hadoop and Spark ecosystems, two prominent frameworks, Apache Mahout and Spark MLlib, provide scalable libraries that integrate directly with distributed storage and computation layers:

- **Apache Mahout:** It was one of the earliest attempts to bring machine learning to the Hadoop ecosystem, offering scalable implementations of algorithms for clustering (e.g., k-means), classification (e.g., Naïve Bayes and Random Forests), and collaborative filtering (e.g., recommendation systems). Originally tied to the MapReduce model, Mahout faced performance limitations because of MapReduce's disk-based I/O. Over time, the project has migrated to more efficient execution engines, such as Apache Spark and Apache Flink, enabling in-memory computation and improved scalability. Today, Mahout focuses heavily on linear algebra frameworks and matrix decomposition methods, which support advanced applications such as text mining, recommender systems, and network analysis in Big Data contexts.

- **Spark MLlib**: By contrast, was built natively for in-memory distributed processing within Apache Spark. It offers a wide range of supervised and unsupervised learning algorithms, including classification, regression, clustering, dimensionality reduction, and recommendation systems, as well as utilities for feature extraction, model evaluation, and optimization. One of its key advantages is its tight integration with Spark's ecosystem, which allows MLlib to seamlessly process data from Spark SQL, Spark Streaming, and GraphX. This makes it particularly suitable for iterative machine learning tasks, where repeated access to the same dataset is required. In practice, MLlib has been widely adopted in genomics to analyze high-dimensional sequencing data, identify genetic variants, and classify disease subtypes, and in computer vision, where it supports large-scale image recognition and feature extraction pipelines [10].

2.4 Challenges in Big Data Ecosystems

Despite their maturity, Big Data ecosystems still face several persistent challenges that limit their effectiveness in domains such as genomics and computer vision:

- **Heterogeneity:** Big Data integrates multiple formats, from structured genomic variant tables (VCF) to unstructured histopathological images. Combining sequencing reads, expression matrices, and clinical imaging requires workflows that can process and align fundamentally different data types without losing biological or diagnostic significance [11] [12].

- **Scalability:** As datasets grow from terabytes to petabytes, workflows such as whole-genome sequencing of national cohorts or large-scale image recognition must be scaled linearly without excessive computational overhead.
- **Privacy:** Genomic data are uniquely identifiable, and medical images may contain sensitive patient information. Sharing such data across institutions requires strong governance frameworks (e.g., GDPR, HIPAA) and technical solutions, such as federated learning, to ensure secure collaboration without exposing raw datasets [13] [14].
- **Integration:** Precision medicine and automated vision diagnostics depend on combinationning of genomic, imaging, and clinical records. However, integrating such multimodal datasets remains challenging because of inconsistent metadata standards, interoperability gaps, and semantic mismatches between biological and imaging ontologies [1] [15].

Addressing these issues is essential to unlock the full potential of big data-driven genomics and vision, enabling robust, secure, and scalable pipelines for knowledge discovery.

3. Big Data Knowledge Discovery Process

Knowledge Discovery in Databases (KDD) in the context of Big Data is a large-scale, computationally intensive process of automatically extracting hidden, previously unknown, and potentially valuable patterns, insights, and knowledge from massive, complex, and often unstructured datasets. It extends beyond traditional databases to include data lakes, streaming data, and distributed storage systems. The process is systematic and exploratory, designed to reveal profound insights that are not apparent through conventional analysis, thereby enabling data-driven decision-making on a large scale (Fig 1.4). The 5Vs of Big Data necessitate adaptations to the traditional KDD process, emphasizing distributed computing, scalable algorithms, and automated pipelines.

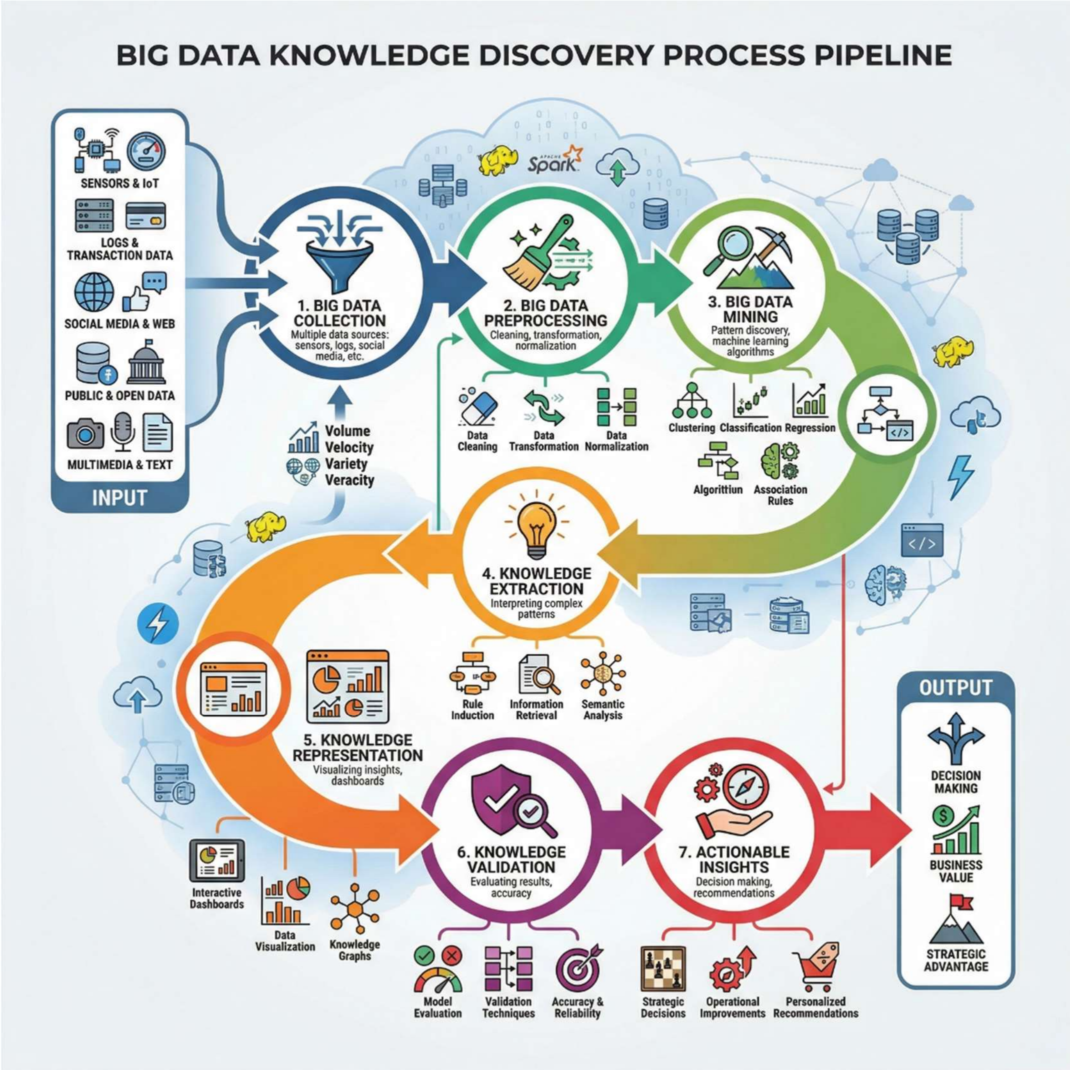

Figure 1.4 Knowledge Discovery Process

Here is an overview of the Big Data KDD process:

3.1 Big Data Selection and Acquisition

In large-scale analytical environments, data acquisition is a complex engineering task and not a simple matter of gathering as much data as possible. These strategies must account for the diversity of incoming sources and operational constraints of downstream processing [16]. The objective was to optimize the informativeness, representativeness, and diversity of the samples while ensuring they met the performance requirements. This often involves balancing conflicting objectives, such as acquiring high-volume streams at speed without diminishing quality and ensuring comprehensive coverage of relevant conditions without over-representing easily accessible subgroups [2]. The acquisition phase thus shapes the eventual analytical value of the data by encoding timeliness, completeness, coherence, and fitness for purpose within raw inputs [17].

3.1.1 The Diversity of Sources and Formats

The heterogeneity of Big Data sources necessitates a nuanced approach to acquisition, with specialized formats and protocols developed to meet domain-specific challenges. Different domains produce data in vastly different structures, ranging from genomic sequencing reads and medical images to financial transactions, IoT sensor streams, social media feeds, large text corpora, and satellite remote sensing, each requiring tailored strategies for efficient storage, processing, and integration [16] [2].

- **Genomic Sequencing Data**

Genomic sequencing exemplifies the challenges of high volume and velocity. A single whole-genome sequencing experiment can generate hundreds of gigabytes of data in text-based formats, such as FASTA or FASTQ, which store raw sequences and associated quality scores. In the next chapter, we focus on this type of data.

- **Medical Imaging Data**

Medical imaging constitutes one of the largest and most complex sources of healthcare Big Data, encompassing modalities such as X-ray, computed tomography (CT), magnetic resonance imaging (MRI), ultrasound, positron emission tomography (PET), and digital pathology. These modalities generate massive, high-resolution datasets that can easily be scaled to terabytes per patient cohort. Standards such as DICOM (Digital Imaging and Communications in Medicine) remain central for storage and exchange, as they encode pixel data and integrate essential clinical metadata, including patient demographics, acquisition parameters, and diagnostic annotations. While this coupling preserves the clinical context and supports interoperability across institutions, it raises ethical and regulatory challenges due to the presence of Personally Identifiable Information (PII) and Protected Health Information (PHI). Effective de-identification of medical imaging data must go beyond removing textual identifiers to include obscuring “burned-in” annotations within pixel arrays, harmonizing metadata, and applying temporal adjustments to acquisition dates [18]. In the era of Big Data, where medical images are increasingly pooled for machine learning, federated analytics, and multi-institutional studies, adherence to regulatory frameworks such as HIPAA (U.S.) and GDPR (Europe) is critical [19]. Thus, medical imaging exemplifies the volume, variety, and veracity challenges of Big Data, while also underscoring the necessity of privacy-preserving infrastructures to unlock its potential for precision medicine and clinical decision support.

- **Digitized Documents and Historical Manuscripts**

Beyond clinical contexts, digitized documents and historical manuscripts have become key components of imaging Big Data. Large-scale digitization initiatives in libraries, archives, and cultural institutions generate vast image repositories of scanned books, newspapers, and handwritten manuscripts. Optical Character Recognition (OCR) systems are employed to unlock their textual content, transforming pixel-level data into machine-readable text. OCR introduces its own Big Data challenges, including handling heterogeneity (different fonts, handwriting styles, degraded or aged paper), veracity (error-prone transcriptions), and integration with structured metadata for indexing and retrieval [20]. Projects such as Google Books, Europeana, and digitized Arabic/Chinese manuscript collections exemplify how scanned imaging data, once processed, become invaluable for linguistic research, digital humanities, and knowledge extraction across centuries of recorded histories.

- **Time-Series and Sensor Data**

Time-series data from continuous monitoring systems, such as ICU vital sign monitors, wearable devices, or distributed IoT sensors, present a challenge in terms of velocity. These sources generate millions of records per hour and require processing in near real-time to detect anomalies and time-sensitive events. For example, neonatal monitoring systems must flag abnormal heart rate patterns within seconds, whereas smart city sensors aggregate traffic, pollution, and energy usage data that must be acted upon dynamically [21]. These demands necessitate low-latency architectures (e.g., Spark Streaming and Apache Flink) capable of horizontal scaling to avoid degradation in utility [22].

- **Financial and Transactional Data**

Beyond health and biology, financial institutions generate vast streams of transactional data, including stock trades, credit card usage and blockchain logs. Here, the variety of formats: relational records, JSON-based API feeds, and real-time market tick data, requires a hybrid processing approach. Fraud detection, for instance, depends on rapid ingestion and anomaly detection pipelines that must combine structured account histories with unstructured event logs in real time [23].

- **Social Media and Textual Data**

Social platforms contribute massive volumes of semi-structured and unstructured data in the form of posts, tweets, videos, and comment threads. Text mining, sentiment analysis, and natural language processing (NLP) pipelines rely on distributed frameworks to handle this heterogeneity, often requiring preprocessing steps such as tokenization, embedding, and noise filtering to achieve this. This domain demonstrates how variety and veracity interact: the same platform may contain valuable behavioral signals alongside misleading or low-quality content [24].

- **Large Text Corpora**

Another major category of Big Data comes from large-scale textual collections, including scientific literature, legal records, books, and multilingual web documents. These corpora are typically stored in formats such as XML, JSON, or plain text, but require extensive preprocessing, such as stemming, stop-word removal, and vectorization, to become analytically useful. Examples include PubMed Central, which hosts millions of biomedical articles [25], or legal corpora used in predictive justice systems [26]. Natural language processing models, including transformers such as BERT and GPT, rely on such corpora for training but face challenges of heterogeneity, ambiguity, and bias across languages and domains [27].

- **Satellite and Remote Sensing Data**

In Earth observation, satellite imagery and radar feeds generate petabyte-scale datasets characterized by high spatial and temporal resolutions. Formats such as GeoTIFF and HDF5 are used for storage, and indexing and tiling strategies are applied for scalable access. These datasets present challenges in terms of volume and integration, as they must often be combined with climate, demographic, or agricultural records to enable downstream applications in environmental monitoring or disaster response [28].

3.1.2 Strategic Choices: Real-time vs. Batch Processing

The choice between real-time and batch processing is a core strategic decision based on the temporal sensitivity of the insights sought.

- **Real-time Architectures**

For situations where the value decays rapidly, such as disease outbreak signals from social media or transient cellular events in video microscopy, acquisition infrastructures are tethered to real-time message queues [29]. These architectures consist of several components: a source (sensors, APIs), a stream ingestion layer (Apache Kafka, Amazon Kinesis), a stream processing engine (Apache Flink, Spark Streaming), and a destination (databases, dashboards) [30] [31]. These systems are designed to handle high volumes of data with minimal delay, often leveraging parallel processing and data partitioning to achieve scale [22].

- **Batch Processing**

In contrast, long-term observational studies prioritize longevity and consistency over immediacy [16]. For these applications, a delayed batch-oriented approach is suitable. The Hadoop ecosystem, for example, is a foundational technology for this model, designed to process vast datasets across clusters of commodity hardware [6] [7]. In this model, data is consolidated over time before undergoing more computationally intensive analysis, a process that is a core part of the MapReduce paradigm [6].

3.1.3 Quality Control at the Point of Capture

A proactive approach to data quality is increasingly recognized as a critical component of modern acquisition strategies, challenging the traditional "schema-on-read" paradigm, which assumes that all raw data can be stored first and cleaned later [1]. Establishing clear specifications for what constitutes a valid sample is essential to avoid wasting resources on low-analytical-utility inputs [16]. For example, in genomic imaging and sequencing, parameters such as spatial resolution, signal-to-noise ratio, coverage depth, and metadata completeness directly determine the usability of the data for downstream applications [11]. Similarly, in medical imaging, enforcing acquisition standards ensures that DICOM objects include consistent metadata fields and sufficient pixel quality to support diagnosis and machine learning applications [18]. Without such upfront validation, storage infrastructures risk being flooded with noisy, incomplete, or redundant records that require expensive cleaning or, worse, compromise the reliability of subsequent analyses. This proactive quality control at the point of capture is thus indispensable for ensuring data veracity and maximizing the efficiency of Big Data ecosystems.

3.1.4 Ethical and Legal Considerations

Ethical and legal dimensions are paramount in Big Data ecosystems and must be embedded from the point of capture, rather than added as post-hoc protections [2]. The scale of modern datasets and the ease of cross-referencing across disparate sources introduce novel risks of re-identification, even when traditional anonymization methods are applied [13]. In highly sensitive domains, such as human genomics and health informatics, the insufficiency of anonymization necessitates a shift toward robust de-identification protocols, encryption, and fine-grained access control mechanisms [32]. For instance, genomic sequences, once considered anonymous, can often be linked back to individuals when combined with demographic or public record data. Regulatory frameworks, such as HIPAA in the United States and GDPR in the European Union, impose strict requirements for consent, purpose limitation, and data minimization, mandating that acquisition pipelines incorporate compliance mechanisms from the outset [33]. This move toward privacy by design reflects the recognition that ethical and legal safeguards must evolve alongside the scale, interconnectivity, and sensitivity of modern Big Data.

3.2 Big Data Preprocessing

Before advanced analytics can be applied, raw Big Data must undergo a crucial preprocessing phase to ensure their quality and usability. This initial step involves cleaning the data to handle inconsistencies, missing values, and noise that are inherent in large, unstructured datasets. Further processes include transformation, such as normalizing numerical values and encoding categorical variables to create a consistent format. Effective preprocessing is fundamental because it directly enhances the accuracy, efficiency, and reliability of subsequent machine learning models and data mining algorithms. Ultimately, this foundational work transforms chaotic raw information into a refined and structured asset ready for analysis.

3.2.1 Normalization and Standardization

Normalization ensures consistency across heterogeneous datasets, preventing biases caused by differences in scale or measurement units. In Big Data pipelines, normalization is typically distributed across clusters and applied in parallel to billions of records.

- **Min–Max Scaling**

This rescales features into a bounded interval [0,1], which is widely used in image pixel normalization and IoT sensor readings. However, outliers in large-scale datasets can distort boundaries, necessitating the use of robust variants such as clipped scaling.

$$x' = \frac{x - \min(x)}{\max(x) - \min(x)} \qquad \mathbf{1.3}$$

- **Clipped Scaling**

Values are first clipped to a predefined percentile range (e.g., 1st–99th percentile, or ±3 standard deviations), before applying Min–Max scaling.

$$x_{clipped} = \min(\max(x, P_l), P_u) \qquad \mathbf{1.4}$$

where P_l, P_u are lower and upper clipping thresholds (percentiles or standard deviation bounds). Then, Min–Max scaling is applied on $x_{clipped}$.

In financial transaction datasets, clipped scaling prevents billion-dollar outliers from skewing fraud detection models. In RNA-seq expression matrices, it avoids distortions caused by a few genes with ultra-high counts.

- **Z-score Standardization**

Standardization is critical in genomic pipelines where gene expression values differ by orders of magnitude, and in financial Big Data where volatility differs across markets. Distributed implementations (e.g., Spark MLlib) compute μ and σ across partitions, then apply transformations in memory to reduce latency.

$$x' = \frac{x - \mu}{\sigma} \qquad \mathbf{1.5}$$

where μ and σ are mean and standard deviation.

- **Nonlinear Transformations**

Many Big Data distributions are highly skewed (hospital billing records, web traffic logs). Skewed distributions lead to heteroscedasticity (variance increasing with the mean), which violates assumptions of many machine learning and statistical models. Nonlinear transformations address this by stabilizing variance, compressing dynamic ranges, and making data more Gaussian-like.

Logarithmic Transformation :

$$x' = \log(x + c) \qquad \textbf{1.6}$$

where c>0 prevents log (0) (c: a positive offset constant added to avoid taking the log of 0)

- Compresses large values while spreading out small values.
- Common in financial transaction analysis (Lawrence et al., 2014).
- Limitation: cannot handle negative values.

- **Domain-Specific Normalization**

For complex data like genomic expression measurements from RNA-seq, standard normalization is insufficient due to the unique characteristics of the data, such as its discrete nature and variance dependence on the mean [34]. Specialized methods like the Trimmed Mean of M-values (TMM) are required to correct for biases arising from sequencing depth and RNA composition [34]. The choice of normalization procedure can lead to significant variability in the results of differential gene expression analysis, underscoring the importance of selecting the right method for the data type [35].

3.2.2 Addressing Batch Effects: A Critical Challenge in Multi-Center Studies

An example of batch effects are non-biological variations that arise from technical differences across different batches of data, such as different scanners, sequencing facilities, or experimental protocols [36]. These systematic discrepancies, if left uncorrected, can compromise the generalizability and robustness of downstream analytical models, obscuring true biological signals [36]. A significant challenge is that models trained on data from one site may not perform well when applied to another, undermining the very purpose of a multi-center study [36]. Algorithms such as ComBat and its variants (ComBat-seq for RNA-seq and ComBat-met for DNA methylation data) have been developed to mitigate these effects [37] [38]. These methods work by estimating the mean and variance differences across batches and adjusting the data to a common level, often using a hierarchical empirical Bayes framework that borrows information across genes to make the adjustment robust, even with small sample sizes [37]. The effectiveness of these methods is a testament to the need for sophisticated, automated solutions to address data quality issues that are a direct result of large-scale data integration.

3.2.3 Noise and Outlier Handling

Managing noise and outliers is a persistent challenge in Big Data pipelines, as imperfections are inevitable when working with heterogeneous, large-scale datasets. Noise may be random, from measurement errors or environmental fluctuations, or systematic, from calibration drift, biased sampling, or batch effects. If left untreated, both forms distort downstream analyses. Common strategies include filtering (low-pass or high-pass filters) to suppress irrelevant fluctuations and smoothing methods (e.g., moving averages and LOESS) to reduce short-term variability [39].

For outliers, automated methods such as Z-score thresholds, Mahalanobis distance, or robust algorithms such as RANSAC and Isolation Forests help detect anomalies [40]. However, there is a fundamental trade-off: aggressive filtering improves data quality but risks discarding rare yet meaningful events such as equipment malfunctions, unusual user behaviors, or fraudulent transactions.

Therefore, noise and outlier handling cannot rely solely on automated algorithm. Domain expertise, hybrid approaches, and sometimes human oversight are required to ensure that anomalies are interpreted correctly. Ultimately, the goal is not to eliminate all irregularities but to distinguish spurious artifacts from valuable signals, reframing anomalies as potential sources of new insights in Big Data contexts.

3.2.4 Missing Values Handling

Handling missing values is a fundamental step in Big Data pipelines, where scale, heterogeneity, and velocity amplify the challenge [41]. Traditional methods, such as row or column deletion, may lead to unacceptable information loss; even a small percentage of missing records can represent terabytes of discarded data. Simple imputation by mean, median, or mode is computationally feasible only when implemented in a distributed manner using aggregation and broadcasting primitives [6]. To overcome these limitations, scalable preprocessing strategies have been developed and integrated into distributed frameworks, such as Spark MLlib, Dask, and TensorFlow data loaders. These strategies can be grouped into three categories (Table 1.2): deletion methods (listwise and feature-wise) are viable only under the strict assumptions of randomness and low missingness. Statistical and model-based imputation methods, including multivariate iterative imputation (MICE), k-nearest neighbors (KNN), and deep learning with autoencoders or variational autoencoders (VAEs), provide more robust solutions by exploiting the inter-feature correlations and latent representations. For categorical data, global mode substitution or encoding "Unknown" categories are common practice. Flagging approaches complement imputation by introducing binary indicators of missingness, which can be predictive. Best practices emphasize profiling the type of missingness (MCAR, MAR, MNAR), using pipeline-optimized transformers (e.g., Spark's Imputer), minimizing costly data shuffling, and supporting real-time streaming through sliding window statistics. Overall, preprocessing missing values in Big Data requires not only methodological rigor but also architectural awareness, ensuring that methods are parallelizable, scalable, and seamlessly integrated with machine learning workflows [42].

Category	Method	Description / Scalability
Deletion	Listwise Deletion	Remove records with missing values; only feasible if % missing is negligible.
	Feature-wise Deletion	Remove features with >60–80% missing values; useful for high-dimensional data.
Imputation	Statistical (Mean/Median/Mode)	Distributed aggregation and broadcasting across partitions.
	Multivariate (MICE)	Iterative modeling of features; distributed implementations in Spark/Dask.
	KNN Imputation	Approximate nearest neighbors (e.g., LSH) for scalability.
	Deep Learning (Autoencoders, VAEs)	Learn latent structures for robust imputation in complex data.
Flagging/Encoding	Binary Indicators	Add "was_missing" feature alongside imputation.
	New Category for Categorical Data	Encode missing values as "Unknown"/"N/A."

Table 1.2 Methods for handling missing values

3.3 Feature Engineering and Dimensionality Reduction

Feature engineering involves two complementary strategies: feature selection, which reduces dimensionality by identifying and retaining only the most informative variables, and feature extraction, which creates compact representations by transforming the original feature space. Selection prioritizes interpretability and computational efficiency, whereas extraction emphasizes compression and representation learning. In Big Data context, both approaches must be designed for scalability and distribution when operating on terabyte- to petabyte-scale datasets.

3.3.1 Feature Selection Methods

Feature selection techniques aim to eliminate irrelevant or redundant variables while preserving the semantics of the original feature space. In the context of Big Data, these methods are crucial for mitigating the curse of dimensionality, enhancing model interpretability, and reducing computational overhead in distributed environments. By identifying a subset of the most informative features, organizations can streamline downstream machine learning pipelines, particularly when processing petabyte-scale datasets across clusters.

- **Filter Methods**

Techniques such as correlation analysis, chi-square tests, and mutual information scoring can be parallelized across nodes, with each worker independently computing univariate statistics [43]. These methods are computationally lightweight and scale efficiently because they do not require iterative model training. Distributed frameworks, such as Spark, leverage in-memory processing to accelerate these computations by partitioning feature sets across nodes for parallel evaluation.

- **Wrapper Methods**

These methods employ distributed cross-validation and ensemble-based search to evaluate feature subsets, balancing predictive accuracy against computational expense [44]. Although more accurate than filter methods, wrapper approaches are computationally intensive. Distributed systems mitigate this by parallelizing model evaluations across multiple nodes using techniques such as grid search or genetic algorithms to explore feature combinations.

- **Embedded Methods**

Techniques such as LASSO regression and tree-based models (e.g., Random Forests, Gradient Boosting) integrate feature selection into the model training process [45]. Distributed optimization algorithms, such as those implemented in MLlib (Spark's machine learning library), enable scalable feature selection by distributing the gradient computations and model updates across clusters.

- **Hybrid and Ensemble Methods**

Hybrid and ensemble methods combine filter, wrapper, and embedded approaches to balance scalability and predictive accuracy [46] [47]. A typical workflow applies filters, such as correlation or mutual information, for pre-selection, followed by wrappers or embedded models, such as LASSO and Random Forests, for refinement [45] [48]. In Big Data environments, these pipelines are implemented on distributed frameworks such as Spark or Dask, where filter steps are parallelized, and wrappers/embedded models leverage distributed training [8]. Hybrid methods are widely applied in domains like IoT and genomics, where noise reduction and predictive accuracy are both critical [44] [40]. Recent advances have emphasized multi-objective optimization to balance accuracy, interpretability, and computational cost, and ensemble feature selection to aggregate rankings from multiple algorithms for improved robustness [49]. The table (Table 1.3) summarizes the key trade-offs, highlighting how embedded and hybrid methods excel in distributed Big Data workflows.

Method	Computational Complexity	Scalability in Big Data
Filter	Low (O(n))	High (parallelizable)
Wrapper	High (exponential)	Medium (ensemble needed)
Embedded	Medium (model-dependent)	High (integrated)
Hybrid	Variable	High (modular)

Table 1.3 Feature Selection Method Comparison

3.3.2 Feature Extraction Methods

Feature extraction is a critical preprocessing step that creates new, more compact, and informative representations from raw data, often at the expense of their direct interpretability. It is indispensable for managing the curse of dimensionality in extremely high-dimensional, multimodal, and unstructured Big Data. The primary goals are to reduce the computational cost, mitigate overfitting, and reveal underlying latent structures that are more amenable to machine learning models.

- **Linear Methods**
  - **Principal Component Analysis (PCA):** For complex datasets, such as genomic expression measurements derived from RNA-seq, standard normalization techniques are inadequate because of the distinct characteristics of the data, including their discrete nature and the variance's dependence on the mean [34]. Specialized methodologies, such as the Trimmed Mean of M-values (TMM), are necessary to address biases resulting from sequencing depth and RNA composition [34]. The selection of a normalization procedure can significantly influence the outcomes of differential gene expression analysis, highlighting the critical importance of choosing an appropriate method for a specific data type [35].
  - **Non-Negative Matrix Factorization (NMF):** Similar to PCA but constrains components to be non-negative, leading to parts-based, interpretable representations often used in text mining (topic modeling) and image decomposition (learned "parts" of faces).
  - **Independent Component Analysis (ICA):** Identifies statistically independent source signals from their linear mixtures, making it highly useful for biomedical data (e.g., EEG artifact removal) and sensor arrays. Its scalability is generally less than that of PCA because of the more complex optimization.
  - **Linear Discriminant Analysis (LDA):** A supervised method that finds feature projections that maximize the separation between classes while minimizing the variance within each class. It is effective for classification tasks but can be computationally expensive for high-dimensional data.
- **Approximate and Randomized Methods**
  - **Random Projections:** Based on the **Johnson–Linden Strauss lemma**[1], this method projects data into a randomly selected lower-dimensional subspace while approximately preserving pairwise distances. It

[1] In mathematics, the Johnson–Linden Strauss lemma is a result named after William B. Johnson and Joram Lindenstrauss concerning low-distortion embeddings of points from high-dimensional into low-dimensional Euclidean space. The lemma states that a set of points in a high-dimensional space can be embedded into a space of much lower dimension in such a way that distances between the points are nearly preserved. In the classical proof of the lemma, the embedding is a random orthogonal projection.

is computationally very efficient and is often used as a preprocessing step for other algorithms like clustering to drastically reduce dimensionality with minimal loss of accuracy [50].

- **Feature Hashing (Hashing Trick):** Primarily for high-dimensional categorical or textual data, a hash function is applied to map the original features directly to indices in a fixed-size vector. This avoids the need to maintain a feature dictionary, enabling minimal memory footprint and one-pass processing of streaming data. A key consideration is managing hash collisions, which can be mitigated by using a signed hash function.

- **Nonlinear Manifold Learning**

  - **t-Distributed Stochastic Neighbor Embedding (t-SNE):** Suited for visualizing high-dimensional data in 2D or 3D by preserving the local neighborhoods. While powerful, it is computationally intensive and non-parametric, meaning it doesn't produce a reusable model.

  - **Uniform Manifold Approximation and Projection (UMAP):** UMAP often outperforms t-SNE in preserving both local and global data structures. It is significantly faster and has GPU acceleration, making it practical for datasets with millions of points (e.g., single-cell RNA-sequencing, image embeddings).

  - **Isomap and Locally Linear Embedding (LLE):** Classic manifold learning techniques that assume that the data lie on an embedded nonlinear manifold. They are effective for certain data types but are generally less scalable than UMAP for very large datasets.

- **Dictionary Learning & Sparse Coding**

This approach learns an over-complete "dictionary" of basis functions from which the input data can be represented as a sparse linear combination. This is highly effective for signals like images and audio. Distributed algorithms for Big Data partition the data across a cluster, enabling parallel updates to the dictionary and the estimation of sparse coefficients for each data point, thus enabling applications in large-scale vision and audio processing.

- **Kernel Methods**

Methods such as Kernel PCA provide a way to perform nonlinear feature extraction by implicitly mapping data into a high-dimensional feature space where linear separation is possible. While powerful, their application to Big Data is challenging due to the $O(n^2)$ or $O(n^3)$ computational complexity.

Approximations using the **Nyström method**[2] or **Random Fourier Features** (rff)[3] are essential to make them scalable.

- **Deep Feature Learning**

Deep learning models inherently perform automatic feature extraction, learning hierarchical representations from raw data.

- **Convolutional Neural Networks (CNNs):** Extract hierarchical spatial features through convolutional and pooling layers. They are the standard for image data in domains from medical pathology to satellite imagery. Pretrained models on large corpora (e.g., ImageNet) can be used for transfer learning, significantly reducing the data required for new tasks.
- **Recurrent Neural Networks (RNNs) and Transformers:** Capture complex sequential and temporal dependencies. RNNs (and their LSTM/GRU variants) were traditionally used for tasks like time-series forecasting. Transformers, with their self-attention mechanism, have become dominant for sequential data like text (e.g., BERT, GPT), genomics, and financial time series due to their superior ability to model long-range context.
- **Autoencoders (AEs) and Variational Autoencoders (VAEs):** Learn compact latent representations in an unsupervised manner. Standard autoencoders learn to compress and reconstruct input data. VAEs learn the parameters of a probability distribution representing the data, enabling generative capabilities. Denoising and contractive autoencoders are variants that improve robustness.
- **Graph Neural Networks (GNNs):** Designed to extract features from graph-structured Big Data (e.g., social networks, recommendation systems, knowledge graphs, and protein-protein interactions). They operate by aggregating information from a node's neighbors, learning powerful representations that encode both node features and graph topology.
- **Self-Supervised Learning (SSL):** A paradigm in which models generate their own supervisory signals from unlabeled data, often by learning to predict hidden parts of the input (e.g., masked language modeling in BERT). This is particularly valuable for Big Data, where unlabeled data is abundant but manual annotation is expensive.

[2] **The Nyström method** is a technique to generate low-rank approximations of matrices by selecting a subset of columns and using them to approximate the full matrix

[3] **Random Fourier Features** approximate kernel functions with low-dimensional projections, enabling scalable kernel methods by replacing expensive kernel computations with efficient linear operations.

- **Automated Feature Engineering (AutoML)**

AutoML frameworks, such as **Auto-sklearn**[4] or **Google's AutoML**[5], use evolutionary search, reinforcement learning, and neural architecture search to generate feature transformations. These methods employ multi-objective optimization to balance the model accuracy with the computational cost. Distributed AutoML pipelines, implemented in frameworks such as **Ray**[6] or **Dask**[7], parallelize feature generation and evaluation across nodes, enabling scalability for large datasets.

3.3.3 Comparative Perspective

To provide a clearer overview of the discussed methods, Table 1.4 presents a comparative summary of feature selection and feature extraction techniques.

Method	Category	Primary Use Cases	Strengths	Weaknesses
Correlation / MI Filters	Selection	Text mining, genomics	Fast, scalable	Ignores feature interactions
Wrapper (CV-based)	Selection	Medium-scale tasks	Captures interactions	High computational cost
Embedded (LASSO, RF)	Selection	Genomics, finance	Built-in selection	Biased by model choice
PCA (Distributed)	Extraction	Omics, IoT, finance	Captures variance	Linear only
Random Projections	Extraction	Text, logs	Efficient, parallelizable	Approximate, less interpretable
t-SNE / UMAP	Extraction	Visualization, biology	Preserves nonlinear structure	Memory-intensive
CNNs, Transformers	Extraction	Images, sequences	Hierarchical, scalable	Require large datasets & compute
GNNs	Extraction	Networks, graphs	Captures relationships	Emerging, still scaling

Table 1.4 Comparative Summary of Feature Selection and Feature Extraction Methods in Big Data Analytics

4 https://www.automl.org/automl-for-x/tabular-data/auto-sklearn/
5 https://cloud.google.com/automl
6 **Ray**: is a high-performance distributed execution framework designed for building and running low-latency, large-scale machine learning applications.
7 **Dask**: is a flexible parallel computing library for analytics and data science in Python.

4. Big Data Mining Techniques

Data Mining represents the core stage of the Knowledge Discovery process, where computational methods are applied to extract patterns, models, and insights from massive, heterogeneous, and fast-evolving datasets. Unlike traditional mining, it must address scalability, real-time processing, and multimodal integration, relying on distributed frameworks and advanced machine learning to convert raw data into useful knowledge. Figure 1.5 presents a taxonomy of Big Data mining techniques, and Table 1.5 summarizes their main categories, underlying algorithms, typical applications, and scalability considerations. These methods, covering clustering, classification, association analysis, and anomaly detection, exploit parallelization,

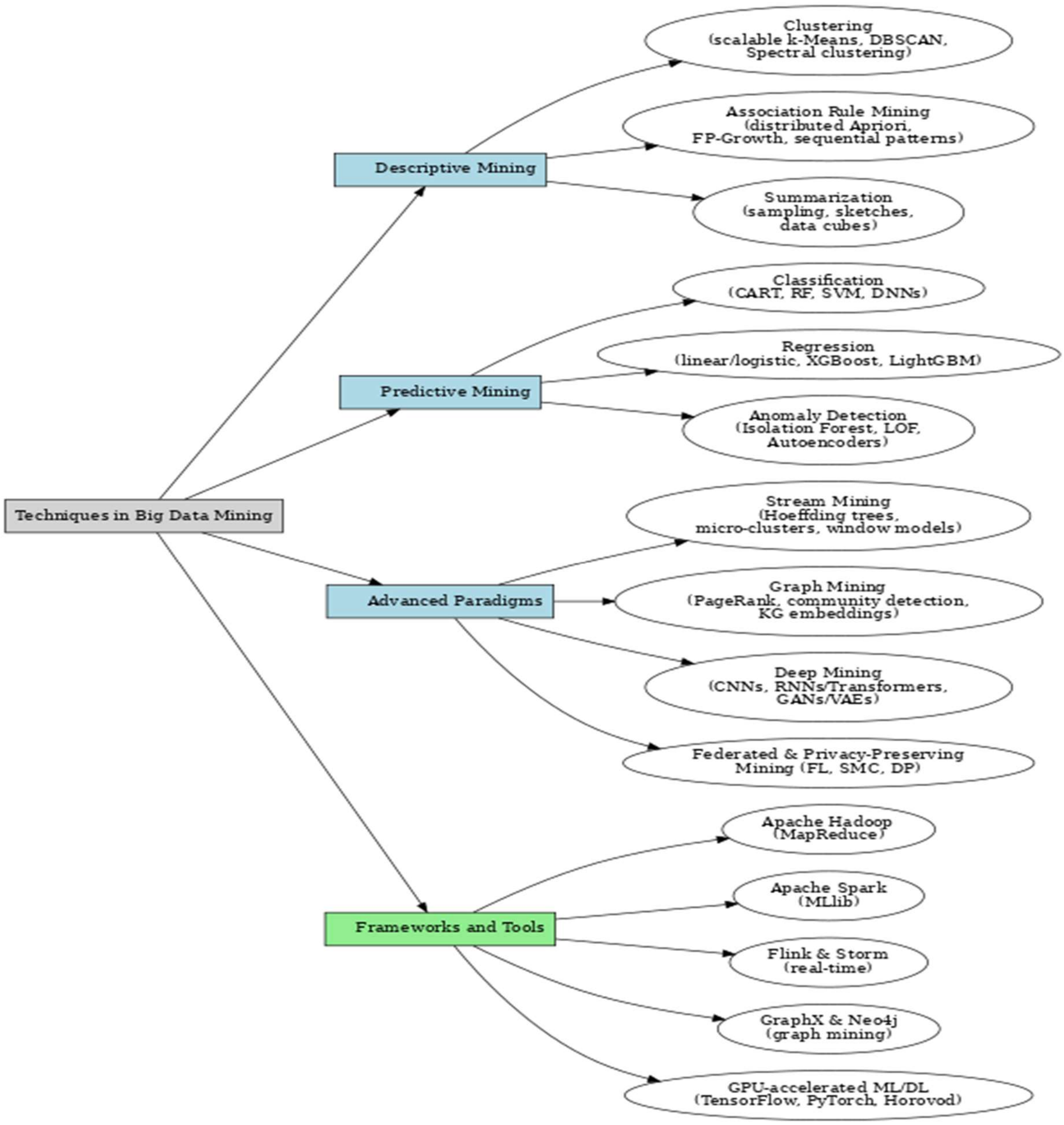

Figure 1.5 Big Data Mining Techniques Taxonomy

approximation, and distributed architectures to ensure that knowledge discovery remains feasible and impactful at scale.

Category	Technique / Algorithm	Main Use Cases	Scalability Considerations
Descriptive Mining	**Clustering** (k-Means, DBSCAN, Spectral)	Customer segmentation, genomic subtyping, document grouping, anomaly detection	k-Means scalable via Spark (mini-batch, k-Means
	Association Rule Mining (Apriori, FP-Growth, Sequential Mining)	Market basket analysis, medical comorbidity mining, text/web usage patterns	Apriori parallelized for candidate generation; FP-Growth scalable with local FP-trees + global aggregation (Spark MLlib); sequential mining adapted for streams
	Summarization and Characterization (Sampling, Sketches, Data Cubes)	OLAP reporting, IoT monitoring, genomic frequency estimation	Sampling for approximation; sketches (Bloom, Count-Min, HyperLogLog) enable sub-linear memory; Data Cubes computed using MapReduce or Spark for multidimensional aggregates
Predictive Mining	**Classification** (Decision Trees, Random Forest, SVM, DNNs)	Fraud detection, medical diagnosis, handwriting recognition, sentiment analysis	Decision Trees easily parallelized; Random Forests distributed via bootstrap samples; SVMs trained with distributed gradient descent; DNNs scaled with GPU clusters + Horovod
	Regression (Linear/Logistic, XGBoost, LightGBM)	Risk scoring, sales forecasting, bioinformatics modeling	Linear/logistic regression via distributed SGD (Spark MLlib); boosting frameworks optimized for parallel tree building and GPU acceleration
	Anomaly Detection (Isolation Forest, LOF, Autoencoders)	Fraud, cybersecurity, sensor fault detection, rare disease detection	Isolation Forest parallelizable (tree ensembles); LOF scaled with approximate nearest neighbors (LSH); autoencoder training distributed across GPUs
Advanced Paradigms	**Stream Mining** (Hoeffding Trees, CluStream, Windows)	Real-time analytics, financial trading, IoT sensor data	Incremental model updates; bounded memory with sliding/damped windows; implemented in Flink, Spark Streaming
	Graph Mining (PageRank, Louvain, Node2Vec, TransE)	Web link analysis, social network mining, knowledge graph discovery	PageRank scalable via iterative MapReduce/GraphX; Louvain community detection parallelized; embeddings trained with stochastic optimization across distributed nodes
	Deep Mining (CNNs, RNNs, Transformers, GANs/VAEs)	Computer vision, speech/NLP, genomics, drug discovery	CNNs/RNNs trained on GPU clusters; Transformers distributed via data/model parallelism; GAN/VAEs require large compute, optimized with mixed precision + multi-GPU frameworks
	Federated & Privacy-Preserving (Federated Learning, SMC, Differential Privacy)	Collaborative medical AI, finance, mobile personalization	Training decentralized, model updates aggregated centrally; SMC ensures secure aggregation; DP adds noise for privacy while preserving utility
Frameworks & Tools	Hadoop (MapReduce), Spark (MLlib), Flink/Storm, GraphX/Neo4j, TensorFlow/PyTorch/Horovod	Generic large-scale mining, batch/stream processing, graph analytics, deep learning	Hadoop for batch jobs; Spark for in-memory iterative ML; Flink/Storm for real-time streams; GraphX/Neo4j for graph mining; GPU frameworks for deep learning and distributed training

Table 1.5 Comparative Overview of Big Data Mining Techniques

In the following section, we focus on a selection of the most widely used and well-established algorithms in Big Data mining, along with the fundamental strategies that enable their parallelization and distribution. This discussion highlights both the methodological foundations and practical techniques that make these approaches scalable and effective in large-scale environments.

4.1 Architectural Models of Parallelization for Scalable Knowledge Discovery

Before detailing the specific algorithms used in Big Data mining, it is essential to first outline the architectural models and types of parallelization that make such algorithms scalable. Understanding these paradigms provides a foundation for analyzing how different methods can be distributed across computing infrastructures. Data and model parallelism represent the two dominant approaches, each with its own advantages, limitations, and technical constraints. Presenting these models in advance clarifies the computational strategies that enable the effective application of mining techniques in large-scale environments.

4.1.1 Data Parallel

Data parallelism is the most common form of parallelism because of its ease of implementation. In data parallel training, the dataset is split into several shards, each of which is assigned to a specific device, a process analogous to parallelizing the training procedure along the batch dimension (Fig 1.6). Each device holds a full copy of the model replica and is trained on the allocated dataset shard. After back-propagation, the gradients of the model are all reduced so that the model parameters on different devices can remain synchronized.

4.1.2 Model Parallelism

Model Parallelism (often called Task Parallelism or Functional Decomposition) is a strategy where the algorithm, program, or model itself is partitioned across multiple computing units (Fig 1.6). Each unit is responsible for a specific subtask or section of the overall problem. A single piece of data must often pass through several different nodes, each performing a different operation to produce a final result.

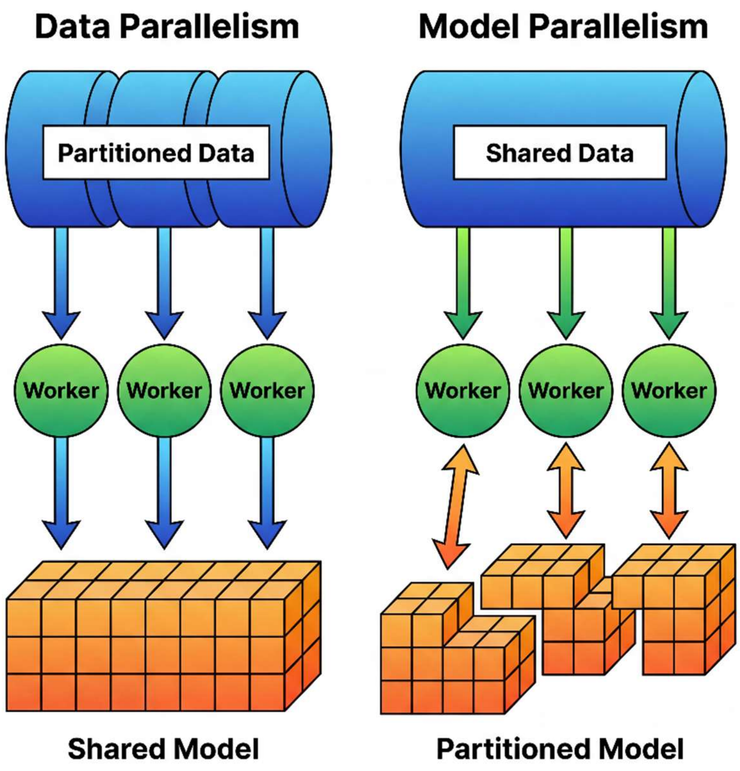

Figure 1.6 Architectural Models of Parallelization

4.1.3 Hybrid Parallelization

Recent advances in distributed training increasingly rely on hybrid parallelism, which combines data and model parallelism to balance memory usage with computational efficiency. For instance, the training of large-scale deep learning transformer architectures typically partitions the model across devices (model parallelism) while simultaneously distributing data batches across nodes (data parallelism) [51]. Emerging frameworks, such as Optimal Sharded Data Parallel (OSDP), introduce automated strategies that shard models into partitions, optimizing the trade-off between communication overhead and memory constraints [52]. Similarly, automatic graph-partitioning systems, such as RaNNC, dynamically split oversized models to fit device memory while balancing pipeline stages, thus reducing idle time and improving throughput [53]. These hybrid and automated approaches illustrate how parallelization continues to evolve to support the ever-growing model sizes and data volumes in Big Data mining and deep learning.

4.1.4 Comparative Analysis of Data and Model Parallelism

To clarify the fundamental differences between parallelization strategies, Table 1.6 contrasts data and model parallelism in terms of their core principles, technical constraints, and scalability features. This comparison provides a foundation for understanding how each paradigm supports distributed learning and Big Data mining, and why hybrid approaches are increasingly adopted in large-scale environments.

Constraint	Data Parallelism	Model Parallelism
Memory Usage	Needs memory for full model replica on each device; plus, optimizers & activations. Can become limiting for large models.	Distributes parameter storage across devices; each device holds only a part, so lower memory per device. But intermediate activations must be transferred, which uses memory and bandwidth.
Computation & Utilization	Devices process data in parallel; good utilization when batch sizes are sufficient. However, large batch sizes can affect convergence/generalization.	Potential under-utilization if pipeline stages or splits are imbalanced or some devices idle waiting for data/activations.
Communication Overhead	High—synchronization (gradients, parameters) among replicas each iteration. Latency & bandwidth become bottlenecks at scale. (Seide et al.; Efficient and Robust Parallel DNN Training)	Also present—inter-device transfers of activations and gradients across model partitions. Pipeline parallelism suffers from "pipeline bubble" delays and weight staleness.
Complexity of Implementation	Relatively simple—many frameworks support data parallelism (e.g., distributed data loaders, All-Reduce).	More complex—requires splitting model architecture, managing dependencies, pipelines, balancing loads, handling splitting of layers. Maintaining correctness (especially during forward/backward passes) is harder.
Scalability	Scales well with many devices, provided communication is efficient and batch sizes are tuned. But diminishing returns when communication dominates.	Allows training ultra-large models that data parallelism cannot handle due to memory constraints. But scalability is limited by dependencies in model structure, communication latency of activations, and potential load imbalance.

Table 1.6 Analysis of Data and Model Parallelism

4.1.5 Frameworks for Distributed Machine Learning

Distributed machine learning (DML) frameworks facilitate the training of machine learning models across multiple machines using CPUs, GPUs, or TPUs. These technologies significantly reduce the training time while effectively managing large and complex workloads that would otherwise exceed the memory capacity. Furthermore, they enable dataset processing, model tuning, and model deployment using distributed computing resources. Table 1.7 summarizes the main characteristics of widely used distributed frameworks.

Feature	PyTorch Distributed	TensorFlow Distributed	Ray	Apache Spark	Dask
Best For	Deep learning workloads	Cloud deep learning workloads	ML pipelines	Big data + ML workflows	Python-native ML workflows
Ease of Use	Moderate	High	Moderate	Moderate	High
ML Libraries	Built-in DDP, TorchElastic	tf.distribute.Strategy	Ray Train, Ray Serve	MLlib	Integrates with Scikit-learn
Integration	Python ecosystem	TensorFlow ecosystem	Python ecosystem	Big data ecosystems	Python ecosystem
Scalability	High	Very High	High	Very High	Moderate to High

Table 1.7 Main Distributed ML Frameworks

4.2 Descriptive Mining Techniques

Descriptive mining techniques aim to characterize the general properties, trends, and patterns of datasets rather than to predict future values. In the KDD process, these methods form the basis for knowledge discovery by summarizing large datasets into human-interpretable formats.

4.2.1 Clustering

Clustering is the process of grouping similar data points together in order to discover natural partitions within a dataset.

- **Scalable k-Means:** The standard k-means algorithm (minimizing within-cluster variance) is adapted for Big Data via parallelization. For example, k-Means (also known as scalable seeding) improves initialization by selecting seed points in a way that reduces the number of data passes required, making it suitable for large-scale datasets [54].

***Input*:** Dataset D (P partitions), clusters K, max_iterations, threshold

Main Algorithm

```
1. Initialize K random centroids
2. For each iteration:
  a. MAP: Assign points to nearest centroids (parallel)
  b. REDUCE: Aggregate sums and counts from all partitions
  c. Update centroids = sums / counts
  d. If centroid_shift < threshold: STOP
3. Return final centroids and assignments
```

Partition Processing

```
AssignPoints(partition, centroids):
  For each point in partition:
    - Find nearest centroid
    - Update local sums and counts
  Return {sums, counts, assignments}
```

- **Distributed DBSCAN:** Because DBSCAN's "neighborhood expansion" is not trivially parallelizable, Big Data implementations partition the space, run DBSCAN locally, and then merge clusters that span partition boundaries. These methods are used in spatial and GIS datasets to maintain clustering quality [55].

Input: ***Dataset D, radius ε, min_points threshold***

Main Algorithm

```
1. Spatial partitioning with ε-overlap
2. MAP: Local DBSCAN on each partition
3. REDUCE: Merge border clusters across partitions
4. Return global cluster assignments
```

Local DBSCAN

```
LocalDBSCAN(partition, ε, min_pts):
  For each unvisited point p:
    neighbors ← RangeQuery(p, ε)
    If |neighbors| ≥ min_pts:
      Create cluster, expand recursively
    Else: Mark as noise
  Return local clusters + border points
```

Border Merge

```
MergeBorderClusters(local_clusters, ε, min_pts):
  For each border point pair across partitions:
    If distance(p1, p2) ≤ ε:
      Union clusters containing p1 and p2
  Return merged global clusters
```

4.2.2 Association Rule Mining (ARM)

Association rule mining discovers frequent co-occurrences among items in transactional or categorical datasets.

- **FP-Growth in distributed:** Spark's implementation of FP-Growth (parallel frequent pattern growth) avoids candidate explosion by building compact FP-trees locally in each partition and then aggregating them globally. This is more efficient than the classic Apriori in large-scale settings. (Spark MLlib documentation). Recent studies have proposed optimizations for FP-Growth for very large datasets, such as improved memory usage or better partitioning strategies [56].

***Input**: Transaction database, min_support*

```
1. Build global frequent item list (sorted by frequency)
2. MAP: Construct local FP-trees per partition
3. For each frequent item (reverse order):
   a. Gather conditional pattern bases
   b. Build conditional FP-tree
   c. Recursively mine sub-patterns
4. Return frequent patterns
```

- **Distributed Apriori:** Although more expensive, some implementations parallelize candidate generation and support counting across nodes, often as baseline comparisons or in cases when datasets are not extremely large.

Input: *Transaction database T, min_support threshold*

1. Find frequent 1-itemsets L_1
2. For k = 1 to |max_itemset|:
   a. Generate candidates C_{k+1} from L_k
   b. MAP: Count candidate support locally
   c. REDUCE: Aggregate global counts
   d. Filter: L_{k+1} = {itemsets ≥ min_support}
3. Return all frequent itemsets

4.2.3 Summarization and Characterization

Summarization and characterization techniques aim to reduce the complexity of massive datasets while preserving their essential properties and their interpretability. In the context of Big Data, they provide compact yet informative representations that allow analysts and decision-makers to gain a high-level understanding of data distributions, patterns, and relationships without processing the full raw dataset.

- **Data Cubes and OLAP:** Multidimensional aggregation structures that allow exploration across different perspectives, such as sales by product, time, or location. Distributed OLAP engines precompute cube fragments using MapReduce or Spark for interactive performance.
- **Sketching data structures:** Bloom filters for membership queries; count-min sketch for approximate frequency estimation in streams; HyperLogLog for approximate distinct counts. These structures allow bounded-error summaries under streaming or high-velocity constraints.

4.3 Predictive Mining

Predictive mining uses historical data to build models that are capable of forecasting the future or unknown values of a target variable. Unlike descriptive mining, which summarizes and explores inherent data structures, predictive mining focuses on constructing models that generalize to unseen instances, enabling applications such as fraud detection, medical diagnosis, genomic prediction and handwriting recognition. In Big Data contexts, predictive mining must address issues of scalability, high dimensionality, streaming, and heterogeneity, leveraging distributed frameworks and advanced machine learning methods [57].

4.3.1 Classification

Classification serves as a quintessential embodiment of predictive data mining, operationalizing the core principles of machine learning to transform historical data into actionable foresight. As a supervised machine learning task, its objective is to infer a function from labeled training data that can map new, unseen instances to predefined categories. This process is at the heart of predictive modeling, where the patterns and correlations discovered within vast datasets are not merely descriptive but are used to forecast future outcomes. Thus, classification acts as a critical nexus: it is the application of machine learning's algorithmic framework to achieve the predictive goals of data mining, transforming raw data into a powerful tool for informed decision-making and automated intelligence.

- **Decision Trees:** Decision trees recursively partition the feature space based on feature values to create a hierarchical decision structure.
  - **ID3 (Iterative Dichotomiser 3)**: Uses information gain as the splitting criterion:

$$\boldsymbol{Information\ Gain(S, A) = H(S) - \sum_{v \in Values\ (A)} \frac{|S_v|}{|S|}\ H(S_v)}, \qquad \mathbf{1.7}$$

Where $\boldsymbol{H(S) = -\sum_{i=1}^{c} p_i\, log_2(p_i)}$, is the entropy of set *S*, and p_i is the proportion of examples belonging to class *i*.

  - **C4.5**: Extends ID3 by using gain ratio to handle bias toward attributes with more values:

$$\boldsymbol{Gain\ Ratio(S, A) = \frac{Information\ Gain(S,A)}{Split\ Information\ (S,A)}}, \qquad \mathbf{1.8}$$

where $\boldsymbol{Split\ Information\ (S, A) = -\sum_{i=1}^{v} \frac{|S_i|}{|S|} log_2 \frac{|S_i|}{|S|}}$, **1.9**

  - **CART (Classification and Regression Trees)**: Uses Gini impurity for splitting:

$$\text{Gini}(\boldsymbol{S}) = \boldsymbol{1 - \sum_{i=1}^{c} p_i^2}, \qquad \mathbf{1.10}$$

In distributed settings, the bottleneck is computing split candidates (e.g., sorting features), which is addressed by sampling, binning, and parallel statistics aggregation. Spark MLlib's implementation uses CART for both classification and regression, supporting Gini/entropy criteria, while custom C4.5 adaptations (e.g., PD-C4.5) employ microservices for cloud scalability.

- **Random Forests:** Random Forests ensemble B bootstrapped trees with random feature subsets (m = √d for classification), aggregated via majority vote or averaging. Robust to overfitting and scalable via independent tree training.
- **Scalable Implementation**:
  - **Spark MLlib**: Builds on DecisionTree; partitions data by rows and trains trees in parallel. Subsampling reduces communication (e.g., broadcasting only m features/nodes). Supports binary/multiclass classification and regression tasks.

Input*: D partitioned, B trees, m = √D, impurity*

Output*: Forest {T_b}*

```
1. For b=1 to B (task-parallel across nodes):
   . Bootstrap: Sample |D| rows with replacement (local per partition)
   . Train Tb: As in distributed CART, but at each node: Random m features
   . Aggregate stats with reduced communication (only m/d fraction)
2. For prediction x: ŷ = mode/mean {Tb(x) for b=1 to B} (parallel eval)
```

```
3. Feature importance: Mean Δimpurity over trees
```

➢ **Enhancements**: Unified batch/streaming in Spark 4.0; Ray integration for hyperparameter tuning.

4.3.2 Regression

Regression is a fundamental supervised learning technique used to predict continuous target variables based on one or more input features. It models the relationship between inputs and outputs, enabling forecasting, trend analysis, and understanding how dependent variables change with variations in independent variables.

- **Linear and Logistic Regression**

These models are widely regarded as baselines for predictive tasks because of their interpretability and efficiency. In Big Data contexts, their scalability relies on distributed optimization methods. Stochastic Gradient Descent (SGD) is commonly parallelized by splitting the training data across worker nodes, each computing partial gradients that are then aggregated at a master node. Mini-batch SGD further improves convergence and reduces the communication overhead. Another approach is the Limited-memory Broyden–Fletcher–Goldfarb–Shanno (L-BFGS) method, a quasi-Newton optimization technique implemented in Spark MLlib, which computes gradient and Hessian approximations in a distributed manner. Parameter updates are coordinated across nodes using synchronous or asynchronous strategies, the latter of which reduces bottlenecks in large clusters [6].

- **Distributed Stochastic Gradient Descent (SGD)**

Input: *Training data D (partitioned), learning rate α, epochs E*

```
1. Initialize weights w randomly across all nodes
2. For epoch = 1 to E:
  a. MAP: Compute local gradients on each partition
    ∇w_local = (1/|partition|) Σ ∇L(w, xi, yi)
  b. REDUCE: Aggregate gradients
    ∇w_global = (1/P) Σ ∇w_local
  c. Update weights: w = w - α * ∇w_global
3. Return final weights w
```

- **Mini-Batch Distributed SGD**

Input: Data D, batch_size B, learning rate α

```
1. Initialize weights w
2. While not converged:
  a. MAP: Sample mini-batches locally
  b. Compute batch gradients in parallel
  c. REDUCE: Average gradients across nodes
  d. Update: w = w - α * avg_gradient
```

3. Return w

- **Distributed L-BFGS**

***Input**: Data D, memory size m, tolerance ε*

1. Initialize w_0, set k = 0
2. While $||\nabla f(w_k)|| > \varepsilon$:
   a. MAP: Compute gradients and function values
   b. REDUCE: Aggregate to get global $\nabla f(w_k)$
   c. Compute search direction using L-BFGS approximation:
      $p_k = -H_k * \nabla f(w_k)$
   d. Line search: find optimal step size α_k
   e. Update: $w_{k+1} = w_k + \alpha_k * p_k$
   f. Update L-BFGS memory vectors
3. Return optimal weights

- **Gradient Boosting Machines (GBM, XGBoost, and LightGBM)**

Gradient boosting sequentially builds ensembles of decision trees, where each tree corrects the residual errors of its predecessors. Although powerful, the sequential nature of these methods traditionally limits their scalability. Modern implementations, such as XGBoost [23] and LightGBM [10], introduce parallelism at multiple levels.

- **Parallel Tree Construction:** Features or data partitions are distributed across nodes, where local histograms of feature splits are computed and aggregated to find the best split.
- **Column Block Compression:** XGBoost stores data in a compressed columnar format, allowing efficient parallel access.
- **Histogram-based Methods:** LightGBM accelerates split finding by discretizing continuous features into bins, reducing complexity and enabling fast parallel computation.
- **GPU Acceleration:** Both XGBoost and LightGBM leverage GPUs to parallelize histogram building, gradient calculations, and split evaluation, drastically reducing the training time on large datasets.
- **Distributed Training:** In cluster environments, boosting frameworks partition the training data across nodes. Each node computes local gradient statistics, which are then reduced (using all-reduce operations) to synchronously update the global models.

5. Deep Learning

Deep learning has emerged as one of the most transformative approaches in Big Data analytics, enabling the extraction of complex hierarchical representations from massive heterogeneous datasets. Unlike traditional machine learning methods, which rely heavily on handcrafted features, deep learning models learn directly from raw data, making them particularly effective in domains such as genomics, medical imaging, natural language processing, and large-scale sensor networks. This ability to uncover hidden structures and nonlinear relationships has made deep learning a cornerstone of modern knowledge discovery, supporting predictive modeling, pattern recognition, and automated decision-making across diverse sectors.

5.1 Main Deep Learning Architectures for Computer Vision and Genomics

In computer vision, DL models process multimodal inputs, such as RGB images or satellite data, whereas in genomics, they handle DNA sequences, read pileups, or epigenetic profiles. This section details the primary architectures, Convolutional Neural Networks (CNNs), and Vision Transformer (ViT), focusing on their design, distributed scalability, and applications in these domains.

5.1.1 Convolutional Neural Networks

CNNs are specialized for extracting spatial hierarchies of features, making them foundational for computer vision tasks and increasingly important in biomedical imaging, remote sensing, and genomic sequence analysis. Their ability to capture local patterns and progressively combine them into higher-level abstractions aligns well with the structures of visual and spatial Big Data.

A CNN is composed of three main types of layers: convolutional layers, pooling layers, and fully connected layers (Fig 1.7). Convolutional layers apply filters (kernels) that slide over the input to extract local patterns such as edges, textures, or shapes. Pooling layers reduce spatial resolution while retaining important features, and fully connected layers map the high level features into outputs such as class probabilities.

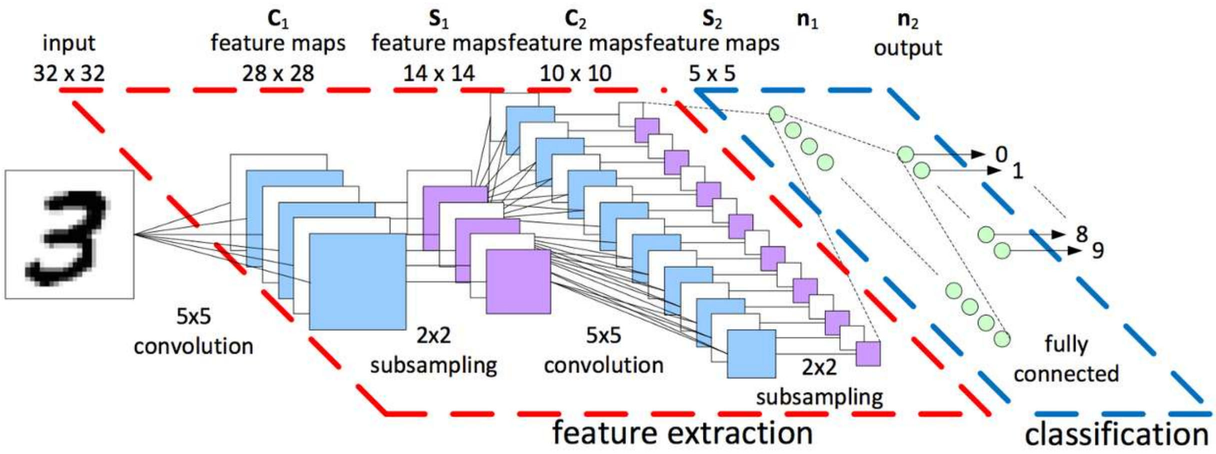

Figure 1.7 CNN Model for Handwriting Digits Recognition

- **CNN-Derived Advanced Architectures**

Convolutional Neural Networks (CNNs) have emerged as foundational architectures in contemporary deep learning, exhibiting exceptional performance across a diverse array of domains. Originally introduced for large-scale image recognition tasks, CNNs revolutionized computer vision by achieving state-of-the-art accuracy on benchmarks such as ImageNet [58]. Their ability to automatically learn hierarchical feature representations, from low-level edges to high-level semantic structures, has enabled breakthroughs in object detection, segmentation, and video analysis [59]. Beyond vision, CNN variants have been successfully adapted to genomics for motif discovery and sequence classification [60], medical imaging for disease diagnosis and tumor segmentation [61], and natural language processing for text classification and sentiment analysis [62]. The scalability of CNNs on distributed GPU and TPU infrastructures further consolidates their role as a cornerstone in deep learning research, paving the way for specialized architectures such as ResNet, U-Net, and EfficientNet. As a result, CNNs have not only transformed pattern recognition but also become a foundational paradigm upon which many advanced architectures and interdisciplinary applications have been built. To provide a structured synthesis of these contributions, Table 1.8 presents a comparative overview of major CNN-derived models, detailing their key use cases, scalability characteristics, and domain-specific relevance.

Architecture	Description	Main Use Cases	Scalability & Parallelization
AlexNet	First deep CNN with ReLU activations, dropout, and GPU training.	Image classification (ImageNet), early CV tasks.	Scales moderately; trained on single GPU; now feasible on distributed multi-GPU systems.
VGGNet	Deep architecture with stacked 3×3 filters.	Image classification, transfer learning in medical imaging.	Memory-heavy due to depth; scales well with model/data parallelism but costly in communication.
GoogLeNet (Inception)	Uses inception modules with multi-scale filters.	Image recognition, mobile vision applications.	Lightweight, efficient; parallelizable with less memory demand; suited for large datasets.
ResNet	Introduces residual connections to avoid vanishing gradients.	CV, medical imaging, genomics, NLP (via CNN backbones).	Highly scalable with distributed SGD; efficient on multi-GPU/TPU clusters.
DenseNet	Dense connections reuse features across layers.	Medical imaging, fine-grained classification.	Communication cost grows with depth; scales with memory optimizations and checkpointing.
MobileNet	Lightweight CNN with depthwise separable convolutions.	Edge computing, mobile vision tasks, IoT.	Scales on edge clusters and GPUs; optimized for low-power, distributed inference.
EfficientNet	Uses compound scaling (depth, width, resolution).	General-purpose image recognition, biomedical imaging.	Achieves SOTA accuracy with fewer resources; scales efficiently with distributed GPUs.
Xception	Extreme Inception with depthwise separable convolutions.	Video classification, object detection.	Efficient for distributed training due to reduced parameters; widely used in transfer learning.
U-Net	CNN encoder-decoder for semantic segmentation.	Medical image segmentation, satellite imaging, rainfall mapping.	Scales via data parallelism; extended to 3D U-Net for volumetric data on GPU clusters.
Mask R-CNN	Extension of Faster R-CNN with segmentation mask branch.	Object detection + instance segmentation.	Requires GPU clusters for real-time inference; parallelizes across regions of interest.
YOLO (You Only Look Once)	Real-time object detection with single-shot CNN.	Autonomous driving, surveillance, embedded vision.	Optimized for low-latency inference; scales for edge devices and GPU clusters.

Architecture	Description	Main Use Cases	Scalability & Parallelization
Faster R-CNN	Region proposal + CNN backbone for object detection.	Object detection in dense scenes (medical, video).	Computationally intensive; scales well with distributed training but requires large memory.
3D CNNs	Extension of CNN to spatiotemporal volumes.	Video analysis, genomics (3D genome structures), medical imaging.	Highly memory intensive; scales via model parallelism, requires GPU/TPU clusters.
Capsule Networks (CapsNet)	CNNs extended with capsules preserving spatial hierarchies.	Handwriting recognition, medical imaging, NLP.	Poor scalability due to routing complexity; active research on distributed implementations.
Attention-CNN Hybrids	CNN backbones integrated with self-attention or transformers.	Multimodal learning (vision+text), biomedical data fusion.	Scales better with pipeline/data parallelism; used in vision transformers (ViT).

Table 1.8 Comparative Overview of CNN-Derived Architectures

5.1.2 Vision Transformers

The Vision Transformer (ViT) represents a paradigm shift in computer vision, challenging the dominance of CNNs. Instead of relying on convolutional filters, ViTs adapt the transformer architecture, originally developed for natural language processing, for image understanding by treating an image as a sequence of patches [63] (Fig 1.8). This sequence-based approach leverages self-attention mechanisms to capture global dependencies, allowing the model to learn the relationships between distant image regions more effectively than CNNs.

- **Architectural Framework**
  - **Patch Embedding Layer:** The initial transformation of visual data in ViTs involves a systematic decomposition of input images into semantically meaningful units. Given an input image

    $\boldsymbol{I} \in R^{H \times W \times C}$ where H, W, and C denote height, width, and channel dimensions respectively, the patch embedding process proceeds as follows:

    The image is partitioned into $\boldsymbol{N} = \frac{HW}{P^2}$ **,** non-overlapping patches of fixed dimensions $P \times P$ where P typically assumes values such as 16 or 32 pixels. Each patch $x_i \in R^{P^2 . C}$ is flattened into a one-dimensional vector and subsequently projected through a learnable linear transformation:

$$\boldsymbol{z_i^{(0)}} = W_e x_i + b_e, \qquad \textbf{1.11}$$

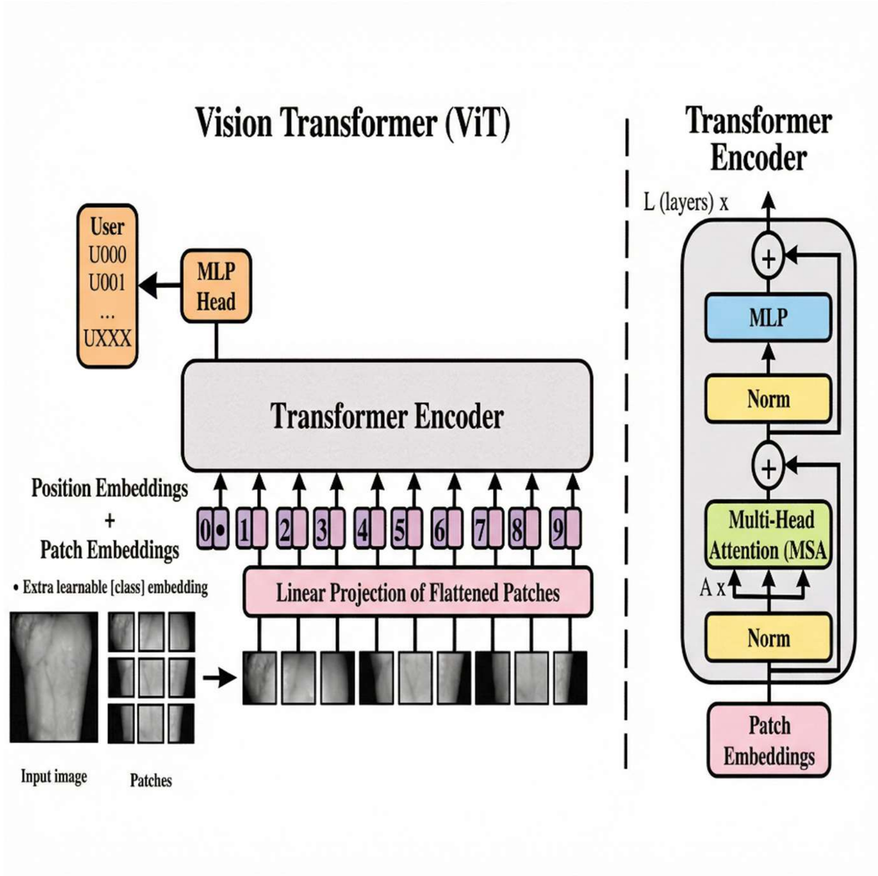

Figure 1.8 Vision Transformers Architecture [63]

where $\boldsymbol{W_e} \in R^{D \times (P^2.C)}$ represents the embedding matrix and $\boldsymbol{b_e} \in R^D$, denotes the bias term, with D representing the latent embedding dimension. This process yields a sequence of patch embeddings $\{z_1^{(0)}, z_2^{(0)}, \dots . z_{iN}^{(0)}\}$, analogous to word tokens in natural language processing applications. A distinctive feature of ViT architecture is the incorporation of a learnable ***class token*** $z_{cls}^{(0)}$, which is prepended to the sequence and serves as an aggregate representation for downstream classification tasks

➢ **Positional Encoding Mechanisms:** The absence of inherent spatial inductive biases in transformer architectures necessitates explicit positional information to preserve spatial relationships within the visual input. ViTs employ positional encodings $E_{pos} \in R^{(N+1) \times D}$, that are element-wise added to the patch embeddings:

$$\boldsymbol{z}^{(0)} = \left[z_{cls}^{(0)}, z_1^{(0)}, z_2^{(0)}, \dots . . z_N^{(0)}\right] + Epos, \qquad \textbf{1.12}$$

Two primary approaches for positional encoding have been investigated:

- ***Learnable positional embeddings***: Parameters learned during training that adapt to the specific spatial patterns of the dataset.

- ***Fixed sinusoidal encodings:*** Deterministic functions that encode positional information through trigonometric patterns

Empirical studies suggest that learnable positional embeddings generally yield superior performance in image classification tasks because they can adapt to the statistical regularities of visual data.

➢ **Transformer Encoder Architecture:** The core computational framework of ViTs consists of *L* identical transformer encoder blocks, each implementing a standardized attention-feedforward structure with pre-layer normalization. The ℓ th encoder block processes input $z^{(\ell-1)}$ through the following sequential operations:

- **Multi-Head Self-Attention (MHSA):** The self-attention mechanism constitutes the fundamental computational primitive for modeling inter-patch relationships. Given input embeddings, three projection matrices generate queries, keys, and values:

$$\boldsymbol{Q} = z^{(\ell-1)}W_Q \text{ , } \boldsymbol{K} = z^{(\ell-1)}W_k \text{ , } \boldsymbol{V}\, z^{(\ell-1)}W_V \text{ ,} \qquad \textbf{1.13}$$

The attention mechanism computes pairwise affinities between all token pairs:

$$\boldsymbol{Attention}(\boldsymbol{Q},\boldsymbol{K},\boldsymbol{V}) = \text{softmax}\left(\frac{QK^T}{\sqrt{d_k}}\right)\text{V} \text{ ,} \qquad \textbf{1.14}$$

where $d_k = \frac{D}{h}$ represents the dimension of each attention head, and h denotes the number of attention heads. Multi-head attention enables parallel computation of diverse attention patterns:

$$\boldsymbol{MHSA}(\boldsymbol{z}) = Concat(head_1, \dots, headh_h)W_O \text{ ,} \qquad \textbf{1.15}$$

where each head captures distinct aspects of inter-token relationships, ranging from local spatial correlations to global semantic dependencies.

- **Feed-Forward Network:** The position-wise feed-forward network applies identical transformations to each token independently:

$$\boldsymbol{FFN}(\boldsymbol{x}) = GELU(xW_1 + b_1)W_2 + b_2 \text{ ,} \qquad \textbf{1.16}$$

The hidden dimension is typically expanded by a factor of four (i.e., 4D) to provide sufficient representational capacity, followed by projection back to the original dimension *D*.

- **Normalization and Residual Connections:** Layer normalization and residual connections ensure stable gradient flow and facilitate deep network training:

$$z'^{(\ell)} = \text{MHSA}(\text{LN}(z^{(\ell-1)})) + \text{z}^{(\ell-1)} \text{ ,} \qquad \textbf{1.17}$$

$$z^{(\ell)} = FFN(LN(z'^{(\ell)})) + z'^{(\ell)} \text{ ,} \qquad \textbf{1.18}$$

➢ **Classification Head:** Upon completion of the encoder stack, the class token $z_{cls}^{(L)}$ encapsulates the global image representation. A linear classification head maps this representation to class probabilities:

$$p(y|I) = \mathrm{softmax}(\, z_{cls}^{(L)} W_{cls} + b_{cls}) \ , \qquad \mathbf{1.19}$$

- **Training Methodologies and Optimization Strategies**

➢ **Large-Scale Pretraining Paradigm:** The empirical success of ViTs is fundamentally contingent on access to large-scale training datasets. Unlike CNNs, which benefit from strong spatial inductive biases, ViTs require extensive data exposure to learn effective visual representation. Typical pretraining regimes employ datasets containing millions to hundreds of millions of images.

- **ImageNet-21k**: 14 million images across 21,000 categories.
- **JFT-300M**: 300 million images with noisy labels.
- **JFT-3B**: 3 billion images representing the current scale frontier.

The pretraining objective typically employs cross-entropy loss over the categorical distribution, with subsequent fine-tuning on downstream tasks using smaller learning rates and specialized augmentation strategies.

➢ **Knowledge Distillation Framework:** Data-Efficient Image Transformers (DeiT), introduced by [64], address the data-hungry nature of ViTs through a sophisticated teacher-student distillation framework. This approach enables effective training on moderately sized datasets, such as ImageNet-1K, through the following mechanisms:

- **Teacher-Student Architecture:** A pre-trained convolutional network (typically RegNetY-16GF or similar high-capacity models) serves as the teacher, providing soft supervision signals to guide the learning process of the ViT student. The student architecture incorporates an additional distillation token, alongside the class token, enabling dual supervision modes.

- **Composite Loss Function:** The training objective combines multiple loss components as follows:

$$L_{total} = \alpha L_{CE}(y, \hat{y}_{cls}) + \beta L_{KL}(\sigma(z_{teacher}/\tau), \sigma(z_{distill}/\tau)) + \gamma L_{CE}(y, \hat{y}_{distill}) \ , \qquad \mathbf{1.20}$$

where L_{CE} represents cross-entropy loss, L_{KL} denotes Kullback-Leibler divergence, τ is the temperature parameter for knowledge distillation, and α , β, γ are weighting coefficients.

➢ **Regularization and Data Augmentation**

Given the reduced inductive bias compared to CNNs, ViTs benefit significantly from aggressive regularization strategies.

- **Stochastic Depth:** Random layer dropping during training to prevent overfitting and improve generalization.
- **Label Smoothing:** Soft label distributions to reduce overconfidence in predictions.
- **Mixup and CutMix:** Sample mixing strategies that create synthetic training examples.
- **RandAugment:** Automated augmentation policy search for optimal data augmentation.
- **Dropout and DropPath:** Stochastic regularization within attention and feed-forward components

- **Attention Mechanisms and Model Interpretability**

➢ **Attention Pattern Analysis:** A distinctive advantage of ViT architectures lies in the interpretability of learned attention patterns. Self-attention weights $A \in R^{(N+1)\times(N+1)}$ provide direct insight into spatial relationships captured by the model. Attention maps revealed several noteworthy patterns.

- **Early layers:** Tend to focus on local spatial neighborhoods, resembling convolutional receptive fields.
- **Middle layers:** Capture intermediate-scale object parts and semantic regions.
- **Deep layers:** Exhibit global attention patterns that span entire objects and contextual relationships.

➢ **Visualization and Explainability:** The attention rollout and attention flow techniques enable the visualization of information propagation through the transformer stack. These methods aggregate attention weights across layers to trace the flow of information from the input patches to the final classification decision. Such visualizations demonstrate that ViTs can:

- Identify semantically relevant image regions without explicit supervision.
- Capture long-range spatial dependencies that may be challenging for CNNs.
- Adapt attention patterns based on task-specific requirements during fine-tuning.

- **ViT Derived Advanced Architectures**

The emergence of the ViTs has catalyzed the development of a wide array of advanced architectures that extend its core principles to address the limitations of scalability, locality, and efficiency across diverse application domains. Models such as DeiT leverage teacher–student distillation to achieve competitive results on limited data [64], while hierarchical variants like the Swin Transformer introduce shifted windows to balance local and global feature extraction, enabling success in detection and segmentation tasks [65]. Other extensions, including CrossViT and CvT, combine multi-scale embeddings and convolutional priors to enhance robustness, whereas hybrid approaches such as CoAtNet bridge the strengths of CNN and transformer for improved generalization [66]. At extreme scales, giant models such as ViT-G/ViT-H serve as foundation architectures trained on billions of parameters, paving the way for zero-shot transfer and multimodal integration [67]. These developments highlight how transformers have evolved into a flexible paradigm adapted to computer vision, medical imaging, video analysis, and other fields. To synthesize this diversity, Table 1.9 provides a comparative overview of transformer-based vision architectures, detailing their design characteristics, use cases and scalability considerations.

Architecture	Description	Main Use Cases	Scalability & Parallelization
ViT (Vision Transformer)	First transformer-based vision model; splits images into fixed-size patches and applies self-attention.	Image classification on large datasets (ImageNet-21k, JFT-300M).	Requires massive data; scales efficiently on TPU/GPU clusters with data parallelism.
DeiT (Data-Efficient Image Transformer)	Introduces knowledge distillation from CNN teachers + heavy augmentation to train ViTs on smaller datasets.	Image classification with limited data.	Efficient training with reduced data; scales well with distillation and augmentation.
Swin Transformer	Hierarchical vision transformer with shifted windows for local-global attention.	Detection, segmentation, dense prediction tasks.	Scales linearly with image size; widely adopted in large-scale CV tasks.
CrossViT	Employs multi-scale patch embeddings and cross-attention between them.	Image recognition, fine-grained classification.	Captures both local and global dependencies; parallelizes across scales.
CvT (Convolutional Vision Transformer)	Combines CNN convolutions for embeddings with transformer layers.	General vision tasks, efficient recognition.	Benefits from CNN inductive biases; scales with hybrid pipelines.
CoAtNet	Hybrid CNN + Transformer backbone designed to leverage both local and global features.	Large-scale classification, multimodal tasks.	Highly scalable across data sizes; strong generalization in distributed setups.
ViT-G/ViT-H (Giant/Huge)	Large-scale ViTs trained with billions of parameters on huge datasets.	Zero-shot learning, multimodal transfer, foundation models.	Requires extreme parallelism (model + data + pipeline); trained on thousands of TPUs.
Video Swin / TimeSformer	Extends ViTs to spatiotemporal sequences for video understanding.	Action recognition, video classification.	Scales via spatiotemporal parallelism; demands high GPU memory.
Medical ViTs	Domain-adapted ViTs (e.g., TransUNet, Swin-Unet) for segmentation and diagnosis.	Tumor segmentation, histopathology, radiology.	Scales via patch-wise decomposition of high-resolution images; often combined with CNN encoders.

Table 1.9 Comparative Overview of Vision Transformer-Derived Architectures

5.2 Scalability Challenges and Distributed Training Strategies for CNNs and ViTs

5.2.1 CNN

CNNs are highly computationally intensive, and their scalability relies heavily on parallel and distributed training strategies. Scaling CNN training across multi-GPU and multi-node clusters enables the efficient processing of massive image datasets such as ImageNet or domain-specific corpora like high-dimensional genomic sequences and medical images that would be infeasible to process on a single machine [58].

- **CNN Data Parallelism:** In data-parallel training, the dataset is partitioned into mini-batches and distributed across worker nodes, each of which hosts a full replica of the CNN (Fig 1.9). Local gradient computations are synchronized using collective operations such as AllReduce, which are implemented in frameworks such as Horovod [68].

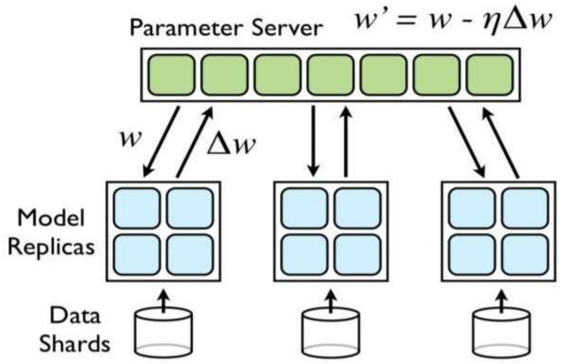

Figure 1.9 Data Parallelism in CNN [68]

Assume that we have a mini-batch of 64 images and four GPUs. In Data Parallelism:

1. The **same identical model** is copied to all four GPUs.
2. A batch of 64 images is split into four **sub-batches** of 16 images (often called *local batches*).
3. Each GPU processes its sub-batch (16 images) independently and concurrently.
   - A **forward pass** is performed to calculate the loss.
   - It performs a **backward pass** to calculate the gradients for the local model.

The Synchronization Step: The crucial part is that after each GPU calculates its own gradients, these gradients must be combined to update the model correctly. This is performed via an all-reduce operation.

- **Gather Gradients:** Gradients from all GPUs are gathered and averaged.
- **Update Models:** The average gradients are then sent back to all GPUs.
- **Synchronized Update:** Every GPU updates its model weights identically using the averaged gradients.

This approach is highly efficient for training small-to-medium-sized models that can fit on a single GPU, as it perfectly parallelizes the computation across devices, often making it the fastest method available. Furthermore, by distributing the data, the batch size is effectively multiplied by the number of GPUs used (local_batch_size * num_gpus), which can, in some cases, aid generalization and lead to faster convergence during training.

However, data parallelism has significant limitations. Its primary drawback is memory inefficiency, as a complete replica of the entire model along with its optimizer states must reside in each individual GPU's memory; consequently, this method offers no solution for training models whose size exceeds the capacity of a single GPU. Compounding this issue is the communication overhead, where the essential all-reduce operation, used to synchronize gradients across all devices can become a severe performance bottleneck, particularly when scaling to a large number of GPUs or when using slower interconnects between them.

- **CNN Model Parallelism (Tensor Parallelism):** Model parallelism distributes layers or filters across the GPUs (Fig 1.10). Parameter servers or pipeline-parallel strategies coordinate the updates between devices.

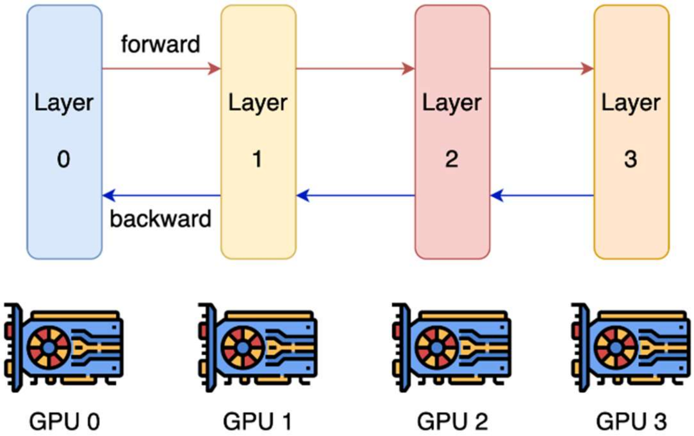

Figure 1.10 Model Parallelism in CNN

Optimization: To mitigate communication bottlenecks, asynchronous stochastic gradient descent (SGD), gradient clipping, and mixed-precision training are commonly employed. Benchmarks show 10–20× speedup for CNNs, such as ResNet, when distributed across 64-GPU clusters using optimized communication strategies [69]. Gradient checkpointing further reduces the memory overhead by re-computing intermediate activations during backpropagation instead of storing them.

The principal advantage of model parallelism is its ability to enable the training of extremely large models by distributing distinct parts of the architecture across multiple GPUs, thus overcoming the memory limitations of any device. Furthermore, when implemented intelligently, such as using Tensor Parallelism within a server equipped with high-speed interconnects, such as NVLink, it can manage communication efficiently. However, these benefits come with significant tradeoffs. In its naive form, model parallelism suffers from critically low GPU utilization, as only one GPU is active at any given time, whereas the others remain idle, leading to poor performance. Moreover, the technique is complex to implement, requiring a deep understanding of the model architecture to manually partition it in a way that balances the computational load across devices.

- **CNN Pipeline Parallelism:** Is essentially a smart version of model parallelism designed to solve the GPU idling problem. The model is split sequentially into "stages" (groups of layers) across the GPUs. Then, a mini-batch is split into smaller "micro-batches" and fed into the pipeline in an overlapping manner. It is particularly well-suited for training extremely deep or wide neural networks that exceed the memory capacity of individual accelerators, such as large-scale transformer architectures (e.g., GPT and BERT), convolutional networks for medical imaging, and multimodal networks in genomics. By distributing different parts of the model across devices, practitioners can leverage limited GPU memory while scaling to billions of parameters. Frameworks such as GPipe, PipeDream, and DeepSpeed implement pipeline parallelism for industrial-scale model training.

5.2.2 Vision Transformers (ViTs)

ViTs present distinct computational challenges, necessitating parallelization strategies that fundamentally diverge from those employed in convolutional architectures. The quadratic complexity inherent in self-attention, characterized by a computational cost that escalates as $O(n^2)$ with the sequence length, leads to substantial memory and processing bottlenecks during training on high-resolution images or extensive datasets [63].

- **ViTs Data Parallelism:** Data parallelism remains the most fundamental and widely adopted approach for scaling ViT training, wherein mini-batches are distributed across multiple GPUs or compute nodes. Each device independently executes forward and backward passes on its data subset, followed by gradient synchronization through collective communication primitives such as AllReduce operations [6]. This strategy enables ViTs to efficiently process massive pretraining datasets, including JFT-300M, JFT-3B, and ImageNet-21k, typically achieving 70-85% parallel efficiency on large-scale GPU clusters, which is notably lower than that of CNNs owing to attention-specific synchronization requirements [63].

  Modern optimization frameworks such as Horovod, DeepSpeed, and PyTorch Distributed mitigate communication overheads through sophisticated techniques, including gradient compression, local gradient accumulation, and computation-communication overlapping. However, the quadratic scaling of attention mechanisms creates unique challenges: as the sequence length increases from standard patches ($14\times14=196$ tokens) to high-resolution inputs ($32\times32=1024$ tokens), both memory consumption and gradient exchange costs grow substantially. This necessitates high-bandwidth interconnects (NVLink, InfiniBand, or NVSwitch) and careful batch size tuning to maintain training stability while maximizing the hardware utilization.

- **ViTs Model Parallelism (Tensor Parallelism):** When ViT architectures are scaled to extreme sizes, such as ViT-G (1.8B parameters), ViT-H (630M parameters), or emerging ViT-22B models, data parallelism alone becomes insufficient owing to GPU memory limitations. Tensor parallelism addresses this constraint by partitioning model parameters and computations across devices rather than data. In ViTs, tensor parallelism naturally aligns with the architecture through several strategies:
  - **Attention Head Parallelism:** Multi-head self-attention (MHSA) heads are distributed across devices, with each GPU computing a subset of the h attention heads independently before concatenation.
  - **Feed-Forward Layer Partitioning**: The MLP blocks within each transformer layer are split along the hidden dimension, typically partitioning the first linear transformation

  $W_1 \in R^{D \times 4D}$, column-wise and the second transformation $W_2 \in R^{4D \times D}$ row-wise.
  - **Embedding Dimension Sharding:** The model's embedding dimension D can be partitioned across devices, though this requires more sophisticated synchronization.

Advanced frameworks such as **Megatron-LM, DeepSpeed ZeRO**, and **FairScale** automate tensor sharding using optimized communication patterns. While tensor parallelism dramatically reduces per-device memory requirements, enabling models that exceed single-GPU memory capacity, it introduces significant communication overhead during attention score computation and layer output aggregation. The trade-off becomes favorable when the model size exceeds the available device memory, typically for models with >1B parameters.

- **ViTs Pipeline Parallelism:** Pipeline parallelism provides orthogonal scaling benefits by distributing transformer encoder layers across multiple devices, thereby creating a computational pipeline in which different stages process different micro-batches concurrently. Mini-batches are subdivided into smaller micro-batches that flow through the pipeline: while stage k processes micro-batch i in the forward mode, stage $k+1$ simultaneously handles micro-batch $i-1$ in the backward mode [70]. This approach offers substantial memory reduction because each device maintains only a subset of the total layers (e.g., layers 1-6 on GPU 0, layers 7-12 on GPU 1 for a 12-layer ViT). Memory savings enable the training of significantly deeper architectures or higher batch sizes within fixed hardware constraints.
  - **ViTs Hybrid parallelization:** combining pipeline and tensor parallelism represents the current state-of-the-art for training the largest ViT models, with systems such as **GPipe**, **PipeDream**, and

DeepSpeed Pipeline enabling the training of models with tens of billions of parameters across hundreds of GPUs while maintaining reasonable training efficiency (typically 60-80% of ideal throughput).

5.2.3 Comparative Scalability of CNNs and ViTs

Understanding the scalability constraints of deep learning models is essential for designing efficient, distributed training strategies. Although CNNs and ViTs share the need for parallel and distributed computation, the nature of their computational bottlenecks and optimization techniques diverges significantly. CNNs primarily face challenges related to large feature maps and convolutional operations, which are well-suited for data parallelism and spatial partitioning. In contrast, ViTs are constrained by the quadratic cost of self-attention and the high communication demands of attention weight synchronization, requiring advanced forms of tensor and pipeline parallelism. To highlight these distinctions, Table 1.10 provides a comparative analysis of the parallelization constraints in CNNs and ViTs, focusing on their computational units, scalability bottlenecks, optimization strategies, and hardware considerations.

Aspect	Convolutional Neural Networks (CNNs)	Vision Transformers (ViTs)
Main Computational Unit	Convolutions (localized kernels sliding over feature maps).	Self-Attention (global pairwise interactions between tokens).
Scalability Bottleneck	Large feature maps, memory bandwidth limitations, and gradient synchronization across devices.	Quadratic cost of self-attention $O(n^2)$ with respect to sequence length (number of patches/tokens).
Parallelization Focus	Data parallelism (batch splitting), spatial parallelism (feature map partitioning), limited model parallelism for very deep networks.	Tensor parallelism (attention heads/projections), pipeline parallelism (layer distribution), sequence parallelism.
Communication Overhead	Gradient exchanges via AllReduce; mitigated by gradient compression and local SGD techniques.	High activation memory transfers between layers and attention weights; mitigated by gradient accumulation and overlapping compute–communication.
Memory Constraints	High consumption from feature maps and intermediate activations; scales with spatial resolution.	Very high footprint from attention matrices ($O(n^2)$); requires checkpointing, mixed precision, and memory-efficient attention.
Optimization Techniques	Activation checkpointing, mixed precision (FP16/BF16), data parallelism optimizations, convolution kernel fusion.	FlashAttention, gradient checkpointing, ZeRO optimizer states, sequence/patch reduction, sparse attention patterns.
Hardware Considerations	Highly optimized on GPUs/TPUs with specialized libraries (cuDNN, oneDNN).	Benefits from high-bandwidth memory (HBM) and fast interconnects; modern attention optimizations reduce communication requirements.
Training Data Needs	Moderate requirements due to strong inductive biases (spatial locality, translation equivariance).	Very high data requirements; large-scale pretraining (e.g., JFT-300M) or knowledge distillation needed due to limited inductive bias.

Table 1.10 CNNs vs ViTs Parallelization Constraints

6. Conclusion

In conclusion, the challenges and opportunities presented by Big Data necessitate methodological rigor and innovation to convert vast, heterogeneous, and rapidly generated datasets into actionable knowledge. This chapter examined the foundations of knowledge extraction and pattern recognition within the Big Data paradigm, highlighting the significance of both scalable computational frameworks and domain-specific understanding. By scrutinizing the limitations of traditional approaches, particularly in the context of data deluge, opacity, and hubris, it becomes apparent that effective solutions must integrate robust data quality management with adaptive strategies. Ultimately, the amalgamation of advanced algorithms, distributed architectures, and cross-disciplinary insights facilitates more reliable, interpretable, and impactful knowledge discovery, ensuring that Big Data transitions from a raw resource into a catalyst for innovation across science, industry, and society.

Chapter 2

Knowledge Discovery in Big Genomic Data

1. Introduction

The advent of high-throughput sequencing has transformed genomics into a defining domain of Big Data. This technological revolution has produced terabytes of heterogeneous genomic information, creating unprecedented computational and analytical demands. Managing this scale requires not only advanced storage infrastructure but also sophisticated algorithms capable of handling complexity. This chapter examines the convergence of large-scale data generation and genomic science. We analyze architectures that enable efficient storage, retrieval, and distributed processing across massive datasets. In addition, we explored advanced computational frameworks and machine learning methods that derive functional and clinical insights from genomic signals. These approaches power essential applications, including variant discovery, transcriptomic profiling and multi-omics integration. Together, these technologies are advancing the boundaries of precision medicine. Ultimately, this chapter provides a roadmap for understanding the computational ecosystem of modern genomics and demonstrates how Big Data solutions are shaping the next era of biomedical innovation.

2. Genomic Data Generation

The generation of genomic data has undergone a profound transformation over the last four decades, driven by advances in sequencing technology. This evolution has been marked by improvements in read length, accuracy, throughput, and cost efficiency, which together define the pace of genome discovery. From the labor-intensive methods of the 1970s to today's high-throughput platforms, each sequencing generation has shaped both the scale and complexity of genomic datasets

2.1 First Generation: Sanger Sequencing

Sanger sequencing, developed in the 1970s, was the foundational genomic technology (Fig 2.1). This enabled the first complete genome sequences and the Human Genome Project [71]. Despite its accuracy, this method is slow, costly, and limited in throughput, generating kilobases of data per run. Its primary value today is in the validation of variants and small targeted sequencing experiments.

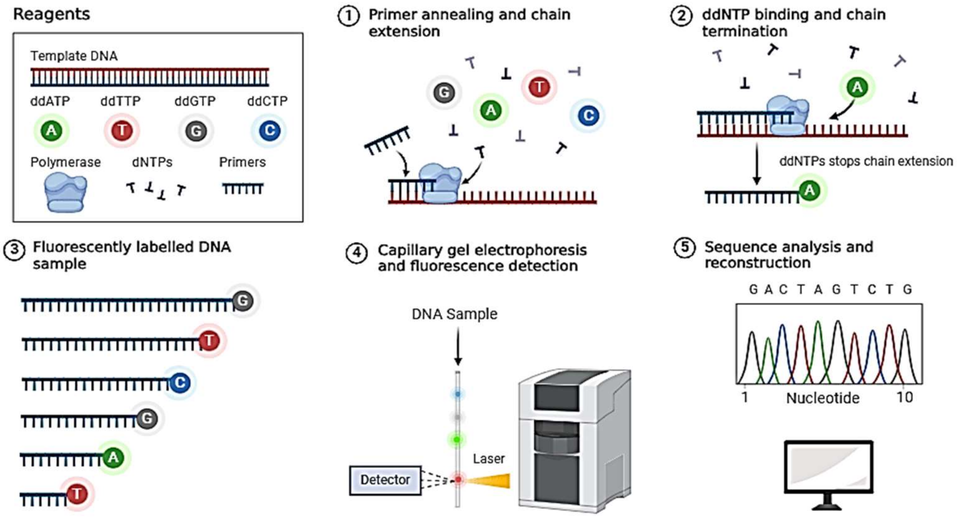

Figure 2.1 Sanger Sequencing Steps [71]

2.2 Second Generation: Massively Parallel Sequencing (NGS)

Next-generation sequencing (NGS) technologies, particularly those developed by Illumina, have revolutionized genomics by introducing massively parallel sequencing (Fig 2.2). Short reads (50–300 bp) are produced in millions or billions per run, enabling cost-effective whole-genome and whole-exome sequencing [72]. NGS remains dominant for population-scale studies and biobank projects because of its balance of **accuracy, throughput, and cost efficiency**. However, its reliance on short reads limits its ability to resolve structural variants, repetitive regions and haplotype phasing.

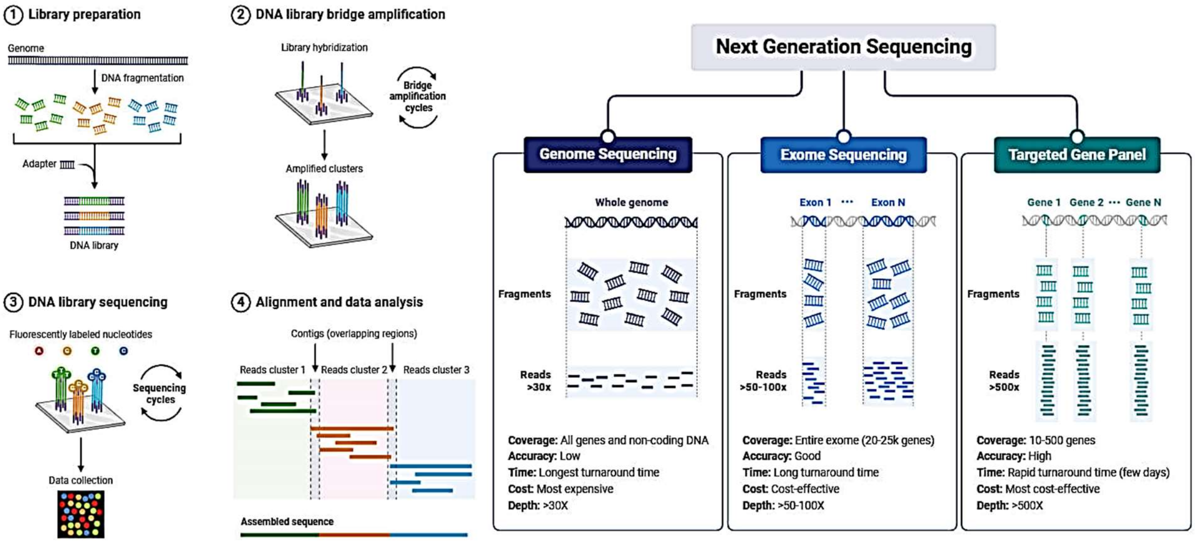

Figure 2.2 Massively Parallel Sequencing Steps [72]

2.3 Third Generation: Long-Read, Real-Time Sequencing

Third-generation sequencing platforms, such as Pacific Biosciences (PacBio) Single Molecule Real-Time (SMRT) sequencing and Oxford Nanopore Technologies (ONT), address the limitations of short reads by producing long reads (up to megabases in length) (Fig 2.3). These methods facilitate de novo assembly, structural variant detection, and the resolution of repetitive genomic regions [73]. Long-read technologies also enable the direct sequencing of RNA and detection of base modifications, adding functional insights beyond sequence content. Although they initially suffered from high error rates, continuous improvements in chemistry and base-calling algorithms have significantly increased their accuracy, making long reads a critical complement to short-read sequencing.

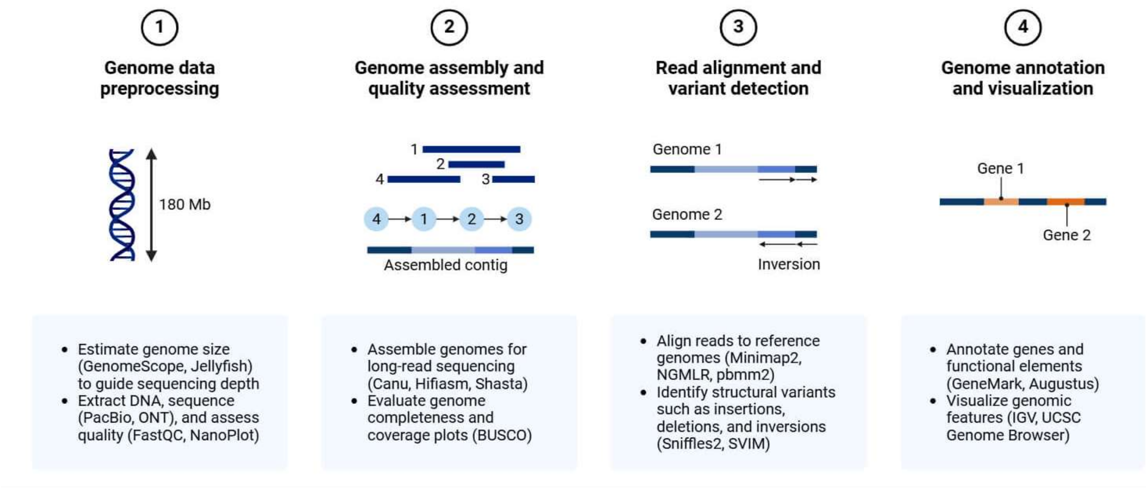

Figure 2.3 Long Read Sequencing Steps [73]

2.4 Current Trends and Outlook

Modern genomic projects increasingly combine short- and long-read sequencing to balance the accuracy, coverage, and structural resolution. The cost of sequencing continues to decline, dropping below $500 for a human genome, while throughput expands toward real-time, portable sequencing for clinical and field-based applications. These trends underscore the continuing expansion of genomic data, laying the groundwork for multi-omics integration, population-scale studies and precision medicine.

3. Genomic Data Representation

The representation of genomic data is central to computational genomics because it determines how sequencing outputs are stored, processed, and shared across analytical pipelines. Over the past two decades, a diverse ecosystem of standardized file formats has emerged, each optimized for a specific stage of analysis, from raw reads to alignments, variants, and higher-level annotations. These formats are complemented by distinct data types that capture the different biological layers of the genome, transcriptome and proteome. Together, these form the foundation of reproducible and large-scale genomic research.

3.1 File Formats

Standardized formats ensure interoperability across sequencing platforms, software packages and databases. Table 2.1 summarizes the most critical file formats used in genomics, grouped by their analytical roles.

Category	Format(s)	Purpose / Typical Contents	Typical Tools / Ecosystem
Raw sequencing	FASTA (.fa)	Reference genome / transcriptome sequences	UCSC/Ensembl, samtools, BEDTools
	FASTQ (.fastq)	Raw reads with Phred quality scores	fastp, seqtk, MultiQC
	SRA	Compressed raw read archives (NCBI)	SRA Toolkit
Alignments	SAM / BAM	Aligned reads; BAM is compressed binary	BWA, Bowtie2, STAR, samtools
	CRAM	Reference-based compressed alignments	samtools, htslib
	BED / BigBed	Genomic intervals, annotation tracks	BEDTools, UCSC utilities
	WIG / BigWig / bedGraph	Coverage or signal tracks (ChIP/ATAC-seq)	deepTools, UCSC tools
Variants	VCF / BCF	Genetic variants (SNPs, indels, SVs); BCF = binary	GATK, bcftools, htslib
	MAF	Somatic mutations (cancer cohorts)	GDC/TCGA, maftools
Annotations	GFF3 / GTF	Gene models (genes, transcripts, exons, CDS)	Ensembl, gffread, agat
	refFlat / GenePred	Tabular gene annotation models	UCSC toolchain
Epigenomics	narrowPeak / broadPeak	ChIP/ATAC-seq peaks (TFs, histone marks)	MACS2, HOMER
	cool / mcool / hic	Hi-C contact matrices (3D genome)	cooler, Juicer, HiCExplorer
Transcriptomics	Counts matrix (.tsv/.csv)	Gene × sample read counts	featureCounts, HTSeq, DESeq2
	FPKM / TPM tables	Normalized expression matrices	edgeR, DESeq2 (R/Bioconductor)
	loom / h5ad	Single-cell RNA-seq (HDF5-based)	Scanpy, Seurat
Proteomics / Multi-omics	mzML / mzXML	Mass spectrometry raw spectra	ProteoWizard, OpenMS
	mzIdentML / mzQuantML	Protein identifications / quantifications	MaxQuant, MS-GF+
	ProBAM / ProBed	Proteogenomics mapped to genome coords	PGTools, R packages
Population genetics	PLINK PED/MAP; BED/BIM/FAM	Genotypes + pedigree; scalable GWAS	PLINK, Hail, BGEN
	Oxford (.gen/.sample)	Imputation formats	IMPUTE2, QCTOOL
Large-scale storage	HDF5	Hierarchical array storage	h5py, rhdf5, AnnData
	Zarr	Cloud-native chunked arrays	zarr, xarray, kerchunk
	Parquet / ORC	Columnar storage for big data	Apache Spark, ADAM, Glow
Other Formats	SBML / BioPAX	Pathway and network models	COPASI, CellDesigner
	Newick / Nexus	Phylogenetic trees	IQ-TREE, BEAST, MrBayes
	CEL / GPR	Microarray raw / processed data	Affymetrix, limma

Table 2.1 Key genomic file formats and their primary applications

This standardized ecosystem enables the seamless integration of different analysis steps, for example, moving from FASTQ raw reads to BAM alignments, to VCF variant calls, and finally to GTF annotations for interpretation. Binary compression (e.g., BAM, CRAM, and BCF) plays a crucial role in managing storage demands at the population and biobank scales.

3.2 Genomic Data Types

Beyond file structures, genomic science is defined by the diversity of its biological data types, each capturing a distinct layer of molecular function and contributing to a multidimensional understanding of biology and disease. These layers form the foundation of multi-omics integration, where the combination of heterogeneous datasets yields insights that cannot be obtained from a single modality.

- **Nucleotide Sequences:** The foundational layer of genomics encodes the genome using four bases (A, C, G, and T) (Fig 2.4). These sequences provide raw substrates for genome assembly, gene prediction, and comparative genomics, enabling the reconstruction of species-specific and pan-genomic references. Advances in long-read sequencing now allow researchers to resolve complex regions, such as centromeres and telomeres, thereby expanding the scope of assembly and structural genomics.

```
TATTTACCATATCAGATTCACATTCAGTCCTCAGCAAAATGAAGGGCTCCATTTTCACTCTGTTTTTATT
CTCTGTCCTATTTGCCATCTCAGAAGTGCGGAGCAAGGAGTCTGTGAGACTCTGTGGGCTAGAATACATA
CGGACAGTCATCTATATCTGTGCTAGCTCCAGGTGGAGAAGGCATCAGGAGGGGATCCCTCAAGCTCAGC
AAGCTGAGACAGGAAACTCCTTCCAGCTCCCACATAAACGTGAGTTTTCTGAGGAAAATCCAGCGCAAAA
CCTTCCGAAGGTGGATGCCTCAGGGGAAGACCGTCTTTGGGGTGGACAGATGCCCACTGAAGAGCTTTGG
AAGTCAAAGAAGCATTCAGTGATGTCAAGACAAGATTTACAAACTTTGTGTTGCACTGATGGCTGTTCCA
TGACTGATTTGAGTGCTCTTTGCTAAGACAAGAGCAAATACCCAATGGGTGGCAGAGCTTTATCACATGT
TTAATTACAGTGTTTTACTGCCTGGTAGAACACTAATATTGTGTTATTAAAATGATGGCTTTTGGGTAGG
CAAAACTTCTTTTCTAAAAGGTATAGCTGAGCGGTTGAAACCACAGTGATCTCTATTTTCTCCCTTTGCC
AAGGTTAATGAACTGTTCTTTTCAAATTCTACTAATGCTTTGAAATTTCAAATGCTGCGCAAAATTGCAA
TAAAAATGCTATAAACCA
```

Figure 2.4 Human Nucleotide Sequences Sample

- **Transcriptomics:** RNA sequencing (RNA-seq) provides a quantitative and qualitative view of gene expression, revealing the transcriptional activity, isoform diversity, and splicing dynamics. Modern approaches, such as single-cell RNA-seq and spatial transcriptomics, extend this layer by capturing heterogeneity across tissues and within individual cells, enabling insights into developmental trajectories, tumor microenvironments, and immune responses.

- **Proteomics and Metabolomics:** Proteins and metabolites represent the functional output of the genome, reflecting enzymatic activity, signaling networks and cellular physiology. Techniques such as mass spectrometry (MS) and nuclear magnetic resonance (NMR) underpin these domains, while advances in quantitative proteomics and metabolite profiling are increasingly integrated with genomics to establish genotype–phenotype links and identify biomarkers for disease.

- **Genetic variants:** Variations in the genome, including single-nucleotide polymorphisms (SNPs), insertions/deletions (indels), copy number variants (CNVs), and large structural rearrangements, represent the substrate of evolutionary change and disease risk (Fig 2.5). Large-scale genome-wide association studies (GWAS) link these variants to phenotypes ranging from simple traits to complex diseases, whereas clinical genomics increasingly applies variant discovery for diagnostics, risk assessment, and pharmacogenomics.

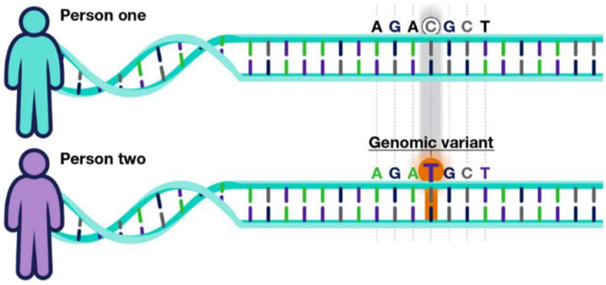

Figure 2.5 Gene Variant

- **Non-coding RNAs (ncRNAs):** Once considered transcriptional ‘’noise” ncRNAs, including microRNAs (miRNAs), long non-coding RNAs (lncRNAs), and circular RNAs, are now recognized as key regulators of gene expression. They modulate transcription, translation, and epigenetic states, influencing processes from development to cancerogenesis. Their dysregulation is increasingly associated with cancer, neurodegeneration, and cardiovascular disorders, positioning ncRNAs as promising diagnostic and therapeutic targets for these diseases.

- **Disease-associated datasets:** Large-scale initiatives, such as The Cancer Genome Atlas (TCGA) and the International Cancer Genome Consortium (ICGC), integrate variants, expression profiles, epigenetic changes, and clinical outcomes, serving as benchmarks for translational genomics. These datasets enable cross-cohort analyses, machine learning–driven biomarker discovery, and identification of molecular subtypes in diseases such as cancer. Expanding beyond oncology, emerging disease-focused cohorts (e.g., Alzheimer’s genomics consortia) are extending this model to other complex conditions.

3.3 Challenges and Multi-Omics Integration

While each format and data type provides unique insights, modern genomics increasingly requires multi-omics integration, the combined analysis of DNA, RNA, protein, metabolite, and epigenomic data, often linked to clinical, lifestyle, and environmental variables. This layered perspective enables researchers to capture the complexity of biological systems more holistically, moving beyond single-dimensional analyses toward a systems-level understanding of health and disease. Multi-omics has proven particularly valuable in precision medicine, where genotype–phenotype associations can be refined through transcriptomic activity, proteomic networks, and metabolic signatures, ultimately informing patient stratification and personalized interventions.

However, this integrative approach introduces significant challenges.

- **Data heterogeneity:** Different measurement technologies produce data with incompatible scales, resolutions and error profiles. For example, whole-genome sequencing yields discrete nucleotide-level variations, whereas mass spectrometry–based proteomics produces relative abundance measures with substantial technical variability. Harmonizing these data requires sophisticated normalization, cross-platform calibration, and metadata curation strategies.

- **Storage and computational demands:** High-resolution multi-omics datasets often involve millions of features across thousands of samples, quickly reaching petabyte-scale storage requirements. The analysis of such datasets requires distributed computing infrastructures, cloud-native workflows, and parallel processing frameworks to maintain efficiency and reproducibility.

- **Standardization and interoperability:** The lack of unified standards across repositories, pipelines, and metadata schemas remains a critical bottleneck. Although initiatives such as FAIR principles (Findable, Accessible, Interoperable, Reusable (FAIR) principles and global consortia, such as GA4GH, promote standardization, inconsistent adoption continues to hinder large-scale data reuse and cross-study integration.

- **Privacy and ethical considerations:** Linking genomic data with electronic health records (EHRs), lifestyle information, and environmental exposure raises complex privacy, consent, and governance issues. Ensuring compliance with regulatory frameworks, such as the GDPR in Europe and HIPAA in the United States, is essential for ethical integration.

- **Interpretability and integration methods:** Even when technical integration is achieved, interpreting cross-layer relationships is challenging. Multi-omics datasets are often high-dimensional but sparse, requiring advanced statistical frameworks, graph-based models, and artificial intelligence-driven approaches to extract biologically meaningful insights.

4. Growth and Complexity of Genomic Data

The scale of genomic data generation has expanded dramatically, evolving from terabytes in early sequencing projects to **petabytes and exabytes** in modern population-level studies [74]. This exponential growth is fueled by decreasing sequencing costs, advances in throughput, and expansion of large-scale collaborative projects.

4.1 From Cohorts to Biobanks

Early efforts, such as the 1000 Genomes Project (~2,500 genomes), provided the first comprehensive catalog of human genetic variation at the population scale [75]. These initiatives were soon surpassed by biobank-scale projects that integrated genomic data with detailed phenotypic and lifestyle information (Table 2.2).

Biobank / Project	Country	Focus	Sample Size	Key Feature
UK Biobank	UK	Population health	~500,000	Gold standard, broad global accessibility
All of Us	USA	Precision medicine	Goal: 1M+	Emphasis on diversity and participant engagement
China Kadoorie	China	Chronic disease	~512,000	Large Asian cohort for population genetics
deCODE Genetics	Iceland	Genetic discovery	~165,000	Leverages isolated population structure
FinnGen	Finland	Genetic discovery	Goal: 500,000	Integration with national health records
23andMe (DTC)	USA	Consumer genetics	10M+ customers	Largest by scale; direct-to-consumer model

Table 2.2 Main Genomic Data File Formats

4.2 Complexity Layers of Modern Genomics

The challenge of genomic big data is not defined solely by its volume but also by its complexity and dimensionality. Beyond the sheer number of sequenced genomes, the integration of multiple data modalities, clinical contexts, and temporal dimensions adds layers of intricacy that strain both computational and analytical frameworks. Several factors contribute to this challenge.

- **Multi-omics integration:** Modern genomic studies increasingly go beyond DNA sequencing to incorporate transcriptomic, epigenomic, proteomic, and metabolomic data sets (Fig 2.6). Each layer offers unique biological insights; for example, transcriptomics captures dynamic gene expression, whereas epigenomics reflects regulatory states and environmental influences. However, integrating these diverse modalities requires sophisticated pipelines for harmonization, normalization, and cross-platform calibration, as differences in resolution, measurement errors, and scale can introduce bias [76]. Effective integration is crucial for systems biology approaches and precision medicine, where disease mechanisms are rarely explained by a single omics layer.

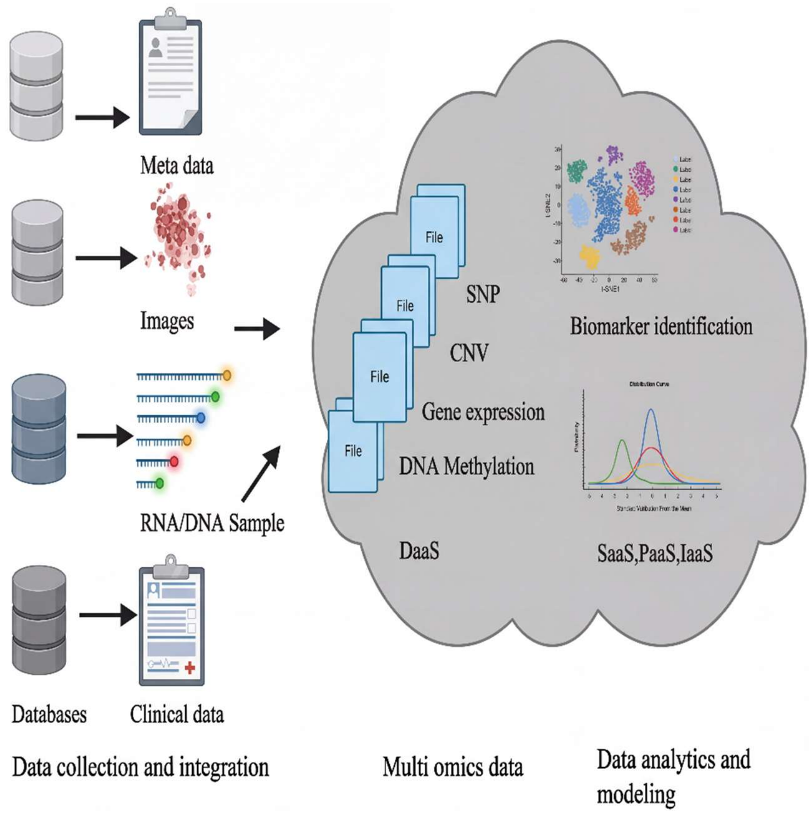

Figure 2.6 Sources of Multi-Omics Data [76]

- **Clinical and lifestyle data:** Linking genomic profiles with electronic health records (EHRs), medical imaging, and lifestyle factors, such as diet, exercise, and environmental exposures, enables a richer and more contextualized understanding of human health [77] [78]. These integrated datasets allow researchers to study not only genetic predisposition, but also gene–environment interactions and the influence of social determinants of health. However, this fusion introduces heterogeneity and interoperability challenges, as clinical data are often unstructured, incomplete, or siloed across institutions. Furthermore, the harmonization of diverse metadata standards remains a major barrier to reproducibility.

- **Longitudinal studies:** Genomic initiatives increasingly adopt repeated sampling over time to capture dynamic changes in molecular and clinical states. Projects such as the GTEx Consortium provide insight into how gene expression varies across tissues and over the lifespan [79], whereas other longitudinal cohorts track disease progression, therapeutic response, and aging [80]. These temporal layers generate multidimensional datasets that multiply the volume and complexity, requiring advanced time-series modeling, statistical methods for missing data, and machine learning frameworks capable of capturing dynamic trajectories.

5. Computational Ecosystem for Big Genomics

The unprecedented growth of genomic data has made computation a critical bottleneck in genomics. Sequencing projects routinely generate datasets in the petabyte range, and biobank-scale efforts anticipate exabyte-level storage demands. The management of this deluge requires a robust ecosystem that integrates high-performance computing (HPC), cloud infrastructure, and standards for data sharing. These systems not only provide storage and processing capabilities but also address issues of security, interoperability, and reproducibility, which are central to translational applications.

5.1 Comparative Ecosystem Overview

In Table 2.3 we introduce a comparative overview of main computational platforms in genomics.

Platform / Initiative	Type	Key Features	Strengths	Limitations
AWS Genomics in the Cloud	Commercial Cloud	On-demand computing; genomics-ready AMIs; S3 storage; integration with ML/AI tools	Elastic scalability; wide adoption by industry and academia	Costs escalate with sustained usage
Google Cloud Life Sciences (Genomics)	Commercial Cloud	BigQuery for large-scale queries; API-driven pipelines; integration with TensorFlow/TPUs	Powerful analytics; strong AI/ML ecosystem	Vendor lock-in; requires cloud expertise
Microsoft Azure for Genomics	Commercial Cloud	Integration with Azure Health Data Services and EHR systems; genomics APIs	Strong healthcare interoperability; secure health data pipelines	Less widespread adoption in genomics compared to AWS/GCP
NIH AnVIL	Public Cloud	Analysis, Visualization, and Informatics Lab-space; FAIR-compliant genomic datasets	Democratizes access to NIH datasets; collaborative workflows	Limited to NIH-funded initiatives; constrained governance
ELIXIR (Europe)	Research Infrastructure	Interoperability for databases, software, and training across European states	Standardization across Europe; sustainability focus	Variable adoption among member states
GA4GH	Standards Body	Defines global standards for responsible genomic data sharing (APIs, schemas, policies)	Promotes global interoperability and ethics	Does not provide direct compute/storage infrastructure

Table 2.3 Comparative overview of major computational platforms in genomics

These infrastructures illustrate the plurality of approaches: commercial providers emphasize elasticity and integration with machine learning, whereas public and academic initiatives prioritize accessibility, standardization, and governance issues.

5.2 Hybrid Cloud–HPC Approaches

The choice between cloud and high-performance computing (HPC) is often not binary. Instead, many institutions now employ hybrid strategies that leverage the complementary advantages of both approaches to balance the cost, performance, and compliance requirements. This hybrid paradigm has become particularly important as genomic datasets grow toward the exabyte scale and demand both stable throughput and flexible scalability.

- **HPC clusters:** Traditional on-premises HPC infrastructures remain the backbone for predictable and compute-intensive workloads, such as read alignment, variant calling, and large-scale batch simulations. Dedicated hardware enables institutions to achieve cost efficiency over time, particularly when pipelines are well-defined and workloads are steady. Additionally, HPC environments offer tight integration with local storage systems and institutional policies, which are essential for research programs operating under strict data governance frameworks.
- **Cloud platforms:** Commercial cloud services provide elastic scaling and global accessibility, making them well-suited for burst workloads, exploratory projects, and international collaborations. Cloud-native genomics platforms also integrate directly with AI/ML frameworks, serverless pipelines, and advanced analytics (e.g., Google BigQuery and AWS Sagemaker), accelerating innovation and pilot projects. However, costs can escalate with long-term use, and vendor lock-in is a recurring concern for institutions managing large-scale operations.
- **Hybrid pipelines:** Institutions increasingly adopt hybrid models that integrate local HPC with cloud resources. For example, workflows may use SLURM-managed HPC clusters for preprocessing steps such as quality control and read alignment, while offloading computationally expensive or collaborative tasks (e.g., variant aggregation and joint genotyping) to cloud platforms such as AWS or GCP. This approach combines the predictability and cost efficiency of HPC with the elasticity and collaborative potential of the cloud, ensuring that resources are allocated according to the workload characteristics.
- **Data locality and compliance:** A key advantage of hybrid models is their ability to maintain data locality, which is critical in regions with restrictions on genomic data transfers. Sensitive datasets can remain on-premises, whereas derived or aggregated results can be processed or shared in the cloud. This structure enables institutions to comply with regulatory frameworks, such as the GDPR in Europe and HIPAA in the United States, while still benefiting from global collaborations.

5.3 Federated and Distributed Genomics

With the increasing globalization of genomics, federated approaches have emerged as key solutions for secure, ethical, and scalable data-sharing (Fig 2.7). Traditional models of centralizing sensitive genomic data in a single repository often face legal, technical, and ethical barriers because of concerns about privacy, consent, and data sovereignty. In contrast, federated systems enable distributed analysis, where computational algorithms are dispatched to local data silos and only aggregated results or model parameters are shared. This paradigm minimizes the risk of data exposure while facilitating large-scale collaboration.

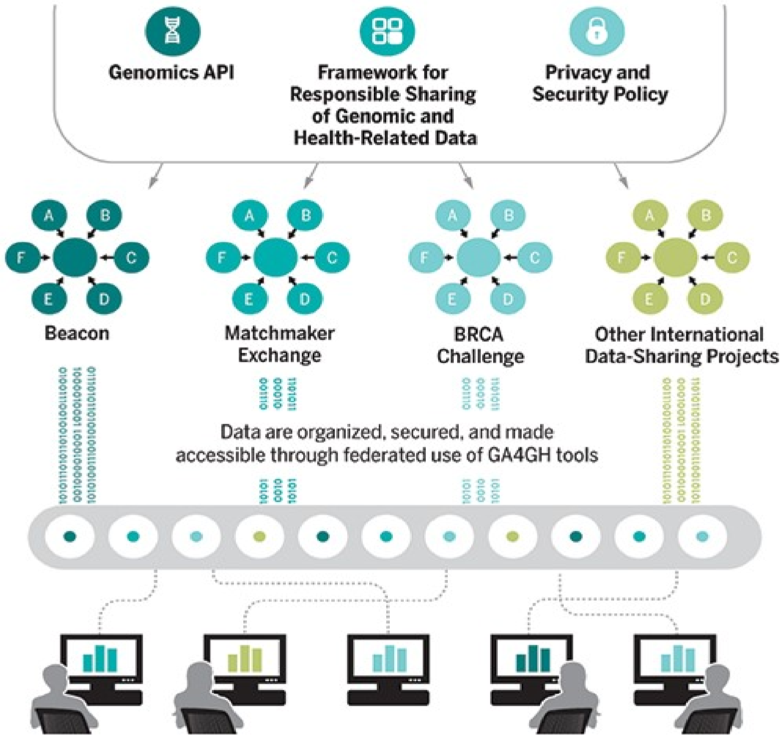

Figure 2.7 The Global Alliance for Genomics and Health (GA4GH) framework, as depicted in the diagram, facilitates secure and responsible sharing of genomic and health-related data across international projects through standardized APIs, policies, and federated tools.

- **GA4GH frameworks:** The Global Alliance for Genomics and Health (GA4GH[1]) has played a central role in defining the technical, legal, and ethical standards for federated analysis. Initiatives such as the Data Use Ontology (DUO) provide a standardized language for consent and permissible data use, while Beacon v2

[1] https://www.ga4gh.org/

allows institutions to share metadata queries without exposing raw data. These frameworks enable interoperability and trust among international genomic consortia.

- **European Genome–Phenome Archive (EGA):** The EGA, along with its federated extension (Federated EGA), exemplifies distributed models that respect national data sovereignty while enabling Pan-European collaboration. Instead of transferring raw genomic files across borders, local nodes securely host data, and researchers can run approved analyses through federated interfaces. This model addresses both GDPR compliance and the need for cross-border genomic research in the EU.

- **Federated learning frameworks:** Beyond query and metadata sharing, federated learning enables the training of machine learning and AI models directly across multi-institutional datasets. In this setup, patient-level data ***never leave local repositories***; instead, model updates are shared and aggregated across the sites. This ensures compliance with privacy regulations, such as the GDPR in Europe and the HIPAA in the US, while maintaining the statistical power required for large-scale or rare disease studies. Emerging federated AI systems also integrate differential privacy and secure multiparty computation (SMPC) to further protect individual-level data.

- **Applications in rare diseases and diversity studies:** Distributed models are particularly critical in contexts where sample sizes are inherently small or population representation is limited. Rare disease genomics often requires collaboration across multiple institutions and countries to achieve sufficient statistical power, whereas ethnically diverse studies rely on distributed cohorts to address biases in genomic reference databases. Therefore, federated genomics enables both equity in representation and scientific rigor by ensuring broader inclusion without compromising privacy.

5.4 Challenges and Future Trends

Despite significant progress in computational genomics, multiple challenges remain in building a robust, scalable, and equitable ecosystem for data analysis and sharing of these data. These challenges span the technical, economic, ethical, and infrastructural domains, reflecting the inherently interdisciplinary nature of genomics.

- **Cost and sustainability:** Although commercial cloud platforms offer unmatched scalability, they impose recurring operational costs for computing, storage, and data transfer. Long-term projects, especially those involving biobank-scale datasets, face sustainability issues because cumulative costs often exceed institutional budgets. This economic burden has led to increased interest in hybrid models and resource pooling among research consortia.

- **Data interoperability:** A major bottleneck is the lack of complete convergence across file formats, metadata standards and APIs. Despite progress from initiatives such as GA4GH and FAIR data principles, many repositories and pipelines remain siloed, limiting cross-study reproducibility and integration. True interoperability requires community-wide adoption of standardized ontologies, APIs, and schema definitions.
- **Security and privacy:** Genomic data are uniquely identifiable, meaning that even anonymized datasets can often be traced back to the individuals. Robust frameworks for encryption, federated data sharing, differential privacy, and fine-grained access control are essential to ensure compliance with regulatory frameworks, such as the GDPR in Europe and HIPAA in the United States. Simultaneously, global research demands collaboration across jurisdictions, making security and governance critical balancing acts.
- **Equity of access:** Many developing regions lack access to sequencing infrastructure, commercial cloud credits, or institutional HPC clusters, leading to global disparities in genomic research capacity. Without intentional strategies to expand infrastructure, training, and funding in low- and middle-income countries, the benefits of genomic medicine may remain confined to resource-rich settings, exacerbating these inequities.

Addressing these challenges requires not only incremental improvements but also paradigm shifts in the conception and deployment of computational genomics. The field is moving beyond reliance on isolated infrastructure toward integrated, intelligent, and sustainable ecosystems. In this context, several emerging trends are beginning to define the trajectory of genomic computation, ranging from hybrid cloud–HPC models that balance performance and scalability to federated AI pipelines that safeguard privacy, green computing practices that mitigate environmental impact, and even quantum-ready platforms that hold the potential to revolutionize optimization and cryptographic security in genomic workflows.

6. Parallel and Distributed Computing

The scale of modern genomic data, which spans millions of samples and petabytes of sequencing reads, necessitates parallel and distributed computing frameworks. Efficient execution depends on exploiting parallelism at two complementary levels: **task-level parallelism**, which distributes independent jobs across compute nodes, and **intra-node acceleration**, which optimizes the performance within individual nodes through multithreading and instruction-level enhancements. Together, these approaches form the foundation for high-throughput genomic analyses.

6.1 Task-Level Parallelism

At the highest level, genomic workflows can be decomposed into independent tasks distributed across nodes in a computing cluster or cloud infrastructure. This strategy is exemplified by the scatter–gather paradigm (Fig

2.8), wherein large datasets are partitioned into smaller segments (scatter), each processed concurrently, and subsequently aggregated into a unified output (gather).

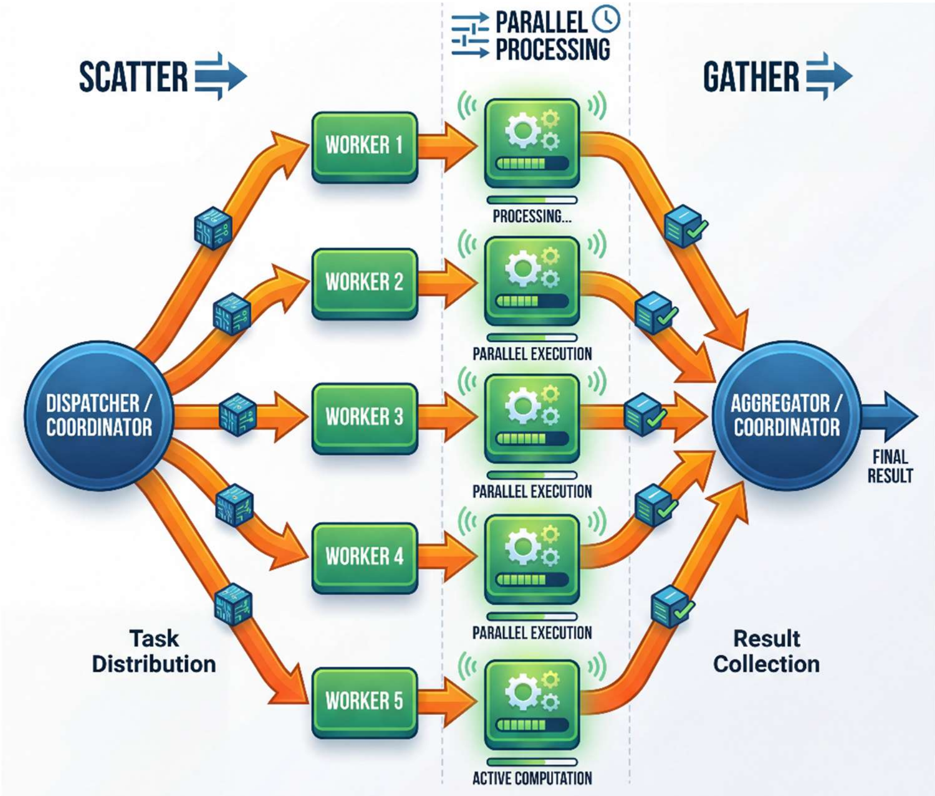

Figure 2.8 Scatter-Gather pattern illustration

This approach is particularly effective for variant calling and population-scale analyses. For instance, the Genome Analysis Toolkit (GATK) HaplotypeCaller applies scatter–gather to subdivide the genome into regions and execute haplotype reconstruction and variant detection in parallel. The integration of GATK4 with Apache Spark further enables distributed execution across clusters, allowing population-scale datasets, such as those from the UK Biobank, to be processed efficiently. By leveraging Spark's in-memory computation and fault tolerance, HaplotypeCaller achieves near-linear scaling across thousands of genomes while maintaining the accuracy.

Other examples of task-level parallelism include sample-level parallelism, where individual genomes or exomes are processed independently in workflows such as read alignment or quality control. These embarrassingly parallel workloads are particularly well-suited for cluster schedulers, such as SLURM (Simple Linux Utility for Resource Management), or cloud-native workflow managers, such as Cromwell, Nextflow, or WDL-based systems (Workflow Description Language).

6.2 Intra-Node Acceleration

While task-level parallelism distributes jobs across nodes, intranode acceleration focuses on maximizing the computational efficiency within a single node. Two strategies dominate this domain:

- **Multithreading:** Modern tools, such as BWA-MEM (Burrows–Wheeler Aligner) and STAR, exploit multithreaded execution, where individual reads or read pairs are processed in parallel threads. This reduces the wall-clock runtime and improves the throughput of multicore processors.
- **Single Instruction, Multiple Data (SIMD):** Vectorized instructions allow simultaneous operations on multiple data points, accelerating key tasks such as Smith–Waterman alignment, sequence scoring and base recalibration. Frameworks such as Intel's Genomics Kernel Library (GKL) integrate SIMD to optimize the GATK workflows.

Intra-node acceleration ensures that even when distributed across clusters, genomic pipelines efficiently use the available CPU cycles and hardware capabilities. This layer of optimization is essential for reducing costs in cloud environments, where the runtime directly influences the expenditure.

7. Computational Tools for Genomics

A diverse suite of computational tools underpins modern genomics, including sequence alignment, variant calling, transcriptomic profiling, and functional inference. Although these tools differ in their algorithms and designs, their comparative strengths and limitations determine their suitability for specific applications.

7.1 Sequence Alignment Tools

To contextualize the role of alignment tools in genomic data processing, Table 2.4 provides a comparative overview of widely used sequence alignment algorithms, summarizing their input types, key strengths, limitations, and typical applications in the field.

Tool	Input Type	Strengths	Limitations	Typical Applications
BLAST	DNA/protein sequences	Fast local alignment; widely adopted; versatile formats	Lower sensitivity for divergent sequences; memory intensive	Homology search, genome annotation, metagenomics
Bowtie	Short reads (<50 bp)	Low memory (<4 GB); extremely fast for small reads	Poor with long reads; struggles in repetitive regions	RNA-seq, ChIP-seq (ENCODE-scale projects)
BWA	Short/medium reads (~100 bp)	Balanced speed and accuracy; widely used in resequencing	Less effective on high-error long reads; not splice-aware	Whole-genome resequencing, population studies
Minimap2	Long/short reads (PacBio, ONT)	Efficient for long reads; robust to sequencing errors	Higher memory demand; less accurate for short reads	Structural variant calling, de novo assembly

STAR	RNA-seq reads	Splice-aware; high sensitivity for junctions; very fast	High memory usage (20–30 GB); sensitive to errors	Differential expression, splicing analysis (GTEx)

Table 2.4 Sequence alignment tools: comparative strengths and applications

7.2 Variant Calling and Downstream Analysis

- **GATK**: Industry standard for SNP and indel discovery; graph-based assembly enhances accuracy but requires high computational resources. It is widely applied in projects such as the UK Biobank [81] [82].
- **SAMtools**: A lightweight toolkit for SAM/BAM manipulation, pileup generation, and variant aggregation. Efficient streaming, but limited by single-threading [83].
- **DESeq2**: RNA-seq differential expression analysis using negative binomial modeling; robust handling of low counts but computationally intensive at biobank scale [84].

7.3 Sensitivity and Probabilistic Methods

- **HMMER**: Employs profile Hidden Markov Models for remote homology detection and functional domain annotation; highly sensitive but computationally demanding for long sequences [85] [86].
- **Clustal Omega**: Scalable multiple sequence alignment for tens of thousands of sequences; suitable for phylogenetic studies, although accuracy depends on guide tree quality and computational cost increases quadratically with dataset size [87].

8. Artificial Intelligence and Machine Learning in Genomics

Artificial intelligence and machine learning are increasingly central to genomics, reshaping the manner in which data are analyzed, interpreted, and translated into actionable insights. The rapid growth of sequencing data, coupled with the complexity of multi-omics integration, has pushed the limits of classical bioinformatics pipelines. Traditional ML algorithms laid the foundation by enabling classification, dimensionality reduction, and feature selection, whereas the advent of deep learning and transformer-based architectures has dramatically expanded predictive power. Today, AI methods are not only advancing basic genomic research but also bridging the gap between precision medicine, drug discovery, and clinical translation.

8.1 Classical Machine Learning Approaches

Classical ML methods remain important because of their interpretability and robustness in scenarios where data are limited or require careful feature selection:

- **Support Vector Machines (SVMs):** Applied to disease subtype classification, gene function prediction, and non-coding vs. coding sequence discrimination [88] [89]. Their ability to handle high-dimensional data is a major advantage, although the computational costs increase quadratically with the dataset size, limiting scalability without distributed frameworks.
- **Genetic Algorithms (GAs):** Inspired by natural selection, GAs are valuable for identifying variant subsets in genome-wide association studies (GWAS). They can capture nonlinear interactions and perform global optimization [90] [91], although stochastic convergence and high computational demand remain challenges. Hybrid GA–deep learning systems have shown promise in multi-omics feature selection.
- **Principal Component Analysis (PCA):** A standard in population genetics, PCA reduces dimensionality and reveals ancestry, population structure, and stratification [92] [93]. PCA is computationally efficient but is constrained by linear assumptions. Nonlinear extensions (e.g., kernel PCA, UMAP, t-SNE) have improved the resolution of complex patterns but often reduce interpretability.

These methods remain critical complements to deep learning, particularly in terms of interpretability and reproducibility.

8.2 Deep Learning Based Approaches

Deep learning has redefined the landscape of genomics by enabling direct modeling of raw sequences, complex regulatory patterns, and multimodal biological data. Unlike classical ML approaches, which rely heavily on handcrafted features, DL architectures learn hierarchical representations directly from data, making them well-suited to capture the nonlinear, context-dependent, and multiscale nature of genomic regulation. Several landmark studies illustrate the breadth of DL applications in genomics.

- **DeepSEA:** One of the first major applications of deep learning in genomics, DeepSEA employs a convolutional neural network (CNN) to predict the regulatory effects of non-coding variants by linking DNA sequence variation to chromatin features, transcription factor binding, and histone marks. Its success demonstrates the potential of DL for noncoding genome annotation and variant interpretation [60].
- **Enformer:** Building on transformer architectures, Enformer extends the receptive field of models to capture long-range (100 kb) sequence dependencies, advancing the prediction of enhancer–promoter interactions and variant impact on gene regulation. By incorporating self-attention mechanisms, Enformer improves interpretability while addressing the limitations of CNN-based models in modeling distal regulatory elements [94].

- **AlphaFold:** A transformative achievement in structural biology, AlphaFold applies attention-based architectures to achieve near-experimental accuracy in protein-structure prediction. Its ability to predict protein folds at scale has redefined structural genomics and accelerated drug discovery. The latest iteration, AlphaFold3, integrates small molecules, thereby expanding its role in ligand–protein interactions and structure-based drug design [95] [96].

- **AlphaGenome**: Building on advances in protein structure prediction and large-scale sequence modeling, AlphaGenome integrates deep neural architectures with evolutionary and functional genomic data. AlphaGenome was designed to predict the functional consequences of genetic variations at both the molecular and organismal levels by combining attention-based modules similar to AlphaFold with genomic and epigenomic features. Early studies have demonstrated its potential in identifying disease-associated variants, regulatory disruptions, and structural impacts of mutations that are difficult to capture using classical variant callers. AlphaGenome exemplifies the next generation of foundation models for genomics, bridging sequence variation, molecular phenotype, and clinical relevance [97].

- **DeepVariant**: Developed by Google, DeepVariant applies deep convolutional neural networks (CNNs) to the task of variant calling, reframing genomic data as image-like tensors. By learning directly from labeled sequencing data, DeepVariant outperforms traditional probabilistic methods in identifying SNPs and indels across diverse sequencing platforms. Benchmark studies have demonstrated its superior accuracy on both whole-genome and whole-exome datasets, with consistent performance across Illumina, PacBio, and Oxford Nanopore platforms [98]. DeepVariant exemplifies how deep learning can replace handcrafted statistical models with end-to-end trainable systems, making it one of the most impactful applications of AI in clinical genomics.

- **DNABERT and transformer-based genomics**: By adapting natural language processing (NLP) methods to DNA, DNABERT demonstrates that genomic sequences can be tokenized into k-mers and modeled as text. Pre-trained on large-scale genomic corpora, DNABERT generalizes effectively to tasks such as promoter recognition, splice-site prediction, and transcription factor binding, highlighting the potential of foundational models for genomics [99].

- **Basenji and BPNet:** Other sequence-based DL models, such as Basenji [100] and BPNet [101], have further advanced regulatory genomics. Basenji uses dilated CNNs to predict epigenomic signals across the genome, whereas BPNet achieves base-pair resolution predictions of transcription factor binding, offering mechanistic interpretability of cis-regulatory grammar.

- **scVI and single-cell DL models:** In transcriptomics, DL frameworks such as single-cell variational inference (scVI) apply variational autoencoders (VAEs) to analyze single-cell RNA-seq data, enabling batch correction, clustering, and trajectory inference across millions of cells [102]. These approaches illustrate how DL supports scalable and high-resolution functional genomics.
- **Graph neural networks (GNNs):** Recently, GNNs have been applied to represent biomolecular structures and interaction networks, supporting protein–protein interaction prediction, pathway inference, and drug repurposing [103] [104]. These models leverage relational structures to integrate diverse biological networks into predictive frameworks.

8.3 Multimodal AI and Precision Medicine

Complex diseases rarely result from a single molecular defect; instead, they emerge from the interplay of genetic, transcriptomic, proteomic, metabolomic, environmental, and lifestyle factors. To address this complexity, multimodal AI models integrate diverse data modalities, including genomics, transcriptomics, proteomics, metabolomics, medical imaging, and electronic health records (EHRs), into a unified predictive framework. By learning cross-layer relationships, these models enable the following:

- **Patient stratification:** Improved grouping of patients not only by genotype but also by disease progression, molecular signatures, and drug response patterns, which supports personalized interventions.
- **Therapeutic targeting:** Identification of causal genetic variants, dysregulated pathways, or protein–metabolite networks that drive the disease, offering novel therapeutic entry points.
- **Population-scale predictions:** Modeling gene–environment interactions by linking molecular profiles with lifestyle and exposure data, enabling risk prediction and preventive strategies across diverse cohorts.

Large-scale initiatives, such as the UK Biobank and All of Us Research Program, provide multimodal datasets that fuel these AI approaches, guiding the development of precision medicine frameworks at the population scale [105] [106]. Importantly, the use of federated learning ensures that AI models can be collaboratively trained across institutions without the need to centralize raw patient data. This approach preserves privacy and data sovereignty while maintaining sufficient statistical power for rare disease studies. By complying with regulations such as the General Data Protection Regulation (GDPR) in Europe and the Health Insurance Portability and Accountability Act (HIPAA) in the United States, federated approaches balance innovation and ethical responsibility.

Looking ahead, multimodal AI is expected to serve as the backbone of precision medicine, bridging molecular mechanisms and clinical outcomes. As data diversity expands, these frameworks will be critical for tackling disease heterogeneity, enabling more accurate diagnosis, prognosis, and therapeutic discovery across populations.

8.4 Emerging AI for Drug Discovery

AI is increasingly reshaping the pharmaceutical pipeline by accelerating compound design, improving hit discovery, and reducing the costs traditionally associated with trial-and-error experimentation. By leveraging deep learning and advanced computational frameworks, AI methods enable a shift from empirical screening to rational, data-driven molecular design.

- **Graph Neural Networks (GNNs):** GNNs provide a natural framework for modeling chemical structures as graphs, where atoms represent nodes and bonds represent edges. These models capture both local substructures and global topologies, making them highly effective for predicting protein–ligand binding affinities, toxicity profiles and pharmacokinetic properties [107]. Applications include virtual screening, where GNNs prioritize candidates from vast chemical libraries, and drug repurposing, where relational graphs across compounds, targets, and diseases inform new therapeutic applications.
- **Generative Models (GANs, VAEs):** Generative adversarial networks (GANs) and variational autoencoders (VAEs) enable de novo molecular design by sampling learned latent spaces of chemical structures. These models can optimize compounds for multiple objectives simultaneously, such as potency, solubility, and toxicity, while expanding chemical diversity beyond existing libraries [108]. More recent extensions have integrated reinforcement learning (RL) with generative models to iteratively refine molecules with desired therapeutic properties.
- **Explainable AI (XAI):** Despite the success of deep learning, black-box predictions remain a barrier to regulatory approval and mechanistic insight. XAI techniques, such as saliency maps, attention mechanisms, and feature attribution methods, improve interpretability by highlighting the substructures or interactions responsible for predictions [109]. These methods are critical for hypothesis generation, lead prioritization, and gaining the trust of medicinal chemists and regulators.
- **Quantum-enhanced AI:** Although still exploratory, quantum computing holds potential for tasks such as molecular docking, conformational sampling, and protein–ligand binding simulation. By combining quantum hardware with AI algorithms, researchers aim to accelerate the solution of NP-hard optimization problems that are inherent in molecular discovery. Early proof-of-concept studies have demonstrated the feasibility of quantum generative models and hybrid quantum–classical approaches for drug discovery [110].

8.5 Challenges and Future Directions

Despite this progress, several persistent challenges limit the widespread adoption of deep learning and AI in genomics. These challenges are not only technical, but also ethical and infrastructural, requiring careful consideration for clinical translation.

- **Interpretability vs. accuracy:** Deep learning models, particularly transformers and multimodal networks, often outperform classical methods in terms of predictive accuracy. However, they remain largely black boxes, offering limited transparency regarding how predictions are made. This opacity reduces trust among clinicians and regulators, and explainability is essential for adoption. Therefore, balancing interpretability and predictive performance is a major frontier in AI-driven genomics [109].
- **Computational cost:** Training and fine-tuning transformers, graph neural networks, and multimodal architectures require extensive computational resources, often relying on GPU/TPU clusters or large-scale cloud infrastructure. This limits accessibility to resource-rich institutions and exacerbates disparities in global genomics research. The growing energy footprint of such models also raises sustainability concerns, linking computation to environmental costs [111].
- **Bias and generalizability:** Genomic datasets are often biased toward populations of European ancestry, leading to models that fail to generalize across diverse contexts. This threatens to exacerbate health disparities if predictions are less accurate for underrepresented groups. Addressing bias requires inclusive data collection, transfer learning strategies, and fairness-aware modeling frameworks that explicitly account for population diversity [112].
- **Data governance:** Genomic data are inherently sensitive and uniquely identifiable. Without robust governance, the risk of privacy breaches remains high. Secure frameworks, including federated learning, differential privacy, and secure multiparty computation (SMPC), are essential for clinical adoption and international collaborations. Regulatory compliance with frameworks such as GDPR in Europe and HIPAA in the United States must be tightly integrated into computational ecosystems [113].

9. Conclusion

This chapter has examined the profound impact of Big Data on modern genomics, driven by high-throughput sequencing technologies that generate massive, heterogeneous, and complex biological datasets. While these data offer unprecedented opportunities for biological discovery and precision medicine, they also introduce significant challenges related to storage, scalability, computational efficiency, and analytical accuracy. The chapter highlighted the role of large genomic repositories and advanced computational infrastructures in enabling large-scale analysis, as well as the growing importance of pattern recognition, machine learning, and deep learning techniques for extracting meaningful information from genomic data. Particular emphasis was placed on the limitations of traditional statistical approaches when confronted with the volume, velocity, and complexity of contemporary sequencing data.

Building on this foundation, the next chapter, focuses on the practical application of these concepts. It presents a scalable, distributed deep learning framework designed to address the computational and methodological challenges of variant calling at population scale, bridging Big Data principles with state-of-the-art artificial intelligence techniques for accurate and efficient genomic analysis.

Chapter 3

Distributed Deep Learning Pipeline for Genomic Variant Calling

1. Introduction

This chapter presents a comprehensive distributed deep learning pipeline designed to address two fundamental challenges in modern genomic variant calling. First, the pipeline tackles the challenge of processing large-scale genomic datasets efficiently through distributed computing. Second, the pipeline addresses the challenge of integrating multiple data modalities to capture the rich, complementary information present in sequencing data. Our approach employs a hybrid transformer-CNN architecture that simultaneously processes one-dimensional sequence information and multi-dimensional pileup images, fusing these heterogeneous data sources through an attention-based mechanism. This multimodal learning strategy enables the model to leverage both the sequential patterns in DNA and the spatial patterns in read alignments, providing a more comprehensive representation of variant characteristics.

2. Data Collection

2.1 Source Data and Rational

Creating effective genomic variant calling systems necessitates the use of high-quality benchmark data that includes well-defined ground truth labels. In this study, we employ data from the Genome in a Bottle (GIAB) consortium, an initiative launched by the National Institute of Standards and Technology (NIST) to supply reference materials and data for human genome sequencing. GIAB sets the gold standard for assessing variant calling methods, providing high-confidence variant calls that have been validated through various sequencing technologies, library preparations, and bioinformatics pipelines.

2.1.1 GIAB Consortium Overview

The GIAB consortium has developed reference materials derived from several well-studied human cell lines, each representing a variety of genetic backgrounds. These reference samples have undergone extensive sequencing through various platforms, including Illumina short-read sequencing, PacBio long-read sequencing, and Oxford Nanopore sequencing. The resulting variant calls have been confirmed through utilizing multiple sequencing technologies allows for cross-validation across various platforms, minimizing biases specific to any one technology. Employing diverse analysis methods, such as integrating results from different variant callers like GATK, FreeBayes, and DeepVariant, enhances accuracy. Family-based validation, through examining Mendelian inheritance patterns in trios, helps confirm variant calls. Additionally, orthogonal validation is achieved through independent methods like array-based genotyping and Sanger sequencing. This thorough validation process ensures that the benchmark variants reflect genuine biological variation, rather than artifacts from sequencing or analysis.

2.1.2 Primary Training Sample: HG002

For training our deep learning model, we selected HG002 (NA24385) as the primary data source. HG002 is the son in an Ashkenazi trio consisting of:

- **HG003** (NA24149): Father
- **HG004** (NA24143): Mother
- **HG002** (NA24385): Son (primary training sample)

Rationale for HG002 Selection:

a. **Comprehensive coverage:** HG002 has been sequenced to high depth across multiple platforms, providing extensive training data.
b. **High-confidence regions:** GIAB has defined confident regions spanning approximately 2.5 gigabases (Gbp) of the human genome where variants can be called with high certainty.
c. **Trio validation:** Parent-child relationships enable Mendelian consistency checks, ensuring label quality.
d. **Community standard:** HG002 is widely used in the variant calling community, facilitating comparison with other methods.
e. **Diverse variant types:** Contains millions of SNPs, insertions, and deletions representative of human genetic variation.

2.1.3 Data Acquisition

The following data components were obtained from public repositories:

- **VCF Files (Variant Call Format)**

VCF files provide ground truth variant annotations for supervised learning, obtained from the GIAB FTP server as HG002_GRCh38_1_22_v4.2.1_benchmark.vcf.gz (version 4.2.1). The structured format contains chromosomal coordinates, reference and alternate alleles, genotype calls, and quality metrics from multiple sequencing platforms. Approximately 4 million high-confidence variant calls are compressed to 250 MB, representing multi-platform consensus. Each entry includes filter flags, quality scores, and allele frequency information enabling selective use of high-confidence variants. The pipeline uses VCF files to provide labeled targets for variant type classification (SNP, insertion, deletion) and genotype determination (heterozygous or homozygous alternate). This establishes correspondence between genomic positions and validated variant status for model training. Multi-platform consensus ensures high reliability of ground truth labels. Quality annotations allow threshold-based variant selection. These files form the foundational truth set for training and evaluation.

- **BAM Files (Binary Alignment Map)**

BAM files provide read-level evidence for feature extraction, obtained from GIAB repositories and NCBI SRA with ~35× coverage from Illumina HiSeq. The files contain 150 bp paired-end reads (350 bp median insert size) compressed to ~180 GB per sample. Each aligned read includes base quality scores (Phred-scaled error probabilities), mapping quality scores, CIGAR strings (alignment operations), and bitwise flags (strand orientation, pairing status). The pipeline extracts two critical features: reference and read sequences provide local genomic context, while read pileups capture base distributions, quality scores, and alignment properties at variant positions. This read-level information distinguishes true variants from sequencing artifacts, alignment errors, and technical noise. Quality scores enable probabilistic interpretation of observations. The substantial file size reflects comprehensive coverage necessary for confident detection. These files bridge raw sequencing data and variant calls, providing empirical evidence for model learning.

- **Reference Genome**

The GRCh38/hg38 reference genome (obtained from NCBI/UCSC) serves as the coordinate system and sequence baseline for variant definition. The primary assembly includes chromosomes 1-22, X, Y, and mitochondrial genome in FASTA format (~3.1 GB uncompressed). It provides sequence context for feature extraction, defines reference points for alternate alleles and coordinates, enables CIGAR string interpretation for read reconstruction, and establishes the coordinate system integrating VCF, BAM, and BED files. Reference sequence quality directly impacts analysis, as errors manifest as apparent variants. GRCh38 represents substantial improvements over previous builds: better genomic diversity representation, corrected assembly errors, and alternative loci for regions with structural variation. The reference establishes the universal framework for genomic position interpretation. Its accuracy is critical for reliable variant identification across all pipeline stages.

- **BED Files (Confident Regions)**

BED files define reliable variant calling regions, serving as quality control filters focusing analysis on analyzable genome portions. The HG002_GRCh38_1_22_v4.2.1_benchmark_noinconsistent.bed file delineates ~2.5 Gbp of confident regions (~80% of genome), excluding technically challenging segments: segmental duplications, centromeric/telomeric regions, areas with inadequate coverage, and regions producing inconsistent results across platforms. The pipeline uses BED files as spatial filters ensuring training examples derive from positions with reliable labels, preventing systematic noise from uncertain regions. This restricts analysis to confident regions where evaluation metrics accurately reflect model performance on reliably callable variants. BED coordinates must align precisely with

VCF and BAM coordinates for consistent position interpretation. These regions represent current technical limits of reliable detection. Their definition evolves as methods improve, potentially expanding callable genome coverage in future studies.

2.1.4 Validation and Test Samples

- **Validation Sample: HG003 (Father):** Used to tune hyperparameters and monitor training progress, and ensures model does not overfit to HG002-specific patterns.
- **Test Sample: HG004 (Mother):** Held out entirely from training and validation, used for final performance evaluation and enables assessment of generalization to unseen individuals.

2.2 Data Quality and Preprocessing

Before training, all data underwent rigorous quality control:

2.2.1 Sequencing Data Quality

Base quality scores are assessed to ensure a mean Phred score above 30, reflecting a 99.9% base-calling accuracy. Reads with low mapping confidence are filtered out by enforcing a minimum MAPQ threshold of 20, ensuring reliable alignment to the reference genome. Coverage uniformity is evaluated, requiring a coefficient of variation below 30% across genomic regions of interest. Additionally, PCR duplicates are identified, marked, and retained at a rate below 10%, maintaining data integrity while preventing artificial inflation of coverage.

2.2.2 Variant Call Quality

Following initial variant detection, results are refined through multiple quality assurance filters. Only variants with a PASS flag in the VCF file are retained, excluding low-confidence predictions. Analyses are restricted to high-confidence genomic regions, avoiding repetitive or poorly mappable loci. Mendelian consistency checks (≥ 99.9%) are applied for trio validation, and variants are cross-validated across at least two sequencing technologies to ensure reproducibility and eliminate platform-specific artifacts.

3. Dataset Description and Statistics

The complete training dataset derived from HG002 encompasses 4,088,122 high-confidence variants spanning chromosomes 1-22 and X, covering approximately 2.5 Gbp of confident callable regions with a density of ~1,620 variants per megabase. The dataset exhibits natural biological distribution characteristics, with SNPs representing the dominant variant class, while insertions and deletions constitute minor classes. The raw data comprises 180 GB of compressed BAM files and 250 MB of compressed VCF files, which expand to 2.3 TB of processed features including 450 GB of sequence encodings, 1.85 TB of pileup images, and auxiliary files.

3.1 Dataset Partitioning

The dataset was partitioned using a chromosome-based strategy to prevent data leakage while ensuring genomic diversity (Table 3.1). The training set contains 3,200,450 examples (98.82% extraction success rate) from alternating autosomal chromosomes (chr1, chr3, chr5, chr7, chr9, chr11, chr13, chr15, chr17, chr19, chr21), representing approximately 80% of total variants. Validation and test sets each comprise 400,056 samples (10% each), with validation on chr2, chr6, chr10, chr14, chr18, chr22 for hyperparameter tuning and early stopping detection from HG003, while test chromosomes (chr4, chr8, chr12, chr16, chr20) from HG004, were completely held out for final evaluation. Chromosome X was excluded from all partitions in the current study.

Partition	Sample Count	Chromosomes	Purpose	Coverage
Training (HG002)	3,200,450 (80%)	chr1, 3, 5, 7, 9, 11, 13, 15, 17, 19, 21	Model learning	~80% of variants
Validation (HG003)	400,056 (10%)	chr2, 6, 10, 14, 18, 22	Hyperparameter tuning, early stopping	~10% of variants
Test (HG004)	400,056 (10%)	chr4, 8, 12, 16, 20	Final evaluation, baseline comparison	~10% of variants

Table 3.1 Dataset Partitioning Strategy

3.2 Class Distribution Characteristics

A critical characteristic of the dataset is severe class imbalance reflecting true biological reality, where SNPs substantially outnumber insertions and deletions with an imbalance ratio exceeding 10:1. This distribution mirrors natural human genetic variation, where SNPs occur approximately every 300 base pairs while small indels are significantly less frequent but often more consequential due to potential frameshift effects. The genotype distribution follows diploid genome expectations, with heterozygous variants (0/1) comprising 65-70% of samples and homozygous alternate (1/1) representing 30-35%, while homozygous reference calls (0/0) were excluded from training to focus on variant genotyping. In the Table 3.2, classes distributions and proportions are summarized.

Category	**Distribution**	**Proportion**	**Notes**
Variant Types			
SNPs	Majority class	>10:1 ratio	Most common genetic variation
Insertions (INS)	Minority class	Significantly underrepresented	Biologically less frequent
Deletions (DEL)	Minority class	Significantly underrepresented	Potential frameshift impact
Genotypes			
Heterozygous (0/1)	Primary	65-70%	Expected diploid pattern
Homozygous alternate (1/1)	Secondary	30-35%	Consistent with population genetics
Allele Frequency			
Common (MAF >5%)	High frequency	~40%	Population polymorphisms
Low-frequency (0.5-5%)	Medium frequency	~25%	Intermediate variants
Rare (MAF ≤0.5%)	Low frequency	~35%	Rare mutations

Table 3.2 Variant and Genotype Characteristics

3.3 Data Quality and Limitations

The dataset demonstrates exceptional quality metrics with 98.82% feature extraction success rate, >99.9% Mendelian consistency in trio validation, and >99.5% multi-platform concordance. Technical quality is maintained through mean base quality of Phred 35+ (99.97% accuracy), mean mapping quality of MAPQ 40+ (99.99% correct alignment), and coverage uniformity with coefficient of variation under 25%. However, several limitations must be acknowledged: genomic coverage is restricted to ~2.5 Gbp confident regions (~80% of genome) excluding difficult regions like centromeres and segmental duplications; sample representation is limited to a single Ashkenazi individual (HG002) from a cell line; variant scope focuses on small variants (1-50 bp) excluding structural and copy number variants; sequencing is primarily Illumina short reads (150 bp) which may harbor platform-specific biases; and sex chromosomes (X and Y) were excluded from the current analysis to focus on autosomal variants. Table 3.3 summarize the data quality metrics characterizations.

Quality Aspect	Metric	Threshold/Value	Notes
Completeness			
Extraction success	98.82%	-	47,780 failures due to low coverage/gaps
Confident regions	100%	By definition	~2.5 Gbp coverage
Label Quality			
Mendelian consistency	>99.9%	Trio validation	High confidence ground truth
False discovery rate	<0.5%	Benchmark regions	Minimal false positives
False negative rate	<1%	Benchmark regions	High sensitivity
Technical Quality			
Mean base quality	Phred 35+	99.97% accuracy	High-quality sequencing
Mean mapping quality	MAPQ 40+	99.99% correct	Reliable alignments
Coverage uniformity	CV <25%	-	Consistent depth
GC bias	<5% deviation	-	Minimal technical bias

Table 3.3 Data Quality Metrics

4. Objective of the Methodology

The primary objective is to develop a scalable, accurate distributed deep learning pipeline for genomic variant calling that addresses two fundamental computational challenges:

4.1 Scalability and Computational Efficiency

The pipeline aims to process population-scale genomic datasets with high computational efficiency. Specific targets include training on datasets containing over 4 million variants while achieving near-linear scalability across multiple GPUs with greater than 90% parallel efficiency. The architecture supports seamless scaling to accommodate datasets of varying sizes and future expansion requirements.

4.2 Multimodal Learning

Integrate heterogeneous data sources to capture complementary variant information through two modalities: sequence context (DNA sequence surrounding the variant position), and alignment patterns (read pileup information showing sequencing evidence).

Genomic variants are best characterized by multiple evidence types. Sequence context reveals biological constraints such as motifs, conservation patterns, and CpG islands, while alignment patterns expose technical artifacts including strand bias, mapping quality issues, and systematic sequencing errors. Fusing these modalities enables comprehensive variant characterization that captures both biological signals and technical quality indicators.

5. Pipeline Overview

The distributed genomic variant calling pipeline (figure 3.1) consists of six major stages that transform raw sequencing data into variant calls through a series of well-defined processing steps. The architecture is designed for modularity, scalability, and production readiness.

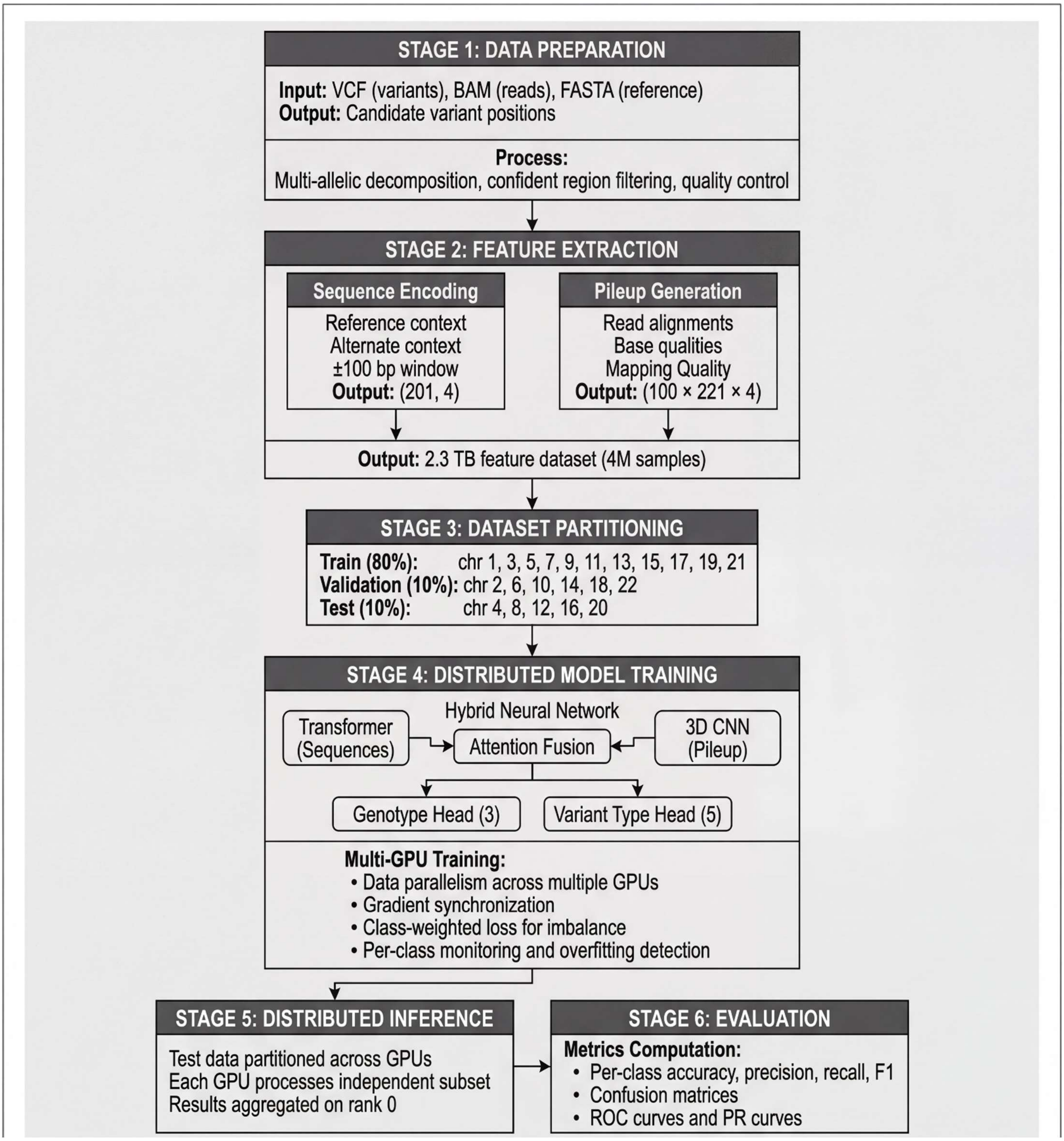

Figure 3.1 Proposed Distributed Variant Calling Pipeline

In the next section we will provides detailed explanation of the major steps in the pipeline.

5.1 Feature Extraction

Extract multimodal features capturing both biological context and technical sequencing evidence for each variant through complementary information sources.

5.1.1 Sequence Feature Extraction

DNA sequence context is extracted using fixed-width windows (±100 base pairs, yielding 201 positions) centered on each variant locus from the reference genome (Figure 3.2). These sequences undergo one-hot encoding where each nucleotide maps to a unique binary vector: A= [1,0,0,0], C= [0,1,0,0], G= [0,0,1,0], T= [0,0,0,1], with ambiguous bases (N) or gaps encoded as [0,0,0,0]. This generates a [201 × 4] matrix preserving nucleotide identity as categorical information without imposing artificial numerical relationships.

One-hot encoding maintains discrete categorical features, provides computational efficiency, ensures fixed-length inputs for batch processing, and enables neural networks to automatically learn sequence patterns including compositional biases, k-mer frequencies, and regulatory motifs without explicit feature engineering.

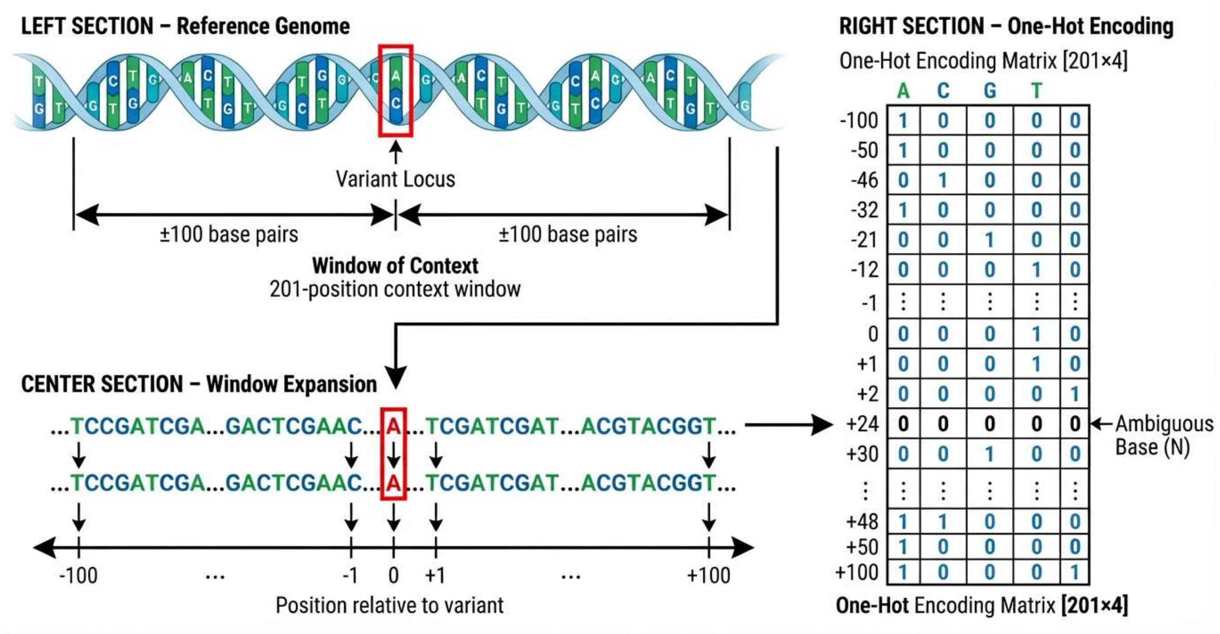

Figure 3.2 DNA Sequence Context Extraction and One-hot Encoding Process

5.1.2 Pileup Image Generation

Read alignments at variant loci are transformed into fixed-size, structured 4D tensors to enable three-dimensional convolutional learning (Figure 3.3). For each candidate variant, reads overlapping a 221-base-pair genomic window are extracted from BAM files and organized into tensors of shape [Batch × 100 × 221 × 4]. The representation captures up to 100 reads ordered by descending mapping quality, ensuring that high-confidence evidence occupies consistent spatial positions. Four channels encode complementary information: base identity, base quality, mapping quality, and strand orientation. Regions with insufficient coverage are padded, while excessive coverage is truncated to retain the most reliable reads. This encoding preserves spatial relationships across read depth, genomic position, and evidence channels, enabling the model to detect strand bias, systematic sequencing errors, and alignment artifacts. The conversion from irregular alignment records to fixed-dimension tensors balances information richness with computational efficiency, facilitating batch processing on GPUs while maintaining the spatial structure essential for accurate convolutional feature extraction.

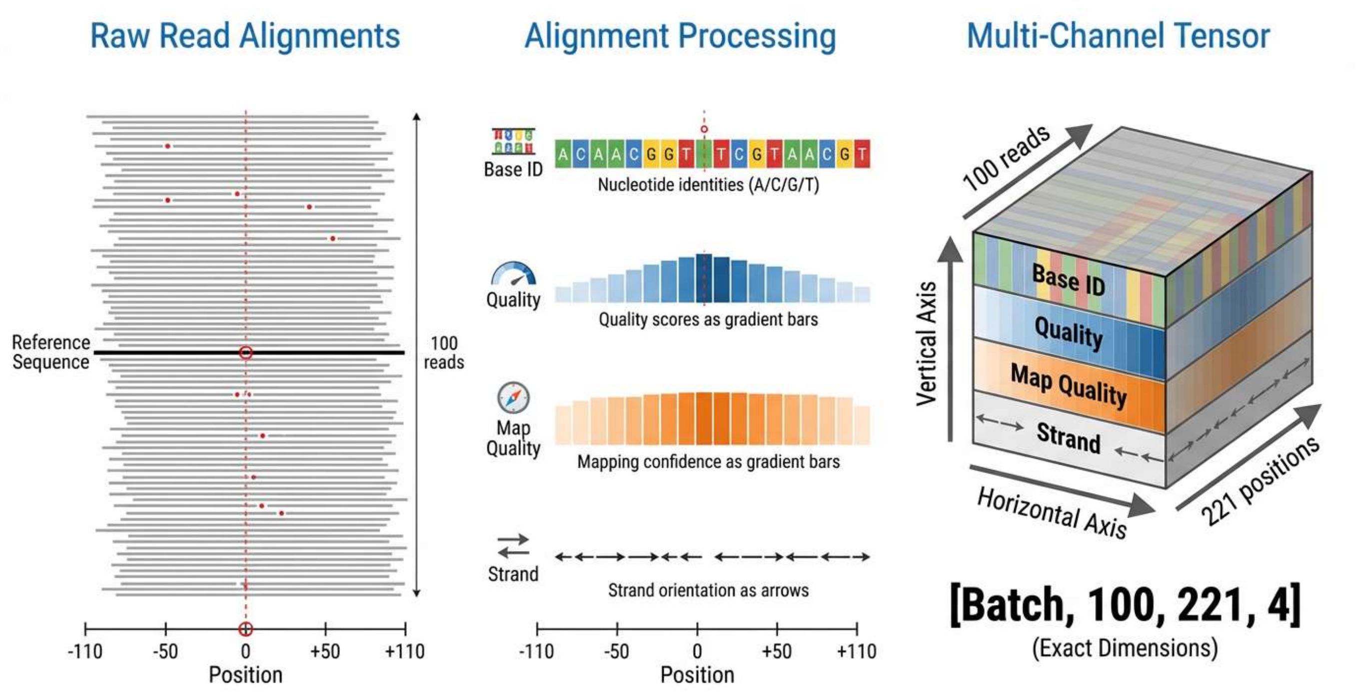

Figure 3.3 Pileup Image Generation Process

Table 3.4 summarizes the encoding procedures, the information captured, and the output dimensions for both the sequence and pileup image representations.

Feature Type	Dimensions	Key Encoding Steps	Information Captured	Storage per Sample
Sequence Context	201 × 4	Extract ±100 bp window → One-hot encode nucleotides	Local sequence patterns, compositional biases, mutational hotspots	3,2 KB
Pileup Image	100 × 221 × 4	Extract overlapping reads → Multi-channel tensor encoding	Read evidence quality, strand bias, mapping confidence, artifact signatures	345 KB

Table 3.4 Feature Extraction Specifications

5.1.3 Label Extraction

Ground truth labels are derived from high-quality benchmark variant callsets through systematic matching procedures using strict criteria encompassing genomic coordinates and allelic identity, assigning binary classifications and extracting genotype information, quality scores, and filter status. Supervised learning reliability fundamentally depends on label quality, necessitating extensively validated benchmark datasets such as those from the Genome in a Bottle Consortium, generated through integration of multiple orthogonal sequencing technologies with extensive manual curation. These benchmarks represent consensus calls with extremely low error rates (typically below 10^{-4} per base), incorporating short-read, long-read, and linked-read platforms validated through pedigree analysis. Anchoring model training to such high-confidence labels ensures learned patterns reflect genuine biological variation rather than systematic errors in training data.

5.2 Neural Network Architecture

5.2.1 Sequence Encoder with Transformer Architecture

The sequence encoding module converts local DNA context into a compact, biologically informed embedding using a hybrid CNN–Transformer architecture. As illustrated in Figure 3.4, the input is a one-hot encoded DNA window of shape [Batch × 201 × 4], representing ±100 bp around the variant with four nucleotide channels (A, C, G, T). An initial 1D convolutional layer with 64 filters and kernel size 7 extracts short-range *k-mer* and motif patterns, producing feature maps of [Batch × 201 × 64] that capture local compositional signals.

To preserve positional information critical for attention, sinusoidal positional encoding is added to the convolutional features, enabling the model to distinguish identical motifs at different genomic locations. The encoded sequence is then processed by four stacked Transformer encoder layers, each with 8-head self-attention operating on 64-dimensional representations. This design allows the model to capture long-range dependencies across the full 201 bp window, modeling interactions between distant bases that are biologically relevant (e.g., regulatory motifs or repetitive contexts). Each encoder layer includes layer normalization, residual connections, a feed-forward network (256 hidden units, ReLU), and dropout (p = 0.1) to stabilize training and reduce overfitting.

Finally, global average pooling aggregates the position-wise outputs [Batch × 201 × 64] into a fixed-length sequence embedding of [Batch × 64]. This embedding summarizes nucleotide composition, motif structure, conservation-related patterns, and long-range contextual dependencies, providing biologically grounded evidence that complements pileup-based alignment features in subsequent multimodal fusion and variant prediction stages.

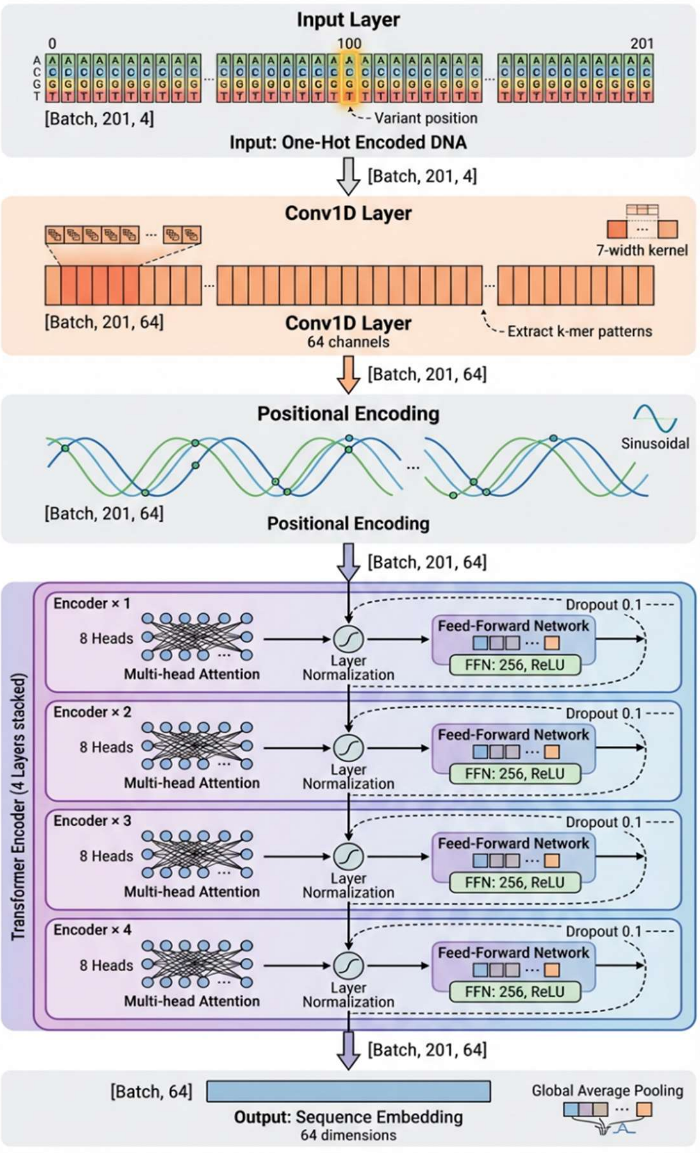

Figure 3.4 Sequence Encoding Module with hybrid CNN–Transformer architecture

5.2.2 Pileup Encoder with Three-Dimensional Convolutional Architecture

The pileup encoding module uses a 3D CNN to transform raw read-alignment data into a compact, informative embedding. As shown in the figure 3.5 , the input is a 4D pileup tensor of shape [Batch ×

100 × 221 × 4], representing 100 aligned reads across 221 genomic positions with four channels (base identity, base quality, mapping quality, and strand).

The network is composed of three hierarchical Conv3D blocks:

- **Block 1**: applies 32 filters with a (3×7×4) kernel, followed by batch normalization, ReLU, and (2×2×1) max pooling, reducing the tensor to [Batch × 50 × 110 × 32].
- **Block 2**: uses 64 filters with (3×5×1) kernels and identical normalization and pooling, producing [Batch × 25 × 55 × 64].
- **Block 3**: applies 128 filters with (3×3×1) kernels, yielding [Batch × 12 × 27 × 128].

This hierarchical design enables multi-scale feature extraction, where early layers capture fine-grained read- and quality-level patterns, while deeper layers aggregate broader spatial context to distinguish true variants from sequencing or alignment artifacts (e.g., strand bias or low mapping quality). Batch normalization stabilizes training across heterogeneous channels.

Finally, adaptive average pooling compresses the spatial dimensions to [Batch × 1 × 1 × 128], which is flattened into a 128-dimensional pileup embedding. This embedding summarizes alignment consistency, quality, and variant evidence, and is suitable for downstream fusion tasks.

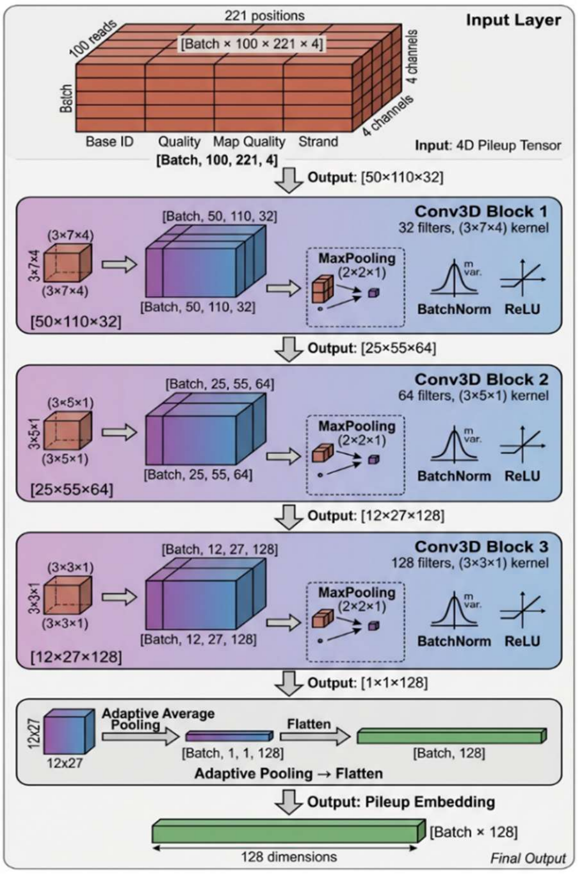

Figure 3.5 Pileup Encoder 3D CNN Architecture

5.2.3 Attention-Based Multimodal Fusion

The fusion module as in Figure 3.6 performs cross-attention–based integration of sequence and pileup information, enabling adaptive, context-aware evidence weighting rather than simple concatenation. The sequence embedding [Batch×64] is first linearly projected to 128 dimensions, while the pileup embedding already resides in [Batch×128] (identity projection). Cross-attention is then applied with sequence features as queries (Q) and pileup features as keys (K) and values (V). Attention weights are computed via scaled dot-product attention :

$$softmax\ (\frac{QK^T}{\sqrt{128}}) \qquad \textbf{3.1}$$

dynamically emphasizing pileup signals that are most relevant to the sequence context. This mechanism allows context-dependent modulation: for example, sequence patterns indicative of homopolymers increase the weight of base-quality cues, whereas repetitive regions shift emphasis toward mapping-quality evidence. The resulting attended pileup vector [Batch×128] is concatenated with the projected sequence vector to form a 256-dimensional representation.

A lightweight MLP refines this joint representation through Linear(256→128) with ReLU and dropout, followed by Linear(128→64) with ReLU and dropout, yielding a compact 64-dimensional fused embedding. This final representation captures synergistic interactions between biological constraints (sequence) and observational evidence (pileup), providing a robust foundation for downstream multi-task prediction.

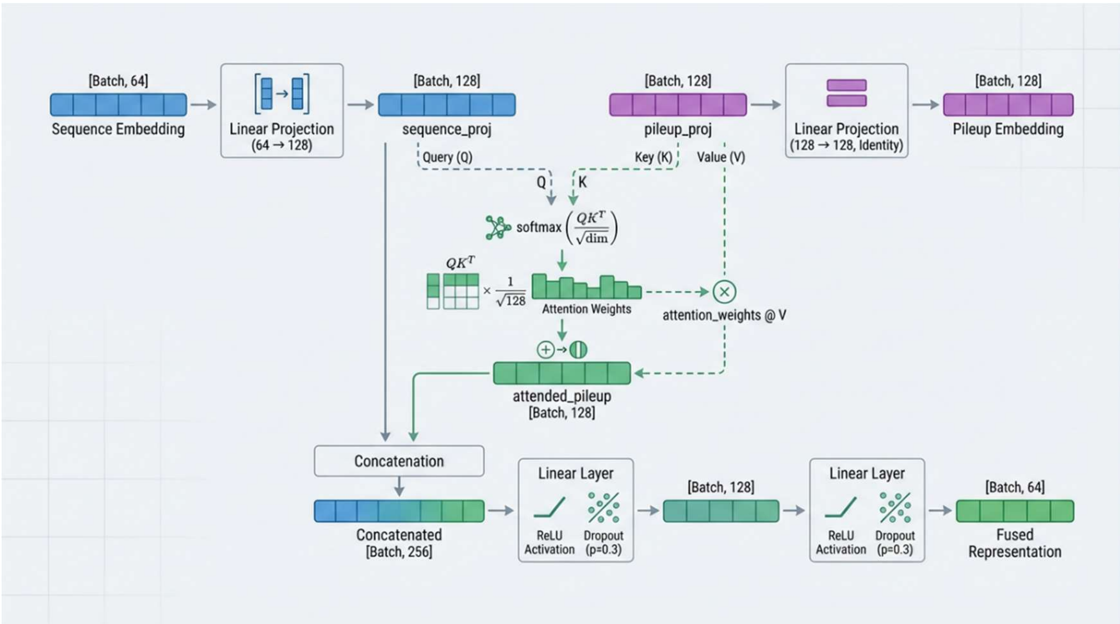

Figure 3.6 Attention-Based Multimodal Fusion Module

5.2.4 Multi-Task Prediction Architecture

The proposed architecture adopts a multi-task learning strategy with four parallel prediction heads operating on a shared fused representation of size [Batch×64]. These heads are jointly trained to perform: variant type classification, genotype prediction, quality score estimation, and variant authenticity classification (Figure 3.7). Each head follows a consistent design a linear projection (64→32), ReLU activation, dropout (p = 0.2), and a task-specific output layer, producing outputs of dimensions

[Batch×5] for variant type, [Batch×3] for genotype, [Batch×1] for quality, and [Batch×2] for authenticity.

This multi-task formulation offers several advantages. First, auxiliary tasks provide complementary gradient signals that improve representation learning in shared encoders. Second, joint optimization acts as an implicit regularizer, reducing overfitting by enforcing representations that generalize across related objectives. Third, the additional outputs enhance interpretability and practical utility by simultaneously delivering variant annotations, genotype calls, confidence scores, and artifact filtering indicators.

To address the pronounced class imbalance in genomic data—where SNPs dominate—the variant type task applies inverse-frequency class weighting. The genotype prediction task reinforces allele dosage learning, exploiting the correlation between expected diploid ratios (e.g., ~50% for heterozygous variants) and variant authenticity. Quality score regression enables calibrated, Phred-scaled confidence estimation, facilitating downstream precision–recall trade-offs, while the authenticity task supports robust discrimination between true variants and sequencing artifacts.

Training is guided by a weighted composite loss:

$$L_{total}=\lambda_1 L_{variant}+\lambda_2 L_{genotype}+\lambda_3 L_{quality}+\lambda_4 L_{authenticity} \qquad 3.2$$

with weights $\lambda_1=1.0$, $\lambda_2=0.5$, $\lambda_3=0.3$ and $\lambda_4=0.8$, reflecting task importance and supervisory contribution. During inference, the model outputs a comprehensive variant characterization: variant class and genotype are selected via maximum probability, quality scores provide continuous confidence estimates, and authenticity is determined through probabilistic thresholding (typically 0.5), enabling effective filtering and ranking of variant calls.

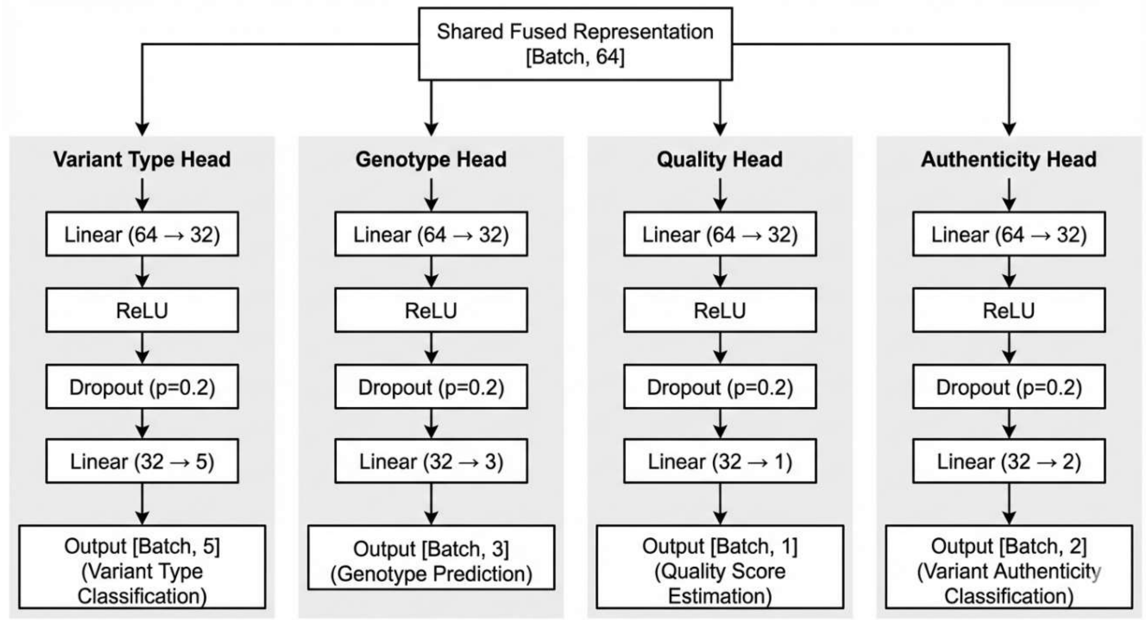

Figure 3.7 Multi-Task Prediction Architecture Module

5.3 Class Imbalance Handling

Genomic variant calling exhibits severe class imbalance, with single nucleotide polymorphisms (SNPs) vastly outnumbering insertions and deletions (indels). Without explicit correction, models trained under standard empirical risk minimization tend to degenerate toward majority-class prediction, achieving high overall accuracy while failing on clinically critical minority variants. The proposed framework addresses this challenge through loss reweighting, multi-task optimization, and per-class monitoring.

5.3.1 Inverse Frequency Class Weighting

To counteract imbalance, class-specific weights are computed using inverse frequency statistics derived from the training data. Each class weight is proportional to the inverse of its sample frequency and normalized to maintain numerical stability. This reweighting increases the contribution of underrepresented variant types to the loss function, ensuring that errors on rare classes (insertions and deletions) are penalized as strongly as errors on frequent SNPs.

This approach effectively transforms the optimization objective from minimizing loss under the empirical (imbalanced) distribution to minimizing loss under a balanced class distribution, preventing trivial solutions where the model predicts only the majority class. As a result, minority class variants exert sufficient influence during training to shape the learned representations.

5.3.2 Weighted Multi-Task Loss Formulation

The overall training objective combines a weighted classification loss with auxiliary task losses in a unified multi-task framework. Variant type classification uses weighted cross-entropy, directly incorporating the inverse frequency weights. Auxiliary objectives genotype prediction and quality estimation, employ standard loss functions (categorical cross-entropy and mean squared error, respectively).

These losses are combined through a weighted summation, where classification is assigned the highest priority as the primary task, and auxiliary tasks receive smaller weights to provide complementary gradient signals without dominating optimization. This design improves shared feature learning while preserving focus on accurate variant classification. Proper tuning of task weights is essential to balance multi-task benefits against potential interference.

5.3.3 Per-Class Performance Monitoring

Model evaluation is performed using per-class metrics rather than aggregate scores. Precision, recall, F1-score, confusion matrices, ROC-AUC, and precision–recall AUC are computed independently for SNPs, insertions, and deletions. This granular monitoring exposes performance disparities that global metrics obscure in imbalanced settings.

Per-class evaluation is particularly important in genomics, where minority variants, especially indels often have disproportionate functional and clinical impact, such as frameshift mutations affecting protein structure. By explicitly tracking class-specific performance, the training process ensures that improvements in overall accuracy do not come at the expense of minority variant detection.

5.4 Distributed Data Parallel (DDP) Training Strategy

Distributed Data Parallel is a parallelization technique that accelerates neural network training by distributing data across multiple computational devices while maintaining identical model replicas on each device. Unlike model parallelism, which partitions the model itself, DDP replicates the entire model architecture and parameters across all devices, enabling simultaneous processing of different data subsets. This approach achieves near-linear scaling efficiency for large batch training by minimizing communication overhead and maximizing computational resource utilization.

5.4.1 Model Replication

In DDP, each computational device (GPU) maintains a complete replica of the neural network with identical architecture and synchronized parameters. At initialization, model weights are broadcast from a master process to all worker processes, ensuring all replicas begin with the same parameter values (Figure 3.8). Throughout training, these replicas remain synchronized through collective communication operations. This replication strategy ensures consistency across devices while allowing independent computation on different data batches, effectively multiplying the throughput without compromising model integrity.

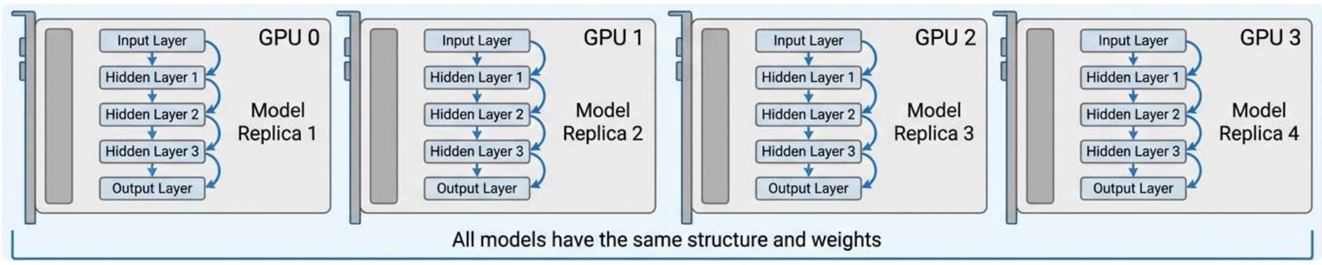

Figure 3.8 Model Replication Across GPUs

5.4.2 Data Partitioning Strategy

The training dataset is partitioned into non-overlapping subsets, with each device processing a unique batch of data during each training iteration (Figure 3.9). The partitioning is performed by a distributed sampler that ensures no data duplication across devices and maintains balanced workload distribution. For a global batch size of N distributed across K devices, each device processes N/K samples independently. This parallel data processing eliminates the sequential bottleneck of single-device training and enables effective utilization of multiple computational resources simultaneously.

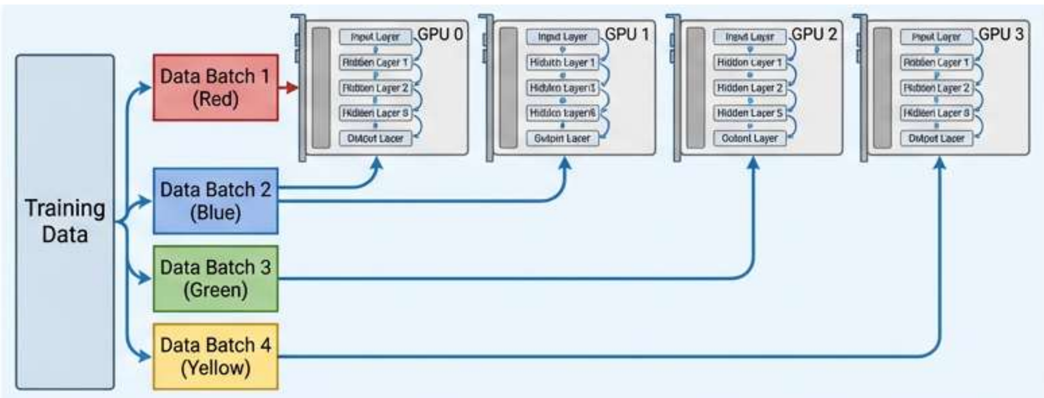

Figure 3.9 Data Distribution Across GPUs Devices

5.4.3 Forward Pass and Loss Computation

Each GPU independently executes the forward pass through its model replica using its assigned data batch. The computation proceeds through the input layer, hidden layers, and output layer without any inter-device communication, as each replica operates on different data (Figure 3.10). After generating predictions, each device computes its local loss value by comparing predictions against ground truth labels. These local losses reflect the model's performance on different data subsets and are used for gradient computation. The independence of forward pass operations across devices maximizes parallel efficiency and minimizes communication overhead.

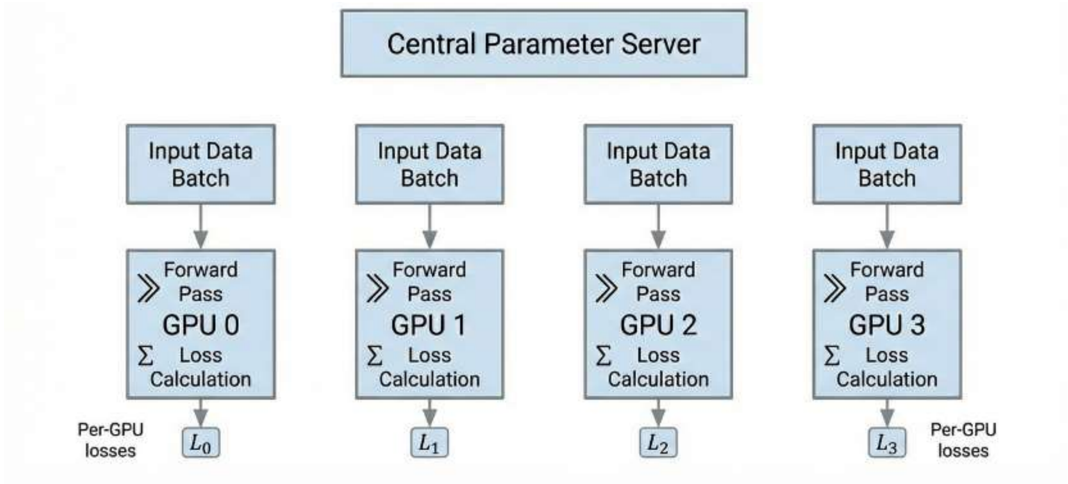

Figure 3.10 Forward Pass

5.4.4 Gradient Synchronization via All-Reduce

Once gradient averaging completes, all devices simultaneously update their model parameters using the synchronized gradients and the chosen optimization algorithm (Adam) (Figure 3.11). The parameter update formula is:

$$W' = W - \eta.\, 1/k \sum_{i=1}^{k} \nabla \mathrm{L}_i \qquad \textbf{3.3}$$

applies identically across all devices, where $\boldsymbol{\eta}$ is the learning rate and $\boldsymbol{\Sigma\nabla L}$ represents the averaged gradient of all GPUs (k=number of GPUs). Since all replicas receive identical averaged gradients and apply the same update rule, parameter consistency is maintained across devices without additional synchronization. This simultaneous update mechanism ensures all replicas remain synchronized for the next training iteration, maintaining model coherence throughout the distributed training process.

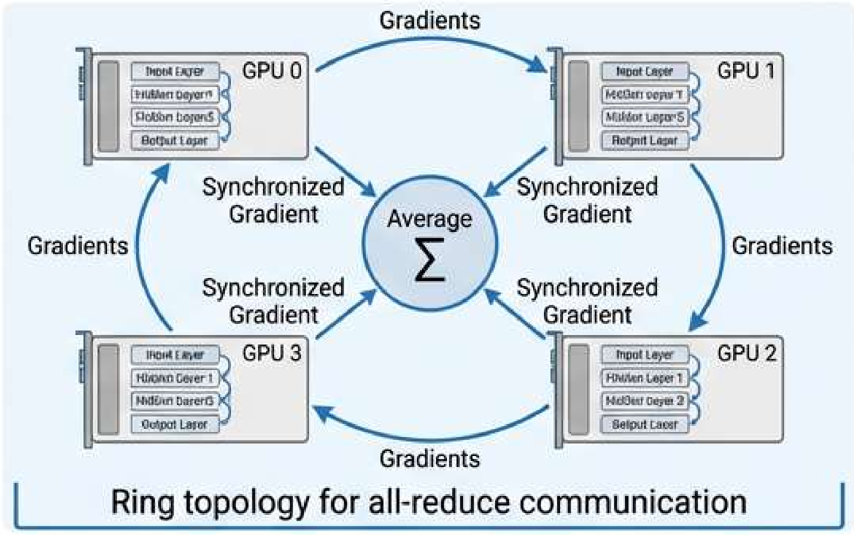

Figure 3.11 Gradients Synchronization

5.4.5 Computational Efficiency and Scalability

DDP achieves significant training acceleration by exploiting data parallelism while maintaining minimal communication overhead. The all-reduce operation scales logarithmically with the number of devices, making DDP efficient for large-scale distributed training. Communication occurs only during gradient synchronization, while computationally intensive operations (forward pass, backpropagation) execute independently on each device. This design enables near-linear speedup as the effective batch size increases proportionally with the number of devices. For large models and datasets, DDP reduces training time from weeks to hours while ensuring numerical equivalence to single-device training with appropriately scaled learning rates.

6. Evaluation Methodology

The experimental protocol establishes a comprehensive and rigorous framework for evaluating the proposed distributed deep learning pipeline for genomic variant calling. This evaluation framework addresses three fundamental research questions that are critical to assessing the scientific contribution and practical utility of the proposed methodology:

- **Performance efficacy:** Does the hybrid transformer-CNN architecture with multimodal learning achieve superior classification accuracy compared to established state-of-the-art variant calling methods?
- **Computational efficiency:** Does the distributed deep learning implementation provide scalable performance improvements that justify the architectural complexity in production genomic workflows?

- **Generalization capability:** Does the model demonstrate robust performance across diverse genomic contexts, variant types, and previously unseen chromosomal regions?

The evaluation methodology employs a multi-dimensional assessment strategy that examines: (i) classification performance stratified by variant type and genomic context; (ii) computational efficiency metrics in distributed computing environments; and (iii) generalization capability through held-out chromosome evaluation. This comprehensive approach ensures that the proposed method is evaluated not merely on aggregate performance metrics, but on its ability to address the specific challenges and limitations identified in current variant calling approaches (Poplin et al., 2018; Zheng et al., 2022).

The experimental design adheres to established best practices in genomic benchmarking (Krusche et al., 2019), including: stratified evaluation on chromosomes completely withheld from training; per-class performance analysis to address the severe class imbalance inherent in genomic variant data; and direct comparison with production-grade baseline methods using identical input data, reference genomes, and high-confidence calling regions. Figure 3.12 illustrates the complete evaluation pipeline, from test data preparation through statistical significance testing.

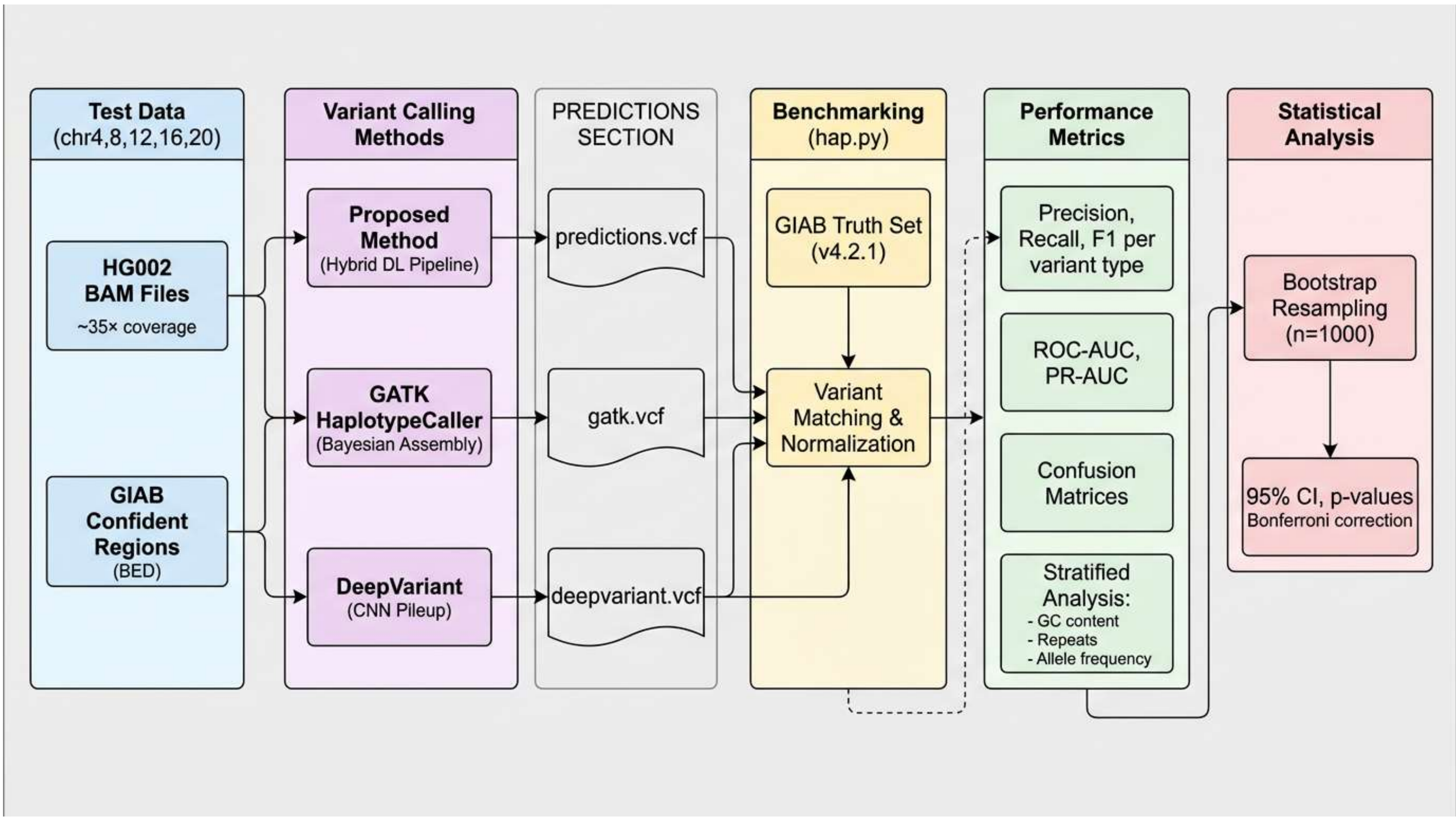

Figure 3.12 Proposed Test Framework

6.1 Test Data Preparation and Curation

The evaluation employs a strict held-out chromosome strategy to assess model generalization to previously unseen genomic regions. Five chromosomes—chr4, chr8, chr12, chr16, and chr20 were selected from the HG002 sample (GIAB Ashkenazi trio son, NA24385) and completely excluded from all training and validation procedures. This selection strategy was designed to satisfy three critical criteria:

- **Criterion 1 Chromosomal diversity:** The selected chromosomes span a range of sizes (chr4: 190.2 Mb; chr8: 145.1 Mb; chr12: 133.3 Mb; chr16: 90.3 Mb; chr20: 64.4 Mb) and represent diverse genomic characteristics, including varying GC content distributions (chr4: 38.2%; chr8: 40.1%; chr12: 40.7%; chr16: 44.8%; chr20: 44.0%), gene densities, and repetitive element compositions.
- **Criterion 2 Variant representation:** Collectively, these chromosomes contain approximately 18.5% of the total high-confidence variant calls in HG002, ensuring sufficient statistical power for performance assessment while maintaining substantial training data for model development.
- **Criterion 3 Community precedent:** The selection aligns with established practices in variant calling benchmarking (Poplin et al., 2018; Zheng et al., 2022), facilitating comparison with published results and ensuring reproducibility.

This held-out strategy represents a more stringent evaluation than k-fold cross-validation within chromosomes, as it tests the model's ability to generalize to entirely new chromosomal contexts rather than merely interpolating within familiar genomic neighborhoods.

6.2 High-Confidence Region Definition

Evaluation is confined to the Genome in a Bottle (GIAB) high-confidence regions (version 4.2.1), which delineate genomic intervals where variant calls are supported by multi-technology consensus and extensive experimental validation, thereby providing a reliable ground truth for benchmarking (Zook et al., 2020). Restricting analysis to these regions minimizes ambiguity arising from alignment artifacts, sequencing biases, and unresolved structural complexity.

Specifically, the GIAB high-confidence set excludes genomic regions known to confound variant detection, including:

- Segmental duplications, defined as duplicated sequences longer than 1 kb with ≥90% sequence identity elsewhere in the genome, which introduce read-mapping ambiguity;

- Centromeric and pericentromeric regions, dominated by highly repetitive α-satellite arrays that are poorly resolved by short-read sequencing;
- Telomeric and subtelomeric regions, characterized by terminal TTAGGG repeats and adjacent duplications;
- Low-complexity sequences, such as simple repeats and homopolymeric runs exceeding 20 base pairs, which are prone to systematic sequencing errors;
- Regions with insufficient sequencing depth, defined as coverage below 10× in any GIAB-supported dataset; and
- Loci exhibiting discordant variant calls across sequencing technologies or analytical pipelines.

6.3 Baseline Methods for Comparative Evaluation

To ensure a rigorous and unbiased evaluation, the proposed framework is benchmarked against two fundamentally different variant calling methodologies that were described in detail in the previous chapter: the statistical, assembly-based approach of GATK HaplotypeCaller and the deep learning based approach of DeepVariant. These baselines represent the two dominant paradigms in modern variant calling probabilistic modeling and convolutional neural inference. All methods are executed on the same input BAM files, reference genome, and GIAB high-confidence test regions, enabling a fair, controlled comparison that isolates methodological differences rather than data- or protocol-induced variability.

6.4 hap.py (haplotype) Variant Matching

Variant call comparisons are conducted using hap.py, a standardized benchmarking framework that evaluates concordance through haplotype-based sequence matching rather than direct positional comparison [114]. Both predicted VCFs and benchmark truth sets are first normalized, left-aligned, and decomposed into primitive variants, after which hap.py reconstructs local haplotypes and performs sequence-level alignment to identify equivalent variant representations, thereby resolving ambiguities arising from indel realignment, MNP decomposition, or complex variant representations (Figure 3.13). Each predicted variant is classified as a true positive (TP), false positive (FP), or false negative (FN), with genotype concordance evaluated separately, while variants outside GIAB high-confidence regions (v4.2.1) are excluded from metric computation [115]. For each evaluated method, hap.py generates a summary report containing aggregate counts of truth and query variants, TP, FP, and FN, along with derived precision, recall, and F1-score, reported independently for SNPs, indels, and the combined variant set.

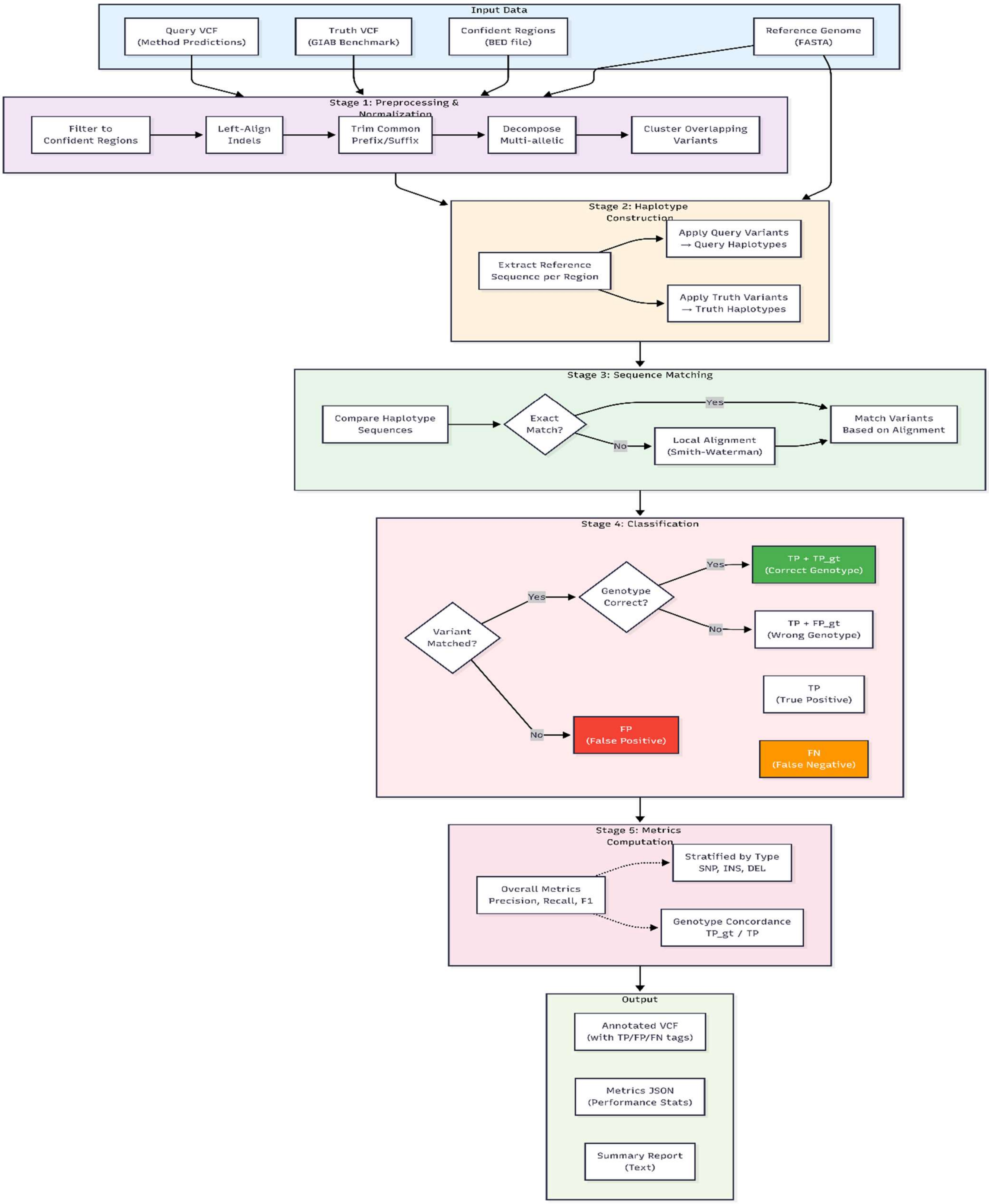

Figure 3.13 Haplotype Benchmarking Framework Architecture

7. Conclusion

This chapter presented a comprehensive distributed deep learning pipeline for genomic variant calling, designed to jointly address scalability constraints and the need for richer variant representations in modern genomics. By combining sequence context modeling with Transformer encoders and alignment-aware pileup modeling using 3D CNNs, the proposed architecture captures both biological signals and technical sequencing evidence in a unified framework. The integration of an attention-based multimodal fusion mechanism enables adaptive weighting of heterogeneous evidence sources, improving robustness across variant types and genomic contexts.

The pipeline was built upon high-confidence GIAB benchmark data, ensuring reliable supervision and rigorous evaluation, and adopted a chromosome-level partitioning strategy to prevent data leakage and assess true generalization. A multi-task learning formulation further enhanced model interpretability by jointly predicting variant type, genotype, quality score, and authenticity. Scalability was achieved through Distributed Data Parallel training, demonstrating near-linear speedup on multi-GPU infrastructure while preserving numerical equivalence with single-GPU optimization.

A rigorous evaluation protocol was defined, including haplotype-based comparison using hap.py, per-class performance analysis, and direct benchmarking against GATK HaplotypeCaller and DeepVariant, representing statistical and deep learning paradigms respectively, as detailed earlier in the manuscript.

The quantitative results and comparative analysis of this framework will be finalized and presented in a dedicated scientific journal article, building upon the methodological foundations established in this chapter and positioning the proposed approach as a scalable, interpretable, and next-generation solution for population-scale variant calling.

Chapter 4

Case Study in Knowledge Discovery: Arabic Handwriting Character Recognition

1. Introduction

Arabic Handwriting Character Recognition (AHCR) is presented as a representative real-world application of knowledge discovery, situated at the intersection of pattern recognition, computer vision, and cultural informatics. The complexity of Arabic script, characterized by high variability, contextual shapes, and rich structural dependencies, poses significant challenges that require advanced feature representation and deep learning techniques. Beyond its technical relevance, AHCR holds strong cultural and historical importance, supporting the digitization and preservation of Arabic manuscripts and documents. The problem naturally embodies Big Data characteristics, including high-dimensional inputs, large-scale datasets, and the need for scalable computational architectures. Building on the theoretical foundations of Big Data mining and pattern recognition established in earlier chapters, this chapter demonstrates the practical application of these concepts through AHCR. In particular, it highlights the effectiveness of hybrid deep neural architectures, such as Capsule Networks combined with Residual Networks in capturing complex spatial relationships in handwritten data. The chapter illustrates a complete knowledge discovery pipeline, from data acquisition and preprocessing to deep feature learning and multi-dataset validation, emphasizing the iterative interplay between domain knowledge, model design, and empirical evaluation.

2. Background on Arabic Handwriting Recognition

Handwriting recognition systems, including digit, character, and word recognition, are widely utilized in various applications. These systems play a crucial role in banking check processing, office automation, document digitization, content-based document retrieval, signature verification, postal code recognition, and digital character identification. By automating these complex tasks, handwriting recognition enhances operational efficiency, reduces human error, and improves accuracy, thereby driving advancements in technological and industrial sectors.

The recognition of Arabic handwritten characters introduces unique challenges and opportunities within the broader field of handwriting recognition. With over 400 million native speakers, Arabic is one of the most widely spoken languages globally [116], holding cultural, historical, and religious significance. Its cursive nature, contextual letterforms, and diacritical marks make character segmentation and recognition more complex compared to non-cursive scripts [117]. Additionally, Arabic has a rich historical manuscript tradition, with numerous texts remaining un-digitized or poorly preserved. These manuscripts, often written in calligraphic styles such as Kufic, Naskh, and Thuluth, present both linguistic and computational challenges in the development of robust recognition models [118]. Despite the growing interest in handwriting recognition, the field of Arabic handwritten character recognition (AHCR) faces a significant shortage of comprehensive and high-quality datasets [119]. The scarcity of well-annotated datasets poses a significant challenge to building robust deep learning models [120], as it hampers their ability to perform consistently across diverse handwriting styles and unseen data. Enhancing the robustness of Arabic OCR systems is essential not only for improving recognition accuracy but also for ensuring reliable performance in real-world applications.

2.1 Characteristics and Challenges of Arabic Writing

The Arabic script consists of 28 distinct characters (letters), written from right to left, and unlike many other writing systems, it does not employ upper-or lower-case forms. A defining feature of Arabic script is the contextual shaping of its characters, where the form of each letter varies depending on its position within a word. Specifically, most letters exhibit two primary forms: disconnected (isolated) and connected, with the latter further categorized into initial (beginning of a word), medial (middle of a word), and final (end of a word) forms (Table. 4.1). This unique morphological characteristic not only contributes to the script's visual elegance and aesthetic appeal but also introduces significant challenges for automated recognition, processing, and computational analysis systems.

In Arabic script, the letter Alif (أ) has a simplified form known as Hamza (ء). The Hamza demonstrates several graphical variations depending on its position within a word, such as in the middle or at the end, and it can appear in combination with other characters. These positional variants are fundamental to the orthographic system of Arabic and contribute to the script's rich visual and structural complexities. Examples include the isolated Hamza (ء), middle form (ـئـ), end form (ئ), above waw (ؤ), above Alif (ـأ), below Alif (ـإ), and initial connected (ئـ). Such diversity illustrates that the Arabic writing system cannot be adequately represented through isolated forms alone, as contextual placement transforms the graphical structure and, in some cases, the semantic interpretation of a character.

N°	Letter	Letter's Form Variations			
		Disconnected (Isolated)	Connected		
			Initial	Medial	Final
1	Alif	أ	-	-	-
2	Baa	ب	بـ	ـبـ	ـب
3	Taa	ت	تـ	ـتـ	ـت
4	Thaa	ث	ثـ	ـثـ	ـث
5	Jeem	ج	جـ	ـجـ	ـج
6	Haa	ح	حـ	ـحـ	ـح
7	Khaa	خ	خـ	ـخـ	ـخ
8	Daal	د	-	-	ـد
9	Dhal	ذ	-	-	ـذ
10	Raa	ر	-	-	ـر
11	Zaa	ز	-	-	ـز
12	Seen	س	سـ	ـسـ	ـس
13	Sheen	ش	شـ	ـشـ	ـش
14	Saad	ص	صـ	ـصـ	ـص
15	Dhad	ض	ضـ	ـضـ	ـض
16	Tta	ط	طـ	ـطـ	ـط
17	Dha	ظ	ظـ	ـظـ	ـظ
18	Ain	ع	عـ	ـعـ	ـع
19	Ghain	غ	غـ	ـغـ	ـغ
20	Faa	ف	فـ	ـفـ	ـف

21	Qaf	ق	قـ	ـقـ	ـق
22	Kaaf	ك	كـ	ـكـ	ـك
23	Laam	ل	لـ	ـلـ	ـل
24	Meem	م	مـ	ـمـ	ـم
25	Noon	ن	نـ	ـنـ	ـن
26	Haa	ه	هـ	ـهـ	ـه
27	Waaw	و	-	-	ـو
28	Yaa	ي	يـ	ـيـ	ـي

Table 4.1 List of All Arabic Letters' Variations

However, widely used datasets, such as the AHCD [121] and ALIF [122], which are restricted to isolated character representations, fail to capture these essential contextual and positional variations. While valuable for initial benchmarking, these corpora are limited in their applicability to real-world handwriting recognition tasks, where characters almost always appear in connected or context-dependent forms. By excluding Hamza variants and positional dependencies, such datasets neglect a fundamental dimension of Arabic orthography, thereby constraining the robustness and generalizability of the recognition systems developed using them.

The challenges of Arabic handwriting recognition extend beyond the omission of positional variant. They are rooted in the cursive nature of the script, where most letters are connected through horizontal strokes or ligatures (Figure 4.1 and 4.2). This connectivity complicates segmentation, as characters often overlap, merge, or share common strokes. Further ambiguity arises from the high structural similarity of many Arabic letters, which are distinguished only by the presence, number, and placement of dots or diacritics (Figure 4.3) [123] [124]. In handwritten text, these diacritics are frequently omitted or stylized, further reducing the discriminative clarity. Moreover, stylistic variability stemming from individual handwriting habits, such as stretching, compression, slanting, or ornamental strokes, introduces additional complexity [125].

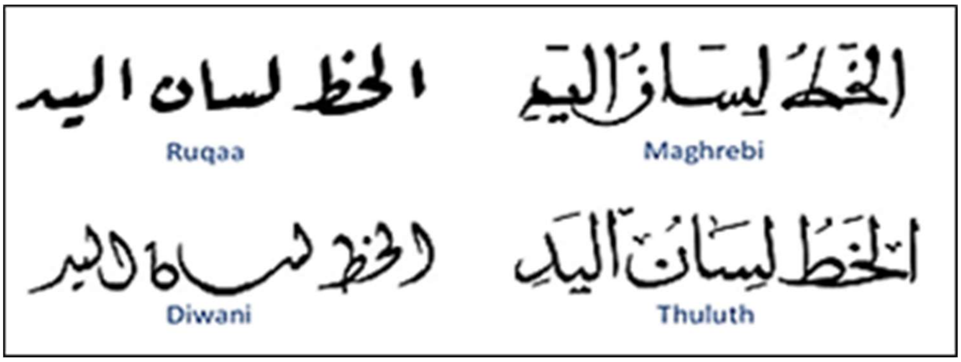

Figure 4.1 Variability in Arabic Handwriting Style.

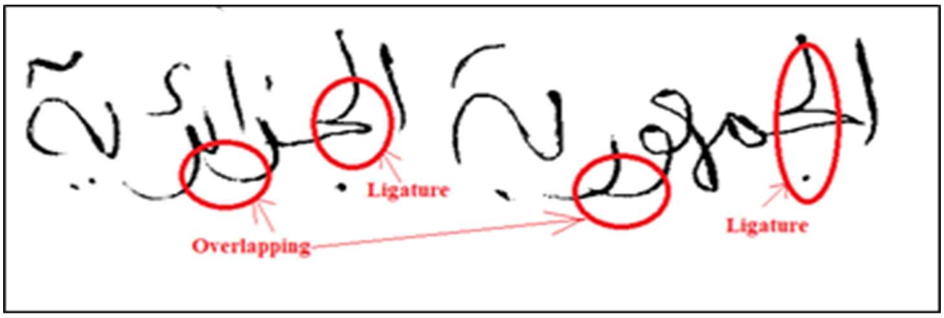

Figure 4.2 Ligature and overlapping.

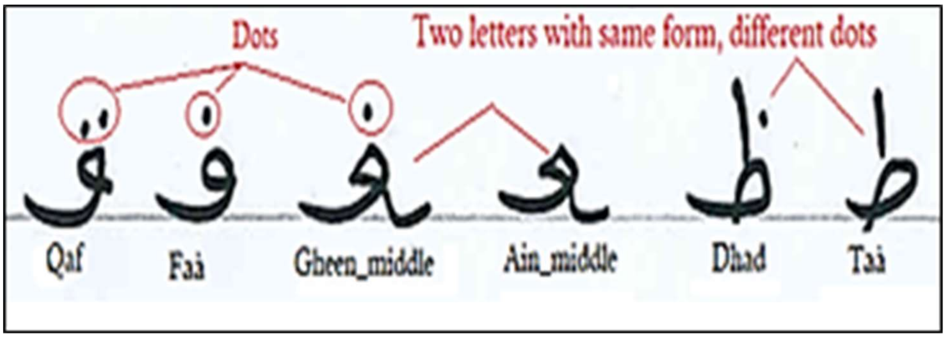

Figure 4.3 Same form with different dots.

Together, these properties make Arabic handwriting recognition a considerably more challenging task than recognition in non-cursive scripts, such as Latin. Addressing these challenges requires a combination of advanced preprocessing techniques (noise removal, normalization, diacritic reconstruction), segmentation-free approaches (e.g., treating entire word images as recognition units), and robust feature extraction and classification models that can capture fine-grained differences while generalizing across diverse writing styles. Recent research increasingly turns to deep learning architectures such as CNNs, Capsule Networks, and Transformers to automatically learn hierarchical representations that are sensitive to both local graphical cues (strokes, dots) and global contextual dependencies (character placement and ligature structure), thereby advancing the state of Arabic handwriting recognition.

2.2 Literature Review

Recent innovations in deep learning have transformed Arabic handwriting recognition through sophisticated architectures including CNNs, transfer learning approaches, and hybrid models. These advancements have systematically addressed the inherent complexities of Arabic script recognition.

2.2.1 CNN-Based Approaches

The effectiveness of CNNs in Arabic script recognition has been extensively validated across numerous studies. Altwaijry et al. [126] pioneered the creation of the Hijja dataset, sourced from children's handwriting, and achieved benchmark accuracies of 88% on Hijja and 97% on the AHCD dataset. To address challenges in processing children's handwriting, Alwagdani and Jaha [127] employed hybrid training using both Hijja and AHCD datasets. Their approach improved recognition accuracy for children's writing to 93%, while additional feature fusion techniques enhanced writer-group discrimination to 94%.

For resource-constrained environments, Kamal et al. [128] introduced the lightweight Huruf model, which maintained strong performance with 96.93% accuracy on AHCD and 99.35% on the MadBase dataset, prioritizing computational efficiency without compromising accuracy. Meanwhile, Balaha et al. [129] achieved ground breaking results using their HMB1 and HMB2 architectures, attaining perfect 100% recognition rates on the CMATER and AIA9K datasets, thereby establishing new benchmarks in Arabic script recognition. Architectural innovations have consistently improved recognition performance. Ullah and Jamjoom [130] enhanced standard CNN frameworks through strategic implementation of batch normalization techniques, reaching 96.78% accuracy on AHCD. Alghyaline [131] conducted a comparative analysis of advanced architectures, including VGG, ResNet, and Inception models, yielding comprehensive insights into their relative strengths, with optimal configurations achieving 98.30% accuracy on AHCD.

2.2.2 Hybrid and Integrated Approaches

Researchers have increasingly explored hybrid approaches to leverage complementary architectural strengths. Najam, R., and Faizullah, S. [132] developed an integrated CNN-RNN model that demonstrated particular efficacy with multi-font datasets, addressing one of the persistent challenges in Arabic script recognition. AlShehri [133] introduced the DeepAHR framework, representing a significant advancement in this direction by incorporating specialized components for improved segmentation and contextual handling of connected characters, the proposed model achieved 98.66% and 88.24% on the AHCD and Hijaa datasets.

Transfer learning strategies have shown considerable promise in this domain. AlMuhaideb et al. [134] adapted the MobileNet architecture to Arabic handwriting recognition, achieving 93.59% accuracy on the Dhad dataset (based on Hijja) while maintaining computational efficiency. This approach has found practical applications in educational technology systems, demonstrating the real-world utility of these research advancements.

2.2.3 Feature Extraction and Advanced Architectures

Sophisticated feature extraction techniques have been instrumental in recognition improvements. Torki et al. [135] combined Scale-Invariant Feature Transform (SIFT) descriptors with Support Vector Machines, achieving 94.28% accuracy on the AIA9K dataset. Loey et al. [136] implemented Stacked Autoencoders that pushed performance boundaries with 98.5% accuracy on MADBase through unsupervised feature learning.

Among advanced architectures, Ghofrani et al. [137] proposed a Capsule Network implementation that stands out for its innovative approach to spatial relationship modeling. Their CapsNet with dynamic routing achieved state-of-the-art 99.87% accuracy on the Hoda dataset, demonstrating exceptional robustness against input variations and noise. Complementarily, Al-Taani and Ahmad [138] leveraged the deep feature learning capabilities of Residual Networks, with their implementation achieving 99.8% accuracy on MADBase through effective gradient flow via skip connections.

Specialized approaches have also emerged for handling distinctive Arabic script features. Lutf et al. [139] developed the diacritic-focused CCRP method, which attained 98.73% accuracy while maintaining low computational overhead significantly outperforming traditional font recognition approaches that struggle with diacritical marks.

These diverse methodological innovations collectively demonstrate the adaptability and effectiveness of deep learning approaches in addressing the unique challenges of Arabic script recognition, from cursive connectivity and diacritical complexity to the considerable stylistic variation found across different writing contexts.

3. Motivation and Problem Statement

As elaborated in the previous section, AHCR presents unique challenges that distinguish it from recognition tasks involving non-cursive scripts. The cursive nature of Arabic, coupled with extensive variability in writing styles, diacritic placement, and contextual character shaping, demands models that not only extract robust features but also capture fine-grained spatial hierarchies in Arabic words. While conventional deep learning architectures, such as CNNs and Residual Networks (ResNets), have achieved remarkable success in hierarchical feature extraction, their reliance on scalar activations inherently constrains their capacity to model spatial relationships. This limitation is particularly critical in AHCR, where ambiguities often arise from subtle variations in stroke curvature, baseline shifts, or the presence and positioning of diacritical marks in the letters.

In contrast, Capsule Networks (CapsNets) were specifically designed to address this gap by representing features as vectors (or capsules) that encode not only the presence of a feature but also its orientation and pose. Through dynamic routing, CapsNets can model part–whole relationships, making them particularly suitable for resolving spatial ambiguities, such as distinguishing between visually similar characters (e.g., ب vs. ت vs. ث). However, despite their theoretical strengths, CapsNets remain hindered by computational inefficiency, high memory requirements, and reliance on relatively shallow backbones, limiting their scalability to complex style-variant handwriting datasets.

Recent research has explored hybrid frameworks that combine the strengths of both paradigms. For example, Capsule Embedded ResNet [140], CapsuleNet–ResNet Fusion Models [141], and Dilated Residual Capsule Networks [142] demonstrate promising results by leveraging the deep hierarchical representation power of ResNet while enriching it with the spatial reasoning capabilities of CapsNet. These approaches underline the potential of hybrid architectures for handwriting recognition, although their application to Arabic scripts remains underexplored. Most prior studies tend to adopt one technique in isolation; for instance, Ghofrani et al. [143] employed CapsNets with limited depth, whereas Al-Taani and Ahmad [138] used ResNets without explicitly addressing spatial hierarchies or contextual shape variation.

To bridge this methodological gap, we propose a novel Residual Capsule Network (ResCapNet) that embeds CapsNet layers within a ResNet backbone, effectively integrating the complementary strengths of both approaches. The design rationale is twofold.

- **Residual Learning (ResNet backbone):** Enables the stable training of deeper networks, enhancing robustness and improving feature extraction across highly diverse and stylistically varied handwriting samples.
- **Embedded Capsules:** Capture spatial hierarchies across multiple receptive fields, enabling the model to distinguish subtle positional variations that are particularly critical in Arabic script (e.g., the distinction between س and ش lies solely in the number and placement of diacritical dots).

This architecture advances Arabic handwriting recognition by unifying hierarchical feature learning with spatial reasoning, directly addressing script-specific challenges, such as cursiveness, contextual character variation, inter-class similarity, and diacritic sensitivity. Thus, ResCapNet not only improves the classification accuracy but also enhances the robustness and generalization across datasets, establishing a strong foundation for scalable applications in real-world AHCR systems.

4. Overview of the Proposed Approach

In our proposed Capsule Embedded ResNet architecture (Figure 4.4), capsule layers are strategically inserted after residual blocks at multiple stages of the ResNet backbone to synergistically combine ResNet's deep feature extraction with capsule networks' ability to model spatial hierarchies.

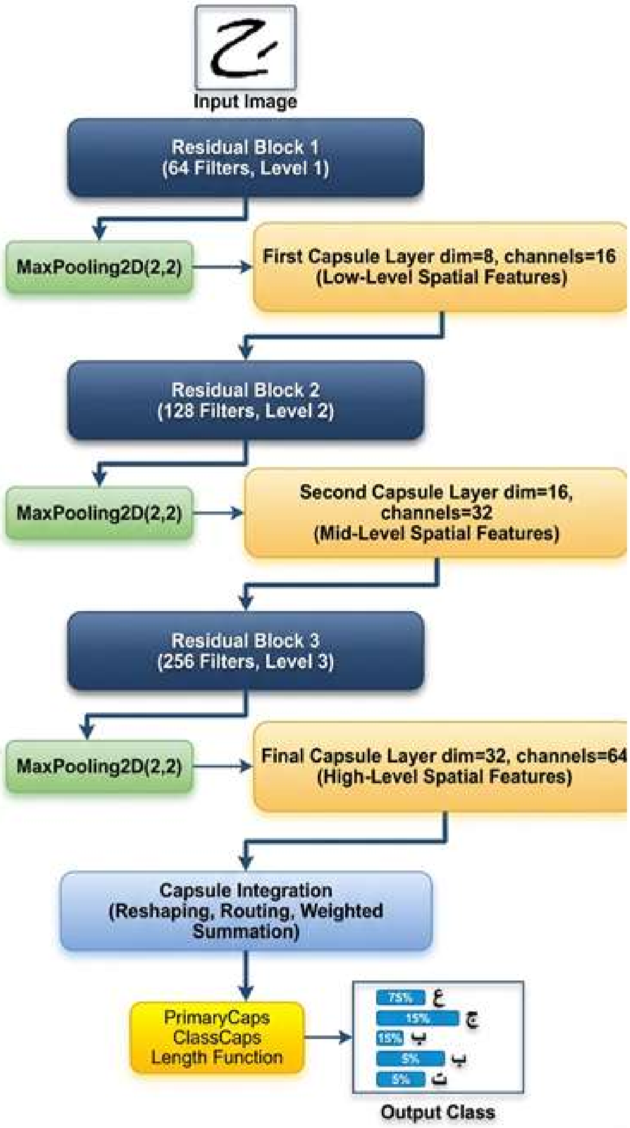

Figure 4.4 Multi-level Capsule Embedding Architecture

4.1 Residual Networks (ResNet)

Deep neural networks have achieved remarkable performance in image classification; however, training very deep architectures often suffers from the degradation problem, where simply stacking additional layers paradoxically leads to higher training errors and reduced accuracy. This issue arises because deeper models encounter difficulties in propagating gradients effectively, leading to vanishing or exploding gradients and suboptimal convergences. To address this, Residual Networks (ResNets), first introduced by He et al. [144], employ the principle of residual learning through shortcut (or skip) connections (Figure 4.5). These shortcuts bypass one or more layers, allowing the network to directly propagate information from earlier to later layers without attenuation.

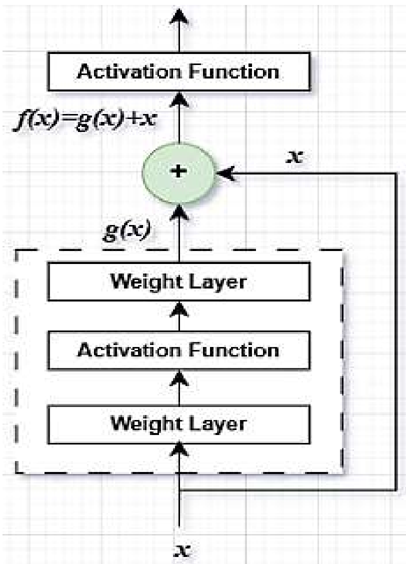

Figure 4.5 Skip Connection in Residual Netwoks

The key insight is that instead of learning an explicit mapping g(x), the residual blocks are designed to learn a residual function F(x) = g(x) + x. This reformulation makes optimization easier because the residual function is often closer to zero than the full mapping, thereby reducing the training difficulty. By enabling gradients to flow more directly through the network, residual connections mitigate vanishing gradient issues and support the effective training of extremely deep networks with hundreds or even thousands of layers.

ResNets have since become foundational in deep learning, achieving state-of-the-art results on large-scale benchmarks, such as ImageNet, where they dramatically improved accuracy while increasing depth. Beyond image classification, their architectural innovations have been widely adopted in diverse applications, such as object detection, semantic segmentation, natural language processing, and medical image analysis. Importantly, for Arabic handwriting recognition, ResNets offer a robust backbone capable of handling the high variability in stroke styles, cursiveness, and diacritic placement, making them an indispensable component of modern hybrid architectures that integrate feature hierarchies with spatial reasoning.

4.2 Capsule Networks (CapsNet)

Capsule Networks (CapsNets), introduced by Sabour et al. [145] in their seminal paper "Dynamic Routing Between Capsules," represent a significant paradigm shift in deep learning by addressing the key limitations of Convolution Networks. While CNNs have dominated image recognition for decades owing to their powerful hierarchical feature extraction, they suffer from a critical drawback: the reliance on max pooling and enforced translation invariance inevitably leads to the loss of fine-grained spatial relationships between features. This is particularly problematic for tasks where part–whole relationships, such as the relative position of strokes in handwritten characters or structural variations in medical images, are essential for correct interpretation.

CapsNets overcome this limitation by introducing capsules, which are groups of neurons that output a vector (or matrix) rather than a scalar (Figure 4.6). These vectors encode not only the presence of a feature but also its pose parameters, such as the position, orientation, scale, and deformation. To capture these relationships more effectively, CapsNets employ dynamic routing mechanisms that allow lower-level capsules to selectively send their outputs to higher-level capsules based on agreement. In other words, if multiple lower-level capsules predict consistent pose information for a higher-level feature, then the connection is strengthened. This mechanism enables the network to explicitly preserve and model spatial hierarchies rather than discarding them through pooling operations.

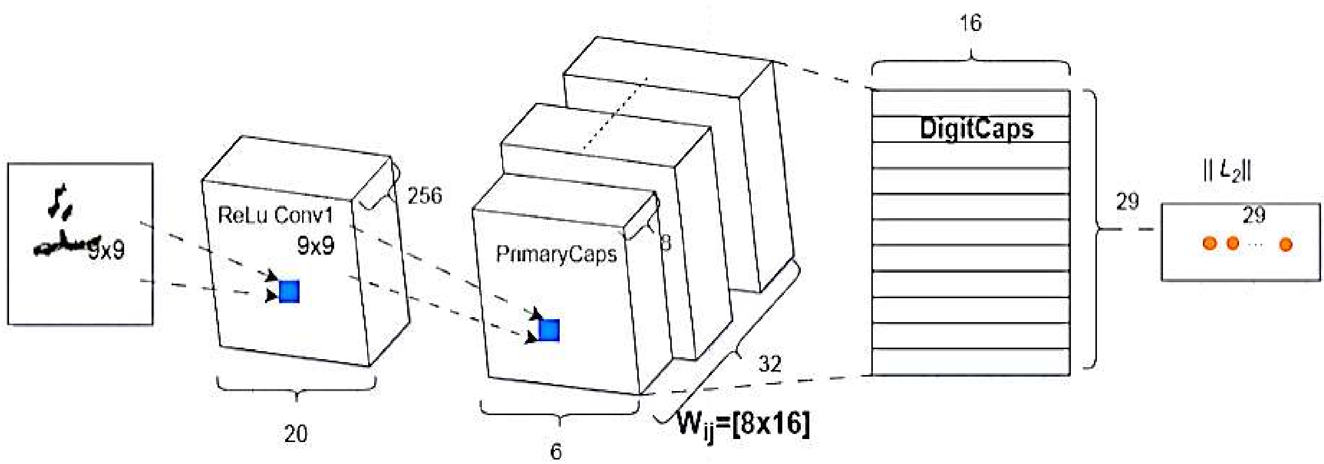

Figure 4.6 CapsNet Encoder Architecture

Table 4.2 below introduce an architectural comparison between traditional neurons and capsule units

		Capsule **Vs**	**Traditional Neuron**
Input from low-level neurons/capsules		**Vector (u_i)**	**Scalar (x_i)**
Operations	Linear/Affine Transformation	$\hat{u}_{j\|i} = W_{ij}u_i + B_j$	$a_{j\|i} = w_{ij}x_i + b_j$
	Weighting	$s_j = \sum_i^n c_{ij}\,\hat{u}_{j\|i}$	$z_j = \sum_{=1}^{3} 1.\, a_{j\|i}$
	Summation		
	Non-linearity activation	$v_i = squash(s_j)$	$h_{w,b}(x) = f(z_j)$
Output		**Vector (v_i)**	**Scalar (h)**
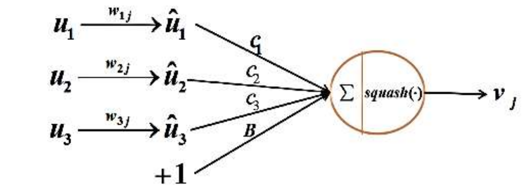 $v_j = \frac{\|\|s_j\|\|^2}{1+\|\|s_j\|\|^2} \cdot \frac{s_j}{\|\|s_j\|\|^2}$			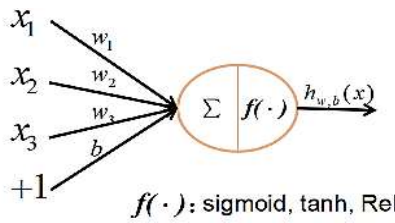 $f(\cdot)$: sigmoid, tanh, ReLU, etc.

Table 4.2 Comparison between capsule network and traditional neural network [145]

- $\boldsymbol{u_i}$: Is the output of capsule *i* in the lower layer.
- $\boldsymbol{W_{ij}}$: Is a weight matrix associated with the connection between a lower-level capsule *i* (e.g., in an earlier layer) and a higher-level capsule *j* (e.g., in a subsequent layer).
- $\boldsymbol{c_{ij}}$: Are coupling coefficients that determine the strength of the connection between capsules and are computed via a ***Softmax*** function.
- $\boldsymbol{s_j}$: The total input to capsule *j* in the higher layer, formed by aggregating weighted predictions from lower-level capsules.

- $\hat{u}_{j|i}$: The prediction vector from capsule *i* to capsule *j*.
- $\boldsymbol{v_i}$: Represents the probability that the entity exists (*squash function*).

CNNs are unable to identify the position of one object relative to another, they can only identify if the object exists in a certain region, or not. This results in difficulty correctly identifying objects that hold spatial relationships between features.

For example, a bunch of randomly assembled face parts will look like a face to a CNN (Figure 4.7), because all the key features are there:

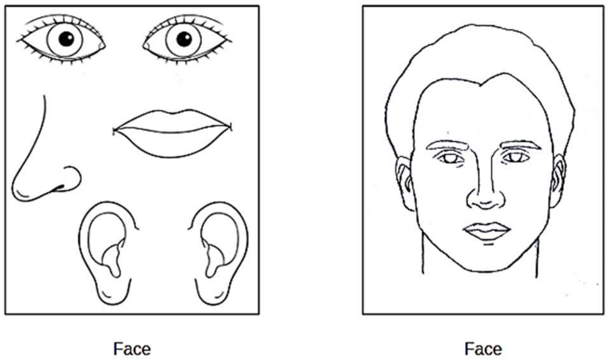

Figure 4.7 Translation Invariance

Capsule Networks is able to identify that the face parts aren't in the correct position relative to one another (Figure 4.8), and label it correctly:

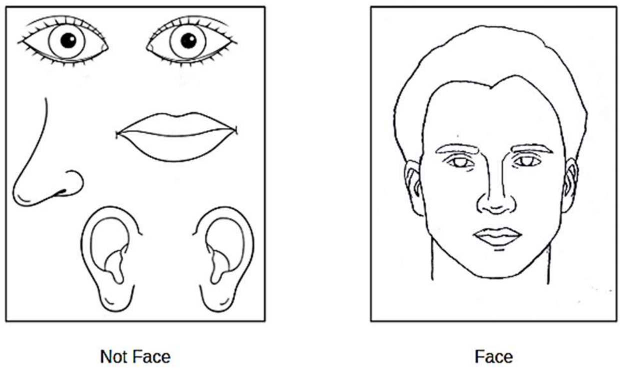

Figure 4.8 Translation Equivariance

This property is particularly beneficial for Arabic script, where subtle differences in diacritic placement, stroke curvature, and the relative positioning of character components determine the semantic distinction between letters. By explicitly modeling part–whole relationships, CapsNets provide a more robust framework for addressing the high variability and structural complexity inherent in Arabic handwriting.

4.2.1 Dynamic Routing Algorithm

Dynamic routing is a central algorithm in Capsule Networks that determines how information flows between capsule layers. Unlike traditional neural networks that use fixed weights determined during training, dynamic routing creates connections on-the-fly based on the agreement between capsules.

Procedure ROUTING ($\hat{u}_{j|i}, r, l$)

1. **for** all capsule *i* in layer *l* and capsule *j* (*l+1*): $b_{ij} \leftarrow 0$
2. **for** *r* iteration **do**
3. for all capsule *i* in layer *l:* $c_i \leftarrow softmax(b_i)$
4. for all capsule *j* in layer *(l+1):* $s_j \leftarrow \sum_i c_{ij}\, \hat{u}_{j|i}$
5. for all capsule *j* in layer *(l+1):* $v_j \leftarrow squash(sj)$
6. for all capsule *i* in layer *l* and capsule *j* (*l+1*): $b_{ij} \leftarrow b_{ij} + \hat{u}_{j|i}.\, v_j$
7. **return** v_j

Dynamic Routing Algorithm [145]

4.2.2 Margin Loss Function

The Margin Loss Function is a specialized loss function designed to evaluate the presence of objects in images while accounting for the unique architecture and properties of capsules.

The Margin Loss Function for Capsule Networks has the following form:

$$L_k = T_K\ max(0, m^+ - \| v_k \|)^2 + \lambda(1 - T_k)\ max(0, \| v_k \| - m^-)^2 \qquad \textbf{4.1}$$

Where:

Lk: is the loss for capsule k.

Tk: is 1 if class kk k is present and 0 otherwise

||vk||: is the length of the output vector of capsule k, which represents the probability of an object of class k being present.

$\boldsymbol{m^+}$: is the upper margin (typically 0.9).

$\boldsymbol{m^-}$: is the lower margin (typically 0.1).

λ: lambda is a down-weighting factor (typically 0.5) that reduces the contribution of absent classes to avoid initial learning from shrinking all capsule outputs [145].

5. Experimental Protocol

This section details our experimental methodology for evaluating the proposed Capsule Embedded ResNet architecture for Arabic handwritten character recognition. Our experiments aim to assess both the performance and robustness of our model through comprehensive cross-dataset validation using samples from diverse writer demographics and various Arabic character formations.

5.1 Used Datasets

We conduct four primary experiments across four complementary Arabic handwriting datasets with total of 16 experiments. Summarized in Table 4.3, used datasets represent diverse writer demographics (children and adults) and contain various Arabic character configurations (isolated, initial, medial, and final positions) with different class distributions, and sizes.

All datasets contain Arabic characters with strokes and diacritics intact (Fig 4.9). These features are critical for distinguishing between similar letters (e.g., س vs. ش or ب vs. ت vs. ث) and are preserved without simplification or removal during preprocessing. This ensures the models learn to recognize the script's morphological and contextual nuances, which are essential for effective Arabic handwriting recognition.

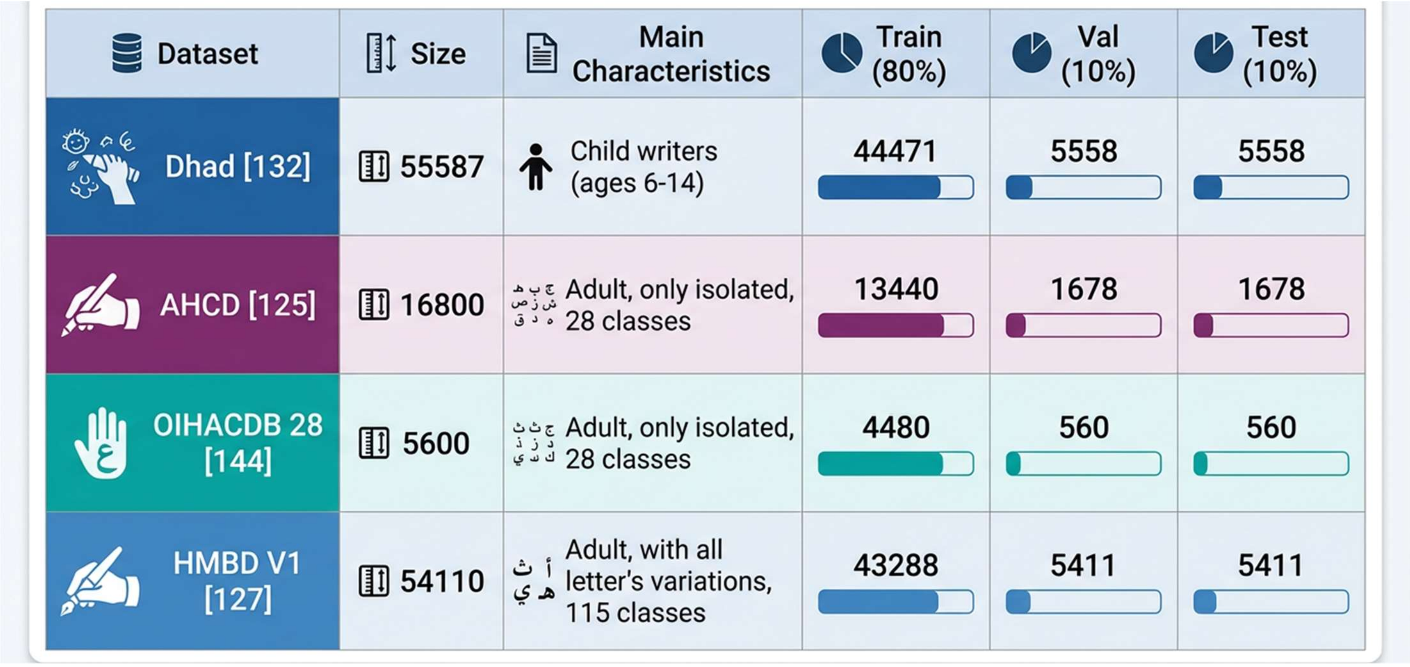

Dataset	Size	Main Characteristics	Train (80%)	Val (10%)	Test (10%)
Dhad [132]	55587	Child writers (ages 6-14)	44471	5558	5558
AHCD [125]	16800	Adult, only isolated, 28 classes	13440	1678	1678
OIHACDB 28 [144]	5600	Adult, only isolated, 28 classes	4480	560	560
HMBD V1 [127]	54110	Adult, with all letter's variations, 115 classes	43288	5411	5411

Figure 4.9 Characteristics of the benchmark datasets used

 HMBD_V1 (Adult)	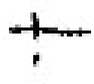 Dhad (Children)	ـبـ Baã middle
 HMBD_V1 (adult)	 Dhad (Children)	ـغـ Gheen middle
 AHCD (adult)	 OIHACDB (Adult)	س Seen isolated

Table 4.3 Samples of characters from used datasets

5.2 Conducted Experiments

5.2.1 Caps-ResNet18

Evaluates the Caps-ResNet18 architecture, where capsule layers are embedded at the end of a ResNet18 backbone. We implement the ResNet18 architecture trained from scratch. This experiment is systematically applied to all four datasets to assess how the integration of capsule networks with residual networks performs across different writing styles and character complexities.

5.2.2 Standalone ResNet18

This experiment **evaluates** standalone ResNet18 architecture without any capsule layers. We implement the ResNet18 model trained from scratch, serving as a baseline to assess the performance of hierarchical feature extraction alone. This configuration isolates the contributions of the ResNet backbone in recognizing Arabic handwritten characters, without the influence of capsule networks.

5.2.3 Caps-ResNet

Investigates a custom-built residual network constructed from scratch, comprising three specialized residual blocks as detailed in the previous section. This experiment aims to determine whether a purpose-built architecture with fewer residual blocks can achieve comparable or superior performance to ResNet18 model.

5.2.4 ResNet with Single Capsule Unit

This experiment investigates a custom ResNet architecture enhanced with a single capsule layer embedded at multiple levels: low, mid, and high. The configuration is designed to explore minimal yet effective integration of capsule networks into ResNet, with the capsule layer responsible for modeling spatial hierarchies at the respective levels of abstraction.

5.3 Pipeline Overview

This section presents a structured framework for handwritten script recognition, encompassing three core stages: data preprocessing, model training, and systematic evaluation (Figure 4.10). Each phase is designed to ensure robustness, reproducibility, and performance across diverse datasets. The subsequent subsections detail the methodology and rationale behind these critical components.

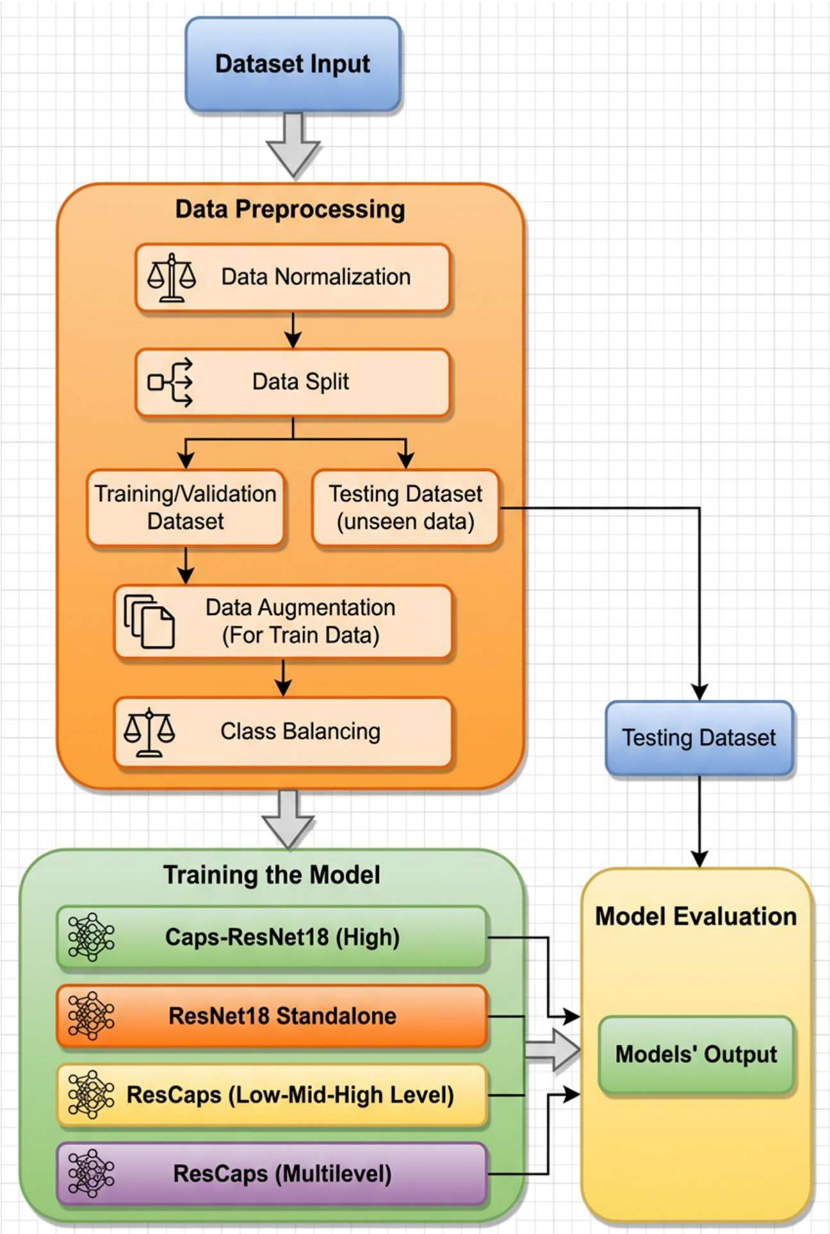

Figure 4.10 Proposed Pipeline

5.3.1 Data Preprocessing

Data preprocessing transforms raw, unstructured data into a refined format suitable for training machine and deep learning models. It addresses challenges like variability in input quality, class imbalance, and limited dataset diversity through normalization, augmentation, and balancing techniques. This foundational step ensures models generalize effectively and achieve reliable performance on real-world tasks.:

A. Min-Max Normalization (0–1 Scaling)

Grayscale images (0–255) are normalized to a 0–1 range to reduce intra-class variability caused by scanning artifacts or ink density differences.

B. Dataset Splitting

The dataset is divided into 80% training (model learning), 10% validation (hyper parameter tuning and overfitting prevention), and 10% testing (unbiased performance evaluation).

C. Data Augmentation

To improve generalization and robustness against real-world variations such as stylized, distorted, or incomplete handwriting, we applied a comprehensive augmentation strategy to the training set. This strategy encompassed handwriting variation simulation and appearance robustness techniques. For handwriting variation simulation, we used geometric transformations, including rotations of up to ±12°, zooming by ±20%, and shearing by ±0.2 radians, along with elastic deformations (σ=5, α=50) to mimic natural handwriting distortions. To ensure appearance robustness, we adjusted contrast by ±30% to handle varying lighting conditions and injected noise, including Gaussian noise (σ=0.05) and salt-and-pepper noise (density=0.03), to emulate capture artifacts.

D. Class Balancing

Addressed imbalance using SMOTE (Synthetic Minority Over-Sampling Technique) to generate synthetic minority-class samples.

These steps collectively improve model robustness, accuracy, and fairness in recognizing diverse handwriting styles.

5.3.2 Training Models

Models training phase employs a systematic exploration of hyperparameters to optimize performance across multiple experimental setups. Key parameters under investigation include batch size (balancing memory efficiency and gradient stability), routing iterations (refining capsule feature dynamics), epochs (controlling training duration and convergence), and optimizer selection (Adam, AdaMax). These experiments aim to identify configurations that maximize recognition accuracy while minimizing computational overhead. Detailed descriptions of used parameters are summarized in the Table 4.4.

Hyper Parameter	Value/Range
Batch Size	32; 64;128
Routing Iterations	3; 5
Epochs	50; 75;100
Optimizer	Adam,AdaMax
Weight Decay	1e-4; 1e-3
Loss Function	Margin Loss, categorical_crossentropy

Table 4.4 Hyperparameters used in Fine Tuning Models

5.4 Baseline and Evaluation Metrics

The model's performance is rigorously evaluated on a comprising unseen data not exposed during training or validation. This ensures an unbiased assessment of its capacity to generalize to new handwriting styles and real-world scenarios. Key metrics include:

- **Accuracy**: Measure the proportion of correct predictions (both true positives and true negatives) across all classes:

$$\text{Acc} = \frac{\text{TP} + \text{TN}}{\text{TP} + \text{TN} + \text{FP} + \text{FN}} \qquad \textbf{4.2}$$

- **Precision**: Measures the accuracy of positive predictions:

$$\text{Precision} = \frac{\text{TP}}{\text{TP} + \text{FP}} \qquad \textbf{4.3}$$

- **Recall**: Measures the ability to identify all relevant instances:

$$\text{Recall} = \frac{\text{TP}}{\text{TP} + \text{FN}} \qquad \textbf{4.4}$$

- **F1-score**: Is the harmonic mean of Precision and Recall, balancing both metrics:

$$\text{F}_1 \text{ score} = \frac{2\times\text{Precision}\times\text{Recall}}{\text{Precision}+\text{Rec}} \qquad \textbf{4.5}$$

Where: TP is the True positive, FP is the False positive, TN is the True negative, and FN is the False negative.

Table 4.5 presents the state-of-the-art accuracy benchmarks achieved by classic approaches on the AHCD, HMBD_V1, Dhad, and OIHACDB-28 datasets, establishing the performance standards against which our proposed Caps-ResNet hybrid architectures will be evaluated.

Authors	Model	Dataset	Accuracy	Loss
Boufenar et al. [146]	AlexNet + TL	AHCD	99.98%	-
Boufenar et al. [147]	Custom-designed CNN	OIHACDB-28	97.32%	-
Balaha et al. [127]	DL-Genetic Algorithm	HMBD_V1	91.96%	0.23
AlMuhaideb et al. [132]	MobilNet	Dhad	93.59%	0.2468

Table 4.5 Baseline Performances across Benchmark

5.5 Computational Setup and Efficiency Analysis

All experiments were conducted on **Google Colab Pro** leveraging the **NVIDIA Tesla A100 GPU**, which offers significant acceleration through its high memory bandwidth (40 GB VRAM), allowing efficient handling of large batches and rapid computation during model training.

Table 4.6 summarizes the number of trainable parameters and average time per epoch across the evaluated architectures

Model	Number of Parameters	Time per Epoch
Custom ResNet Low-level	61,134,272	36s
Custom ResNet Mid-level	63,094,464	46s
Custom ResNet High-level	238,796,992	73s
Custom ResNet Multilevel	484,622,016	96s
ResNet18 High-level	501,927,088	95s
ResNet18 Standalone	326,365,785	85s

Table 4.6 Computational Parameters

The Low-level and Mid-Level Custom ResNet models involve relatively fewer parameters (~61–63 million), making them computationally efficient while still achieving strong performance on simpler recognition tasks. In contrast, the High-level and multilevel embedding models particularly the Custom ResNet Multilevel (484 million parameters) and ResNet18 High-level (502 million parameters), introduce substantially greater model complexity. This increase corresponds with improved capacity to capture nuanced spatial hierarchies in Arabic script, enhancing both recognition accuracy and prediction confidence, though at the expense of higher computational cost. The Standalone ResNet18 model, with approximately 326 million parameters, offers a middle ground in terms of complexity; however, its elevated test loss across datasets indicates reduced prediction certainty and highlights the added value of capsule-augmented architectures in achieving more robust feature representation.

6. Results and Discussions

Our proposed architectures, Caps-ResNet18 and Caps-ResNet with multi-level embedding, were rigorously evaluated on four Arabic handwriting datasets: Dhad, AHCD, OIHACDB-28, and HMBD_V1. Table 4.7 provides a comprehensive comparison of our models' performance.

Model	Metrics	Dataset			
		Dhad	**AHCD**	**HMBD V1**	**OIHACD 28**
Custom ResNet Low-level	Loss	0.047	0.0565	0.1244	0.1838
	Acc	90. 77%	98.57%	90.80%	98.75%
	M-F1	90.14%	98.57%	90.77%	98.74%
	W-F1	90.73%	98.57%	90.83%	98.74%
Custom ResNet Mid-level	Loss	0.0732	0.0557	0.0945	0.0505
	Acc	93.90%	**98.48%**	**91.39%**	99.64%
	M-F1	93.30%	**98.48%**	**91.34%**	99.64%
	W-F1	93.88%	**98.48%**	**91.40%**	99.64%
Custom ResNet High-level	Loss	0.0497	0.0167	0.078	0.0152
	Acc	93.67%	98.15%	89.96%	98.57%
	M-F1	93.00%	98.15%	89.95%	98.56%
	W-F1	94.00%	98.15%	89.99%	98.56%
Custom ResNet Multi-level	Loss	0.0549	0.0364	0.0843	0.013
	Acc	93.24%	98.42%	89.98%	98.93%
	M-F1	92.61%	98.42%	89.95%	98.93%
	W-F1	93.22%	98.42%	90.01%	98.93%
ResNet18 High-level	Loss	**0.0467**	**0.0169**	**0.2048**	**0.0285**
	Acc	**94.14%**	98.12%	88.91%	99.46%
	M-F1	**93.50%**	98.00%	88.61%	99.46%
	W-F1	**94.10%**	98.00%	88.69%	99.46%
Standalone ResNet18	Loss	0.283	0.137	0.294	0.298
	Acc	93.24%	97.11%	87.60%	**99.64%**
	M-F1	92.60%	97.12%	87.17%	**99.64%**
	W-F1	93.26%	97.11%	87.26%	**99.64%**

Table 4.7 Empirical Results Across Experiments

6.1 Result Discussion and Analysis

6.1.1 Capsule Embedding Effect on Custom ResNet models

Capsule units, integrated into the Custom ResNet models, enhance feature representation by capturing spatial hierarchies and part-whole relationships through vector-based embeddings, unlike traditional convolutional layers that rely on scalar activations. This dynamic routing mechanism allows Capsules to model complex patterns, improving robustness to variations in data. In the Custom ResNet models, Capsule embeddings are applied at different feature extraction levels (Low-level, Mid-level, High-level) and combined in the hybrid Caps-ResNet (Multilevel), enabling a nuanced analysis of their impact.

Low-level Capsule Embedding

The Custom ResNet Low-level model, which injects capsule embeddings in the earliest convolutional layers to capture fine-grained spatial cues (e.g., diacritics, dots), delivers competitive—but dataset-dependent—performance. On Dhad it attains a Test Accuracy of 90.8 % with a Test Loss of 0.0470, indicating strong detail extraction yet limited robustness for complex character shapes. For OIHACDB, accuracy rises to 98.8 % but the higher Test Loss of 0.1838 signals less efficient optimisation. On the more structured AHCD dataset, the model achieves 98.6 % accuracy with a moderate loss of 0.0565, whereas on HMBD-V1, accuracy drops to 90.8 % and loss rises to 0.1244, underscoring that fine-grained features alone cannot fully capture the contextual variability of this set. Overall, low-level capsule embeddings excel at preserving local patterns but exhibit limited generalisation when higher-level semantics dominate.

Mid-level Capsule Embedding

The Custom ResNet Mid-level model, applying Capsule embeddings at intermediate layers to capture abstract features (e.g., Hamza above), demonstrates strong and consistent performance by balancing fine detail and abstraction. On Dhad, it achieves a Test Accuracy of 93.9 % with a Test Loss of 0.0732, showing improved classification due to enhanced feature hierarchies. On OIHACDB-28, it attains an outstanding Test Accuracy of 99.64 % and a low Test Loss of 0.0505, reflecting excellent generalization and optimization. On AHCD, the model reaches 98.48 % accuracy with a Test Loss of 0.0557, and on HMBD-V1, it records 91.39 % accuracy with a Test Loss of 0.0945, outperforming other variants. These results highlight the effectiveness of mid-level Capsule embeddings in capturing intermediate semantic features, making this architecture particularly robust across datasets with varied structural complexity.

High-Level Embedding

The Custom ResNet High-level model, incorporating Capsule embeddings at deeper layers to capture semantic features (e.g., base forms of Arabic letters), demonstrates strong performance on datasets with clear class boundaries. On Dhad, it achieves a Test Accuracy of 93.67 % and a Test Loss of 0.0497, showing effective semantic-level abstraction for character classification. It performs exceptionally well on OIHACDB-28 and AHCD, reaching 98.57 % and 98.15 % accuracy, respectively, with very low-test losses (0.0152 and 0.0167), indicating efficient optimization and robustness for structured datasets. However, performance drops on HMBD-V1, with a Test Accuracy of 89.96 % and a Test Loss of 0.0780, suggesting that semantic features alone are insufficient for datasets requiring fine-grained or multi-scale discrimination. These findings highlight the strength of high-level Capsule embeddings in capturing semantic relationships, while also pointing to their limitations in scenarios that demand more localized or hierarchical feature modeling.

Multilevel Embedding

The Custom ResNet Multilevel model, or hybrid Caps-ResNet, integrates Capsule embeddings across low-, mid-, and high-level layers, yielding consistent and robust performance across all datasets. On Dhad, it achieves a Test Accuracy of 93.24 % with a Test Loss of 0.0549, demonstrating balanced feature extraction and effective optimization for Arabic character recognition. On OIHACDB-28, the model excels with 98.93 % accuracy and the lowest Test Loss of 0.0130 across all configurations, highlighting its superior generalization and optimization for structured data. For AHCD, it achieves 98.42 % accuracy with a Test Loss of 0.0364, maintaining strong performance on clean, well-structured input. On HMBD-V1, it records a Test Accuracy of 89.98 % and a Test Loss of 0.0843, showing resilience to complex or ambiguous patterns, though slightly trailing the Mid-level variant in accuracy. The key strength of this hybrid Caps-ResNet lies in its ability to combine fine-grained, abstract, and semantic features through multi-scale Capsule integration, enabling improved robustness and generalization across datasets of varying complexity. Figure 4.11 illustrates the comparative test loss achieved by each of the proposed Custom ResNet architectures.

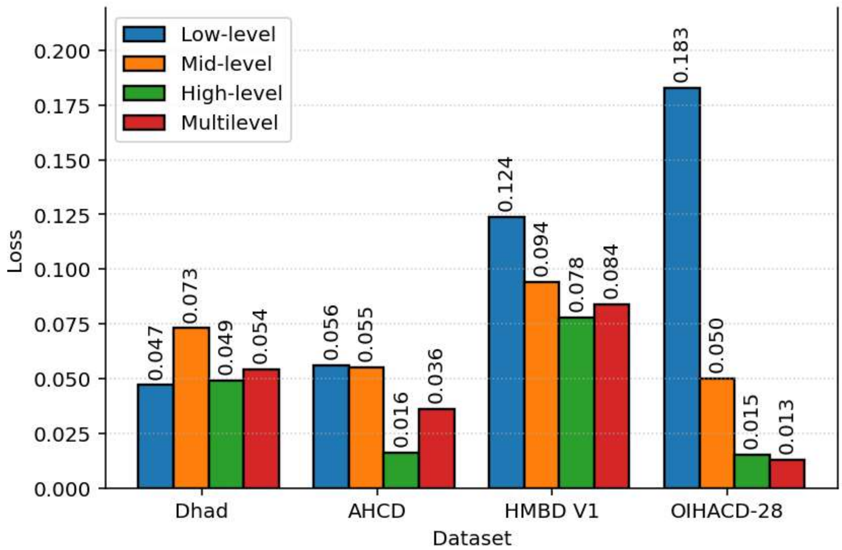

Figure 4.11 Comparative Test Loss (Custom CapsNet)

Figure 4.12 presents the test accuracy of the same Custom ResNet variants across the evaluated datasets

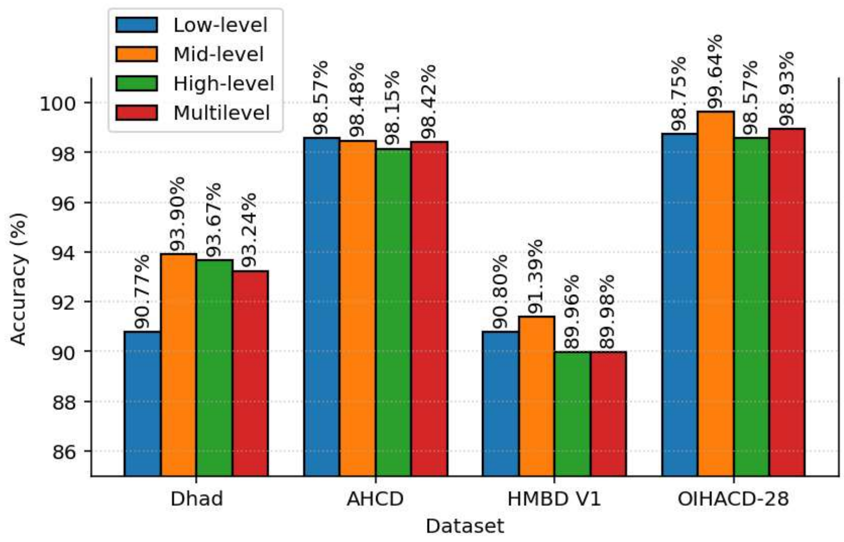

Figure 4.12 Comparative Test Accuracy (Custom CapsNet)

6.1.2 Capsule Embedding Effect on ResNet18 models

The experiments evaluate the impact of Capsule units in the ResNet18 High-level model, which applies Capsules at deeper layers to capture semantic features, compared to the ResNet18 Standalone model using standard convolutions, across evaluated datasets.

ResNet18 High-level Capsule Embedding

The ResNet18 High-level model, incorporating Capsule embeddings at deeper layers to capture semantic features (e.g., letter base forms), demonstrates strong performance across datasets with distinct class boundaries. On Dhad, it achieves a Test Accuracy of 94.14 % and a Test Loss of 0.0467, reflecting effective semantic-level abstraction for Arabic character recognition. On OIHACDB-28, it reaches 99.46 % accuracy with a low-Test Loss of 0.0285, confirming efficient optimization and strong performance for structured scripts. For AHCD, the model yields 98.12 % accuracy with a Test Loss of 0.0169, showcasing its reliability on well-structured datasets. However, on HMBD_V1, it records a lower accuracy of 88.91 % and a significantly higher Test Loss of 0.2048, indicating limitations in handling complex, variable patterns where semantic features alone are insufficient. These results underline the model's strength in capturing high-level relationships but also reveal that deeper semantic embeddings, in isolation, may not generalize as well as multi-scale Capsule-based approaches.

ResNet18 Standalone

The ResNet18 Standalone model, based on the standard ResNet18 architecture without Capsule embeddings, demonstrates consistent but generally lower performance compared to Capsule-integrated variants across most datasets. On Dhad, it achieves a Test Accuracy of 93.24 % with a notably high-Test

Loss of 0.283, suggesting less precise classification despite reasonable accuracy. For OIHACDB-28, it ties for the highest accuracy at 99.64 %, but with a significantly elevated Test Loss of 0.298, pointing to suboptimal generalization. On AHCD, the model reaches 97.11 % accuracy and a Test Loss of 0.137, reflecting moderate performance for structured inputs. On HMBD_V1, it records the lowest performance among models, with a Test Accuracy of 87.60 % and a high-Test Loss of 0.294, indicating substantial challenges in handling variability and complexity. These outcomes highlight that while the ResNet18 Standalone model performs adequately on datasets with clear feature hierarchies, its high-test losses and reduced robustness on complex data emphasize the value of Capsule embeddings in enhancing feature representation and model generalization. Figure 4.13 presents the test loss of the Caps-ResNet18 across the evaluated datasets.

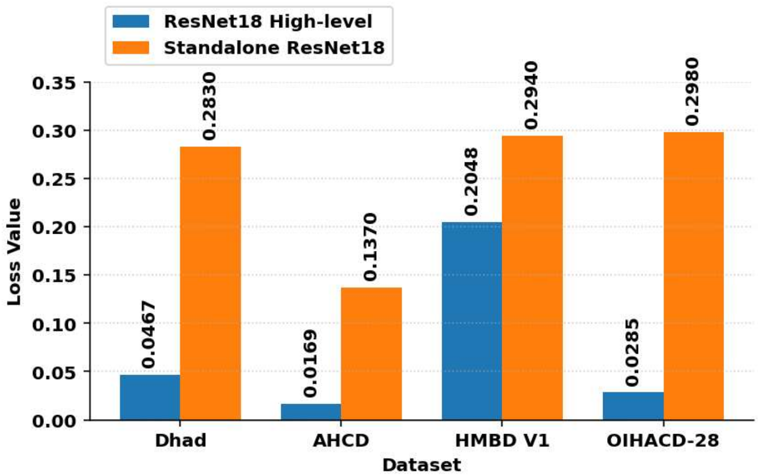

Figure 4.13 Comparative Test Loss (Caps-ResNet18)

Figure 4.14 presents the test accuracy of the Caps-ResNet18 across the evaluated datasets

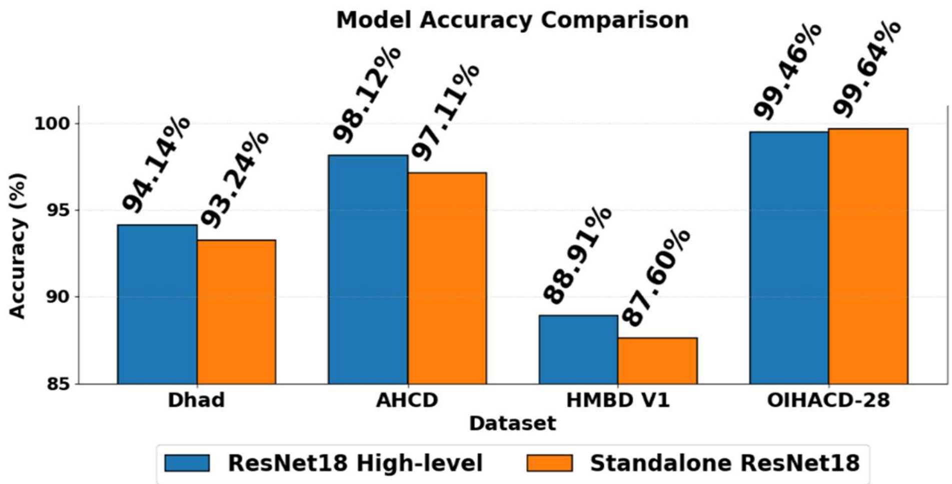

Figure 4.14 Comparative Test Accuracy (Caps-ResNet18)

6.1.3 Performance Comparison of Models Across Datasets with Baseline

This section presents a comparative analysis of the proposed models against baseline methods across multiple evaluated datasets, focusing on key performance metrics such as test loss and test accuracy to highlight improvements and robustness. Table 4.9 summarizes the key comparisons.

Dataset	Model	Accuracy	Test Loss	Macro F1	Weighted F1
Dhad	Baseline	93.59%	0.2468	94.00%	94.00%
Dhad	ResNet18 High-level	94.14%	0.0467	93.50%	94.10%
Dhad	Custom ResNet Mid-level	93.90%	0.0732	93.30%	93.88%
AHCDBaseline	Baseline	99.98%	--	--	--
AHCDBaseline	ResNet18 High-level	98.12%	0.0169	98.00%	98.00%
AHCDBaseline	Custom ResNet Low-level	98.57%	0.0565	98.57%	98.57%
HMBD V1	Baseline	91.96%	0.23	--	--
HMBD V1	ResNet18 High-level	88.91%	0.2048	98.48%	98.48%
HMBD V1	Custom ResNet Mid-level	91.39%	0.0945	91.34%	91.40%
OIHACDB-28	Baseline	97.32%	--	--	--
OIHACDB-28	ResNet18 Standalone	99.64%	0.2989	99.64%	99.64%
OIHACDB-28	Custom ResNet Mid-level	99.64%	0.0505	99.64%	99.64%

Legend:
- High Accuracy / High F1 Score / Low Test Loss
- Medium Accuracy / Medium F1 Score / Medium Test Loss
- Low Accuracy / Low F1 Score / High Test Loss
- Best Performance in Dataset

Table 4.8 Comparative performance analysis of our proposed models against established baselines

Dhad Dataset

On the Dhad dataset, the baseline model achieved a Test Accuracy of 93.59% with an estimated Test Loss of 0.2468. Capsule-integrated models, particularly those using mid- and high-level embeddings, outperformed the baseline in both accuracy and optimization. The ResNet18 High-level model led with the highest accuracy (94.14%) and the lowest loss (0.0467), indicating strong robustness to character complexity. The Custom ResNet Mid-level model followed closely (93.90%, loss: 0.0732), while the Custom High-level variant also performed well (93.67%, loss: 0.0497). The Custom Multilevel and ResNet18 Standalone models matched in accuracy (93.24%), but the former achieved better optimization (loss: 0.0549) than the latter (0.2830). The Custom Low-level model recorded the lowest accuracy (90.77%) despite a low loss (0.0470), suggesting limited generalization from fine-grained features alone. These results highlight that Capsule integration at deeper or mid-levels significantly enhances performance on challenging datasets like Dhad.

AHCD Dataset

On the AHCD dataset, the baseline model achieved a near-perfect Test Accuracy of 99.98%, outperforming all other models in accuracy. Despite this, several Capsule-integrated models demonstrated competitive performance and significantly lower Test Losses, indicating better optimization. The Custom ResNet High-level and ResNet18 High-level models achieved accuracies of 98.15% and 98.12% with the lowest losses of 0.0167 and 0.0169, respectively, suggesting effective semantic abstraction. The Custom Multilevel model offered the best balance between accuracy (98.42%) and Test Loss (0.0364), while the Low-level and Mid-level models maintained solid accuracy (~98.5%) with moderate losses (~0.056). The ResNet18 Standalone model lagged with the lowest accuracy (97.11%) and highest loss (0.1370). These findings indicate that while the baseline excels on AHCD's structured data, Capsule-based architectures optimize better, offering enhanced generalization and robustness.

HMBD_V1 Dataset

On the HMBD_V1 dataset with 115 classes, all Capsule-based and ResNet18 models underperformed the baseline accuracy of 91.96%. Among them, the Custom ResNet Mid-level model performed best, with a Test Accuracy of 91.39% and a moderate Test Loss of 0.0945, indicating reasonable robustness to complex patterns. Models with high-level or multilevel Capsule embeddings showed slightly lower accuracies (~89.9%) but had better optimization (lower losses). The ResNet18 Standalone model had the lowest accuracy (87.60%) and highest loss (0.2940), reflecting poor generalization. Overall, while none of the models surpassed the baseline, the Mid-Level Capsule model stood out as the most balanced in handling HMBD_V1's fine-grained discrimination challenges.

OIHACDB-28 Dataset

On the OIHACDB-28 dataset, all models outperformed the baseline accuracy of 97.32%, underscoring the effectiveness of Capsule-enhanced architectures. The Custom ResNet Mid-level and ResNet18 Standalone models tied for the highest accuracy (99.64%), though the Standalone model exhibited a much higher loss (0.2980) compared to the Mid-level's more optimized performance (0.0505). The Custom ResNet Multilevel model achieved the lowest Test Loss (0.0130) with a strong accuracy of 98.93%, reflecting excellent generalization. Similarly, the Custom ResNet High-level model recorded a low loss (0.0152) with 98.57% accuracy. The ResNet18 High-level model reached 99.46% with a loss of 0.0285, while the Custom Low-level model performed well (98.75%, loss: 0.1838). These results highlight that Capsule integration, particularly at multilevel and high-level layers, enables precise and efficient classification on structured datasets like OIHACDB-28.

Figures 4.15 and 4.16 present performance comparisons between the two proposed models (Caps-ResNet18 and Custom CapsNet) and the baseline, highlighting the best achieved results.

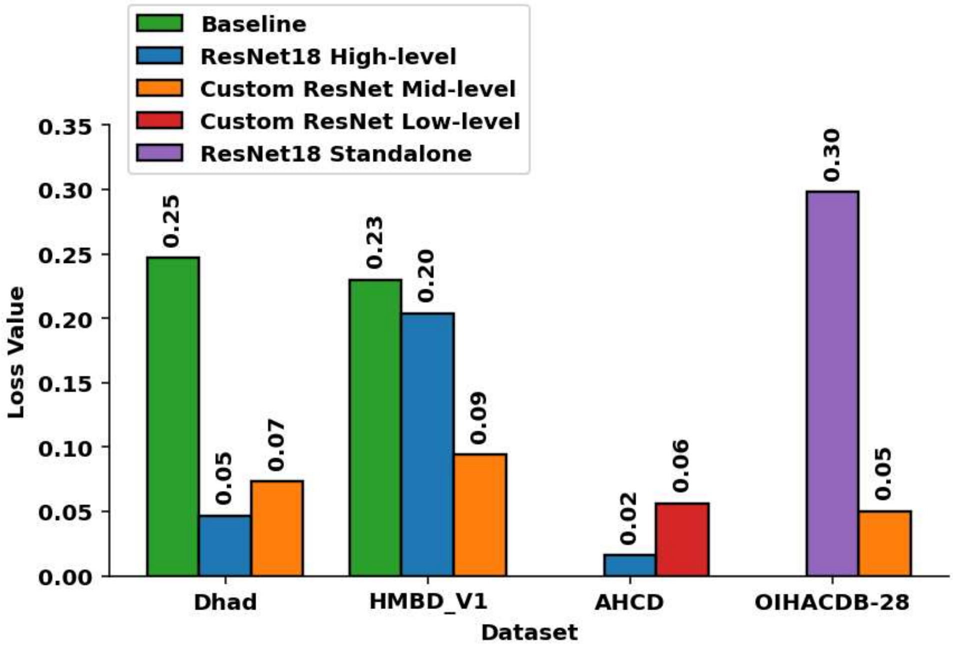

Figure 4.15 Test Loss Comparison with Baseline

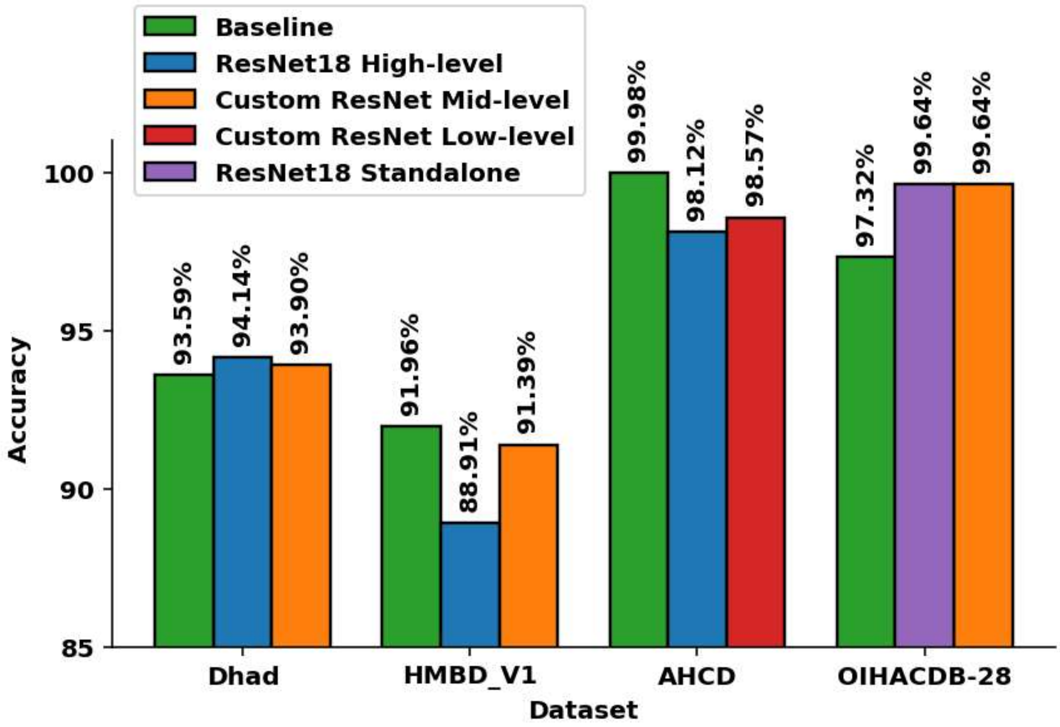

Figure 4.16 Test Loss Comparison with Baseline

7. Conclusion

This study introduced novel Custom ResNet architectures augmented with capsule embeddings at distinct hierarchical levels—low, mid, high, and multilevel, to improve the recognition of Arabic handwritten characters. Evaluations were conducted across four benchmark datasets: AHCD, IOHACDB-28, Dhad, and HMBD_V1, each representing varying structural complexities and character morphologies.

The performance variation across embedding strategies reflects how different feature abstraction levels influence recognition capability. Low-level embeddings excel at capturing fine-grained spatial features like diacritics and localized strokes, which benefited cleaner, isolated-character datasets such as AHCD. However, they proved less effective for complex or context-rich datasets like Dhad and HMBD_V1, where broader structural and semantic cues are essential. Mid-level embeddings demonstrated consistent robustness by balancing local and abstract features, achieving top performance on moderate-complexity datasets like OIHACDB-28. The High-level embedding variant performed strongly on datasets with clear semantic boundaries but underperformed where fine morphological distinctions were critical.

The Multilevel Caps-ResNet, combining all three embedding levels, emerged as the most balanced architecture, achieving stable and strong results across all datasets. It delivered the best test loss on OIHACDB-28 (0.0130) and robust accuracy on challenging datasets like HMBD_V1 (89.98%), indicating its capacity to generalize across various handwriting styles and complexities.

In summary, the integration of capsule embeddings at strategic abstraction layers significantly enhances the spatial hierarchy modeling of ResNet architectures. These findings confirm that such hybrid models not only boost classification accuracy but also improve prediction certainty and feature robustness. Consequently, these advancements bring Arabic handwriting recognition closer to reliable deployment in real-world applications involving diverse and challenging handwritten input.

General Conclusion

The research presented in this dissertation addresses the central challenge of Knowledge Discovery in Big Data, where exponential growth in data volume, velocity, and heterogeneity demands methodological innovation and scalable computational frameworks. This work establishes theoretical foundations, extends them through distributed deep learning architectures, and validates effectiveness across domain-specific applications.

The dissertation progresses methodologically from theoretical foundations of Big Data analytics and knowledge discovery frameworks to their application in genomics, a domain exemplifying computational challenges at massive scale. A comprehensive distributed deep learning pipeline for genomic variant calling demonstrates how multimodal fusion, attention mechanisms, and Distributed Data Parallel training address both accuracy and scalability in production environments. The methodology extends to Arabic handwriting recognition, where hybrid Capsule-embedded Residual Networks capture hierarchical features and spatial relationships in complex cursive scripts.

This multidisciplinary exploration demonstrates that scalable knowledge discovery requires integrated innovation: algorithmic advancement, architectural adaptation through parallelization and distribution, multimodal data integration, and domain-specific design. The contributions span methodological frameworks for Big Data mining, distributed architectures for genomic analytics demonstrating near-linear parallel efficiency, and hybrid neural networks balancing accuracy with computational feasibility across diverse pattern recognition tasks.

Through this multidisciplinary investigation spanning theoretical foundations, computational genomics, and pattern recognition, we have gained deep insights into the convergence of Big Data methodologies and advanced deep learning architectures. This cross-domain experience reveals that many computational challenges share fundamental characteristics scalability constraints, data heterogeneity, representation learning complexity, and the tension between model expressiveness and computational efficiency, yet manifest differently across domains. These observations, combined with emerging technological paradigms and evolving application requirements, suggest several promising research directions that warrant systematic exploration and may lead to concrete methodological advances and practical innovations.

Perspectives

- **In genomics**: integrating graph neural networks with multi-omics datasets, extending pipelines to long-read sequencing technologies, and developing interpretable models remain critical directions for advancing clinical genomics and personalized medicine.
- **In distributed computing**: exploring model and pipeline parallelism beyond data parallelism, leveraging emerging hardware accelerators, and implementing federated learning frameworks offer pathways to petabyte-scale knowledge discovery while preserving privacy.
- **In quantum computing**: quantum machine learning algorithms present transformative potential through exponential speedups for high-dimensional pattern recognition and optimization. Hybrid classical-quantum architectures could revolutionize genomic sequence alignment and variant annotation by exploiting quantum superposition and entanglement. However, realizing this potential requires addressing quantum algorithm design, noise mitigation, and scalable quantum-classical interfaces.
- **In pattern recognition**: transformer-based attention mechanisms and self-supervised learning approaches offer enhanced robustness and reduced dependency on labeled datasets, particularly valuable for low-resource languages and multilingual contexts.

1. Hashem, I. A. T., Yaqoob, I., Anuar, N. B., Mokhtar, S., Gani, A., & Ullah Khan, S. (2015). The rise of "big data" on cloud computing: Review and open research issues. *Information Systems, 47*, 98–115.
2. Kitchin, R. (2014). The data revolution: Big data, open data, data infrastructures and their consequences. Sage.
3. Ward, J. S., & Barker, A. (2013). Undefined by data: A survey of big data definitions. *arXiv preprint arXiv:1309.5821*.
4. Fan, W., Han, J., & Liu, H. (2014). Challenges of big data mining algorithms. *ACM SIGKDD Explorations Newsletter, 14*(2), 1–10.
5. Manyika, J., Chui, M., Brown, B., Bughin, J., Dobbs, R., Roxburgh, C., & Byers, A. H. (2011). *Big data: The next frontier for innovation, competition, and productivity*. McKinsey Global Institute.
6. Dean, J., & Ghemawat, S. (2008). MapReduce: Simplified data processing on large clusters. *Communications of the ACM, 51*(1), 107–113.
7. White, T. (2015). *Hadoop: The definitive guide* (4th ed.). O'Reilly Media.
8. Meng, X., Bradley, J., Yavuz, B., Sparks, E., Venkataraman, S., Liu, D., ... & Zaharia, M. (2016). MLLib: Machine learning in Apache Spark. *Journal of Machine Learning Research, 17*(34), 1–7.
9. Vavilapalli, V. K., Murthy, A. C., Douglas, C., Agarwal, S., Konar, M., Evans, R., ... & Curino, C. (2013). Apache Hadoop YARN: Yet another resource negotiator. *Proceedings of the 4th Annual Symposium on Cloud Computing*, 1–16.
10. Ke, G., Meng, Q., Finley, T., Wang, T., Chen, W., Ma, W., ... & Liu, T. Y. (2017). LightGBM: A highly efficient gradient boosting decision tree. *Advances in Neural Information Processing Systems (NeurIPS)*, 30.
11. Koboldt, D. C., Steinberg, K. M., Larson, D. E., Wilson, R. K., & Mardis, E. R. (2013). The next-generation sequencing revolution and its impact on genomics. *Cell, 155*(1), 27–38.
12. Litjens, G., Kooi, T., Bejnordi, B. E., Setio, A. A., Ciompi, F., Ghafoorian, M., ... & Sánchez, C. I. (2017). A survey of deep learning in medical image analysis. *Medical Image Analysis, 42*, 60–88.
13. Erlich, Y., & Narayanan, A. (2014). Routes for breaching and protecting genetic privacy. *Nature Reviews Genetics, 15*(6), 409–421.
14. Rieke, N., Hancox, J., Li, W., Milletarì, F., Roth, H. R., Albarqouni, S., ... & Cardoso, M. J. (2020). The future of digital health with federated learning. *NPJ Digital Medicine, 3*(119), 1–7.
15. Marx, V. (2013). Biology: The big challenges of big data. *Nature, 498*(7453), 255–260.
16. Jagadish, H. V., Gehrke, J., Labrinidis, A., Papakonstantinou, Y., Patel, J. M., Ramakrishnan, R., & Shahabi, C. (2014). Big data and its technical challenges. *Communications of the ACM, 57*(7), 86–94.
17. Gandomi, A., & Haider, M. (2015). Beyond the hype: Big data concepts, methods, and analytics. *International Journal of Information Management, 35*(2), 137–144.
18. Meystre, S. M., Savova, G. K., Kipper-Schuler, K. C., & Hurdle, J. F. (2010). Extracting information from textual documents in the electronic health record: A review of recent research. *Yearbook of Medical Informatics, 19*(01), 128–144.
19. Gerstmair, A., Dawe, H., & Jones, C. (2013). Privacy-preserving sharing of medical images. *Journal of Digital Imaging, 26*(1), 60–69.
20. Smith, R. (2007). An overview of the Tesseract OCR engine. *Proceedings of the Ninth International Conference on Document Analysis and Recognition (ICDAR)*, 629–633.
21. Bonomi, F. L., Milito, R., Zhu, J., & Addepalli, S. (2012). Fog computing and its role in the internet of things. *Proceedings of the First Edition of the MCC Workshop on Mobile Cloud Computing*, 13–16. ACM.

22. Akidau, T., Bradshaw, R., Chambers, C., Chernyak, S., Fernández-Moctezuma, R. J., Lax, R., ... & Whittle, S. (2015). The dataflow model: A practical approach to balancing correctness, latency, and cost in massive-scale, unbounded, out-of-order data processing. *Proceedings of the VLDB Endowment, 8*(12), 1792–1803.
23. Chen, T., & Guestrin, C. (2016). XGBoost: A scalable tree boosting system. *Proceedings of the 22nd ACM SIGKDD International Conference on Knowledge Discovery and Data Mining*, 785–794.
24. Ghani, R., Probst, K., & Liu, Y. (2019). Data mining for business applications. In *Encyclopedia of Database Systems* (pp. 1–6). Springer.
25. Roberts, K., Demner-Fushman, D., & Voorhees, E. M. (2016). Biomedical literature mining and information retrieval. *PLOS Computational Biology, 12*(11), e1005205.
26. Ashley, K. D. (2017). *Artificial intelligence and legal analytics: New tools for law practice in the digital age*. Cambridge University Press.
27. Devlin, J., Chang, M. W., Lee, K., & Toutanova, K. (2019). BERT: Pre-training of deep bidirectional transformers for language understanding. *Proceedings of NAACL-HLT*, 4171–4186.
28. Gorelick, N., Hancher, M., Dixon, M., Ilyushchenko, S., Thau, D., & Moore, R. (2017). Google Earth Engine: Planetary-scale geospatial analysis for everyone. *Remote Sensing of Environment, 202*, 18–27.
29. Kreps, J., Narkhede, N., & Rao, J. (2011). *Kafka: A distributed messaging system for log processing*. In Proceedings of the NetDB Workshop.
30. Zaharia, M., Das, T., Li, H., Hunter, T., Shenker, S., & Stoica, I. (2013). *Discretized streams: Fault-tolerant streaming computation at scale*. In Proceedings of the 24th ACM Symposium on Operating Systems Principles (SOSP) (pp. 423–438). ACM.
31. Carbone, P., Katsifodimos, A., Ewen, S., Markl, V., Haridi, S., & Tzoumas, K. (2015). *Apache Flink™: Stream and batch processing in a single engine*. IEEE Data Engineering Bulletin, 38(4), 28–38.
32. Gymrek, M., McGuire, A. L., Golan, D., Halperin, E., & Erlich, Y. (2013). Identifying personal genomes by surname inference. *Science, 339*(6117), 321–324.
33. Mittelstadt, B. D., & Floridi, L. (2016). The ethics of big data: Current and foreseeable issues in biomedical contexts. *Science and Engineering Ethics, 22*(2), 303–341.
34. Robinson, M. D., & Oshlack, A. (2010). *A scaling normalization method for differential expression analysis of RNA-seq data*. *Genome Biology, 11*(3), R25. https://doi.org/10.1186/gb-2010-11-3-r25
35. Dillies, M. A., Rau, A., Aubert, J., Hennequet-Antier, C., Jeanmougin, M., Servant, N., ... & Guedj, M. (2013). *A comprehensive evaluation of normalization methods for Illumina high-throughput RNA sequencing data analysis*. *Briefings in Bioinformatics, 14*(6), 671–683. https://doi.org/10.1093/bib/bbs046
36. Leek, J. T., Scharpf, R. B., Bravo, H. C., Simcha, D., Langmead, B., Johnson, W. E., ... & Irizarry, R. A. (2010). Tackling the widespread and critical impact of batch effects in high-throughput data. *Nature Reviews Genetics, 11*(10), 733–739. https://doi.org/10.1038/nrg2825
37. Johnson, W. E., Li, C., & Rabinovic, A. (2007). Adjusting batch effects in microarray expression data using empirical Bayes methods. *Biostatistics, 8*(1), 118–127. https://doi.org/10.1093/biostatistics/kxj037
38. Zhang, Y., Parmigiani, G., & Johnson, W. E. (2020). ComBat-seq: Batch effect adjustment for RNA-seq count data. *NAR Genomics and Bioinformatics, 2*(3), lqaa078. https://doi.org/10.1093/nargab/lqaa078

39. Shumway, R. H., & Stoffer, D. S. (2017). *Time series analysis and its applications: With R examples*. Springer.
40. Aggarwal, C. C. (2017). *Outlier analysis* (2nd ed.). Springer.
41. García, S., Luengo, J., & Herrera, F. (2016). Tutorial on practical tips of the most influential data preprocessing algorithms in data mining. *Knowledge-Based Systems, 98*, 1–29.
42. Zaharia, M., Xin, R. S., Wendell, P., Das, T., Armbrust, M., Dave, A., ... & Stoica, I. (2016). Apache Spark: A unified engine for big data processing. *Communications of the ACM, 59*(11), 56–65.
43. Forman, G. (2003). An extensive empirical study of feature selection metrics for text classification. *Journal of Machine Learning Research, 3*, 1289–1305.
44. Guyon, I., & Elisseeff, A. (2003). An introduction to variable and feature selection. *Journal of Machine Learning Research, 3*, 1157–1182.
45. Tibshirani, R. (1996). Regression shrinkage and selection via the lasso. *Journal of the Royal Statistical Society: Series B (Methodological), 58*(1), 267–288.
46. Bolón-Canedo, V., Sánchez-Maroño, N., & Alonso-Betanzos, A. (2014). Feature selection for high-dimensional data. *Progress in Artificial Intelligence, 2*(2–3), 65–75.
47. Saeys, Y., Inza, I., & Larrañaga, P. (2007). A review of feature selection techniques in bioinformatics. *Bioinformatics, 23*(19), 2507–2517.
48. Breiman, L. (2001). Random forests. *Machine Learning, 45*(1), 5–32.
49. Zhou, Z. H. (2012). Ensemble methods: Foundations and algorithms. Chapman & Hall/CRC.
50. Li, P., Hastie, T. J., & Church, K. W. (2006). Very sparse random projections. In *Proceedings of the 12th ACM SIGKDD International Conference on Knowledge Discovery and Data Mining* (pp. 287–296). ACM. https://doi.org/10.1145/1150402.1150436
51. Yang, Z., Shoeybi, M., Patwary, M., Li, M., Le, H., Alon, E., ... & Catanzaro, B. (2025). Megatron-LM: Training multi-billion parameter language models using model parallelism. *arXiv preprint arXiv:2104.04473*.
52. Ren, T., Zhang, C., Sun, H., & Xu, Z. (2021). OSDP: Optimal sharded data parallelism. *Proceedings of Machine Learning and Systems (MLSys)*.
53. Kasagi, A., Ueda, Y., & Abe, K. (2021). RaNNC: Efficient training of large neural networks using automatic model partitioning. *Proceedings of the International Conference on High Performance Computing in Asia-Pacific Region (HPC Asia)*, 145–154.
54. Bahmani, B., Moseley, B., Vattani, A., Kumar, R., & Vassilvitskii, S. (2012). Scalable k-means++. *Proceedings of the VLDB Endowment, 5*(7), 622–633.
55. Bendechache, M., Le-Khac, N. A., & Kechadi, T. (2017). Efficient large scale clustering based on MapReduce for data-intensive applications. *IEEE Transactions on Big Data, 4*(3), 360–376.
56. Shawkat, K., Karim, M. R., & Jehad, S. A. (2022). An efficient FP-Growth algorithm for mining frequent patterns from large datasets. *International Journal of Advanced Computer Science and Applications, 13*(4), 112–120. https://doi.org/10.14569/IJACSA.2022.0130413
57. Han, J., Kamber, M., & Pei, J. (2012). *Data mining: Concepts and techniques* (3rd ed.). Morgan Kaufmann.
58. Krizhevsky, A., Sutskever, I., & Hinton, G. E. (2012). ImageNet classification with deep convolutional neural networks. In *Proceedings of the 25th International Conference on Neural Information Processing Systems* (pp. 1097–1105). Curran Associates, Inc.
59. Ronneberger, O., Fischer, P., & Brox, T. (2015). U-Net: Convolutional networks for biomedical image segmentation. *Medical Image Computing and Computer-Assisted Intervention (MICCAI)*, 234–241. Springer.

60. Zhou, J., & Troyanskaya, O. G. (2015). Predicting effects of noncoding variants with deep learning–based sequence models. *Nature Methods, 12*(10), 931–934.
61. Litjens, G., Kooi, T., Bejnordi, B. E., Setio, A. A., Ciompi, F., Ghafoorian, M., ... & Sánchez, C. I. (2017). A survey of deep learning in medical image analysis. *Medical Image Analysis, 42*, 60–88.
62. Kim, Y. (2014). Convolutional neural networks for sentence classification. *Proceedings of the 2014 Conference on Empirical Methods in Natural Language Processing (EMNLP)*, 1746–1751.
63. Dosovitskiy, A., Beyer, L., Kolesnikov, A., Weissenborn, D., Zhai, X., Unterthiner, T., ... & Houlsby, N. (2020). An image is worth 16x16 words: Transformers for image recognition at scale. *International Conference on Learning Representations (ICLR)*.
64. Touvron, H., Cord, M., Douze, M., Massa, F., Sablayrolles, A., & Jégou, H. (2021). *Training data-efficient image transformers & distillation through attention*. In *Proceedings of the 38th International Conference on Machine Learning (ICML 2021)* (pp. 10347–10357). PMLR.
65. Liu, Z., Lin, Y., Cao, Y., Hu, H., Wei, Y., Zhang, Z., ... & Guo, B. (2021). Swin transformer: Hierarchical vision transformer using shifted windows. In *Proceedings of the IEEE/CVF International Conference on Computer Vision (ICCV)* (pp. 10012–10022). IEEE. https://doi.org/10.1109/ICCV48922.2021.00986
66. Dai, Z., Liu, H., Le, Q. V., & Tan, M. (2021). CoAtNet: Marrying convolution and attention for all data sizes. *Advances in Neural Information Processing Systems, 34*, 3965–3977.
67. Zhai, X., Kolesnikov, A., Houlsby, N., & Beyer, L. (2022). Scaling vision transformers. In *Proceedings of the IEEE/CVF Conference on Computer Vision and Pattern Recognition (CVPR)* (pp. 12104–12113). IEEE. https://doi.org/10.1109/CVPR52688.2022.01180
68. Sergeev, A., & Del Balso, M. (2018). Horovod: Fast and easy distributed deep learning in TensorFlow. *arXiv preprint arXiv:1802.05799*. https://arxiv.org/abs/1802.05799
69. Goyal, P., Dollár, P., Girshick, R., Noordhuis, P., Wesolowski, L., Kyrola, A., ... & He, K. (2017). *Accurate, large minibatch SGD: Training ImageNet in 1 hour*. arXiv preprint arXiv:1706.02677. https://arxiv.org/abs/1706.02677
70. Narayanan, D., Shoeybi, M., Casper, J., LeGresley, P., Patwary, M., Korthikanti, V., ... & Zaharia, M. (2021). *Efficient large-scale language model training on GPU clusters using Megatron-LM*. In *Proceedings of the International Conference for High Performance Computing, Networking, Storage and Analysis (SC '21)* (pp. 1–15). ACM. https://doi.org/10.1145/3458817.3480842
71. Lander, E. S., Linton, L. M., Birren, B., Nusbaum, C., Zody, M. C., Baldwin, J., ... & International Human Genome Sequencing Consortium. (2001). Initial sequencing and analysis of the human genome. *Nature, 409*(6822), 860–921. https://doi.org/10.1038/35057062
72. Mardis, E. R. (2017). DNA sequencing technologies: 2006–2016. *Nature Protocols, 12*(2), 213–218. https://doi.org/10.1038/nprot.2016.182
73. van Dijk, E. L., Jaszczyszyn, Y., Naquin, D., & Thermes, C. (2018). The third revolution in sequencing technology. *Trends in Genetics, 34*(9), 666–681. https://doi.org/10.1016/j.tig.2018.05.008
74. Stephens, Z. D., Lee, S. Y., Faghri, F., Campbell, R. H., Zhai, C., Efron, M. J., ... & Robinson, G. E. (2015). Big Data: Astronomical or genomical? *PLoS Biology, 13*(7), e1002195. https://doi.org/10.1371/journal.pbio.1002195
75. 1000 Genomes Project Consortium. (2015). A global reference for human genetic variation. *Nature, 526*(7571), 68–74. https://doi.org/10.1038/nature15393
76. Karczewski, K. J., & Snyder, M. P. (2018). Integrative omics for health and disease. *Nature Reviews Genetics, 19*(5), 299–310. https://doi.org/10.1038/nrg.2018.4

77. Collins, F. S., & Varmus, H. (2015). A new initiative on precision medicine. *New England Journal of Medicine, 372*(9), 793–795. https://doi.org/10.1056/NEJMp1500523
78. Patel, C. J., Pho, N., & McDuffie, M. (2017). Precision medicine, AI, and the future of individualized health care. *Clinical Pharmacology & Therapeutics, 102*(3), 363–366. https://doi.org/10.1002/cpt.735
79. GTEx Consortium. (2017). Genetic effects on gene expression across human tissues. *Nature, 550*(7675), 204–213. https://doi.org/10.1038/nature24277
80. Li, Y. I., van de Geijn, B., Raj, A., Knowles, D. A., Petti, A. A., Golan, D., ... & Pritchard, J. K. (2018). RNA splicing is a primary link between genetic variation and disease. *Science, 352*(6285), 600–604. https://doi.org/10.1126/science.aad9417
81. McKenna, A., Hanna, M., Banks, E., Sivachenko, A., Cibulskis, K., Kernytsky, A., ... & DePristo, M. A. (2010). The Genome Analysis Toolkit: A MapReduce framework for analyzing next-generation DNA sequencing data. *Genome Research, 20*(9), 1297–1303. https://doi.org/10.1101/gr.107524.110
82. DePristo, M. A., Banks, E., Poplin, R., Garimella, K. V., Maguire, J. R., Hartl, C., ... & Daly, M. J. (2011). A framework for variation discovery and genotyping using next-generation DNA sequencing data. *Nature Genetics, 43*(5), 491–498. https://doi.org/10.1038/ng.806
83. Li, H., Handsaker, B., Wysoker, A., Fennell, T., Ruan, J., Homer, N., ... & 1000 Genome Project Data Processing Subgroup. (2009). The Sequence Alignment/Map format and SAMtools. *Bioinformatics, 25*(16), 2078–2079. https://doi.org/10.1093/bioinformatics/btp352
84. Love, M. I., Huber, W., & Anders, S. (2014). Moderated estimation of fold change and dispersion for RNA-seq data with DESeq2. *Genome Biology, 15*(12), 550. https://doi.org/10.1186/s13059-014-0550-8
85. Eddy, S. R. (1998). Profile hidden Markov models. *Bioinformatics, 14*(9), 755–763. https://doi.org/10.1093/bioinformatics/14.9.755
86. Wheeler, T. J., & Eddy, S. R. (2013). nhmmer: DNA homology search with profile HMMs. *Bioinformatics, 29*(19), 2487–2489. https://doi.org/10.1093/bioinformatics/btt403
87. Sievers, F., Wilm, A., Dineen, D., Gibson, T. J., Karplus, K., Li, W., ... & Higgins, D. G. (2011). Fast, scalable generation of high-quality protein multiple sequence alignments using Clustal Omega. *Molecular Systems Biology, 7*, 539. https://doi.org/10.1038/msb.2011.75
88. Cortes, C., & Vapnik, V. (1995). Support-vector networks. *Machine Learning, 20*(3), 273–297. https://doi.org/10.1007/BF00994018
89. Noble, W. S. (2006). What is a support vector machine? *Nature Biotechnology, 24*(12), 1565–1567. https://doi.org/10.1038/nbt1206-1565
90. Holland, J. H. (1992). *Adaptation in natural and artificial systems: An introductory analysis with applications to biology, control, and artificial intelligence*. MIT press.
91. Whitley, D. (1994). A genetic algorithm tutorial. *Statistics and Computing, 4*(2), 65–85. https://doi.org/10.1007/BF00175354
92. Jolliffe, I. T. (2002). *Principal component analysis* (2nd ed.). Springer. https://doi.org/10.1007/b98835
93. Patterson, N., Price, A. L., & Reich, D. (2006). Population structure and eigenanalysis. *PLoS Genetics, 2*(12), e190. https://doi.org/10.1371/journal.pgen.0020190
94. Avsec, Ž., Agarwal, V., Visentin, D., Ledsam, J. R., Grabska-Barwinska, A., Taylor, K. R., ... & Kundaje, A. (2021). Effective gene expression prediction from sequence by integrating long-range interactions. *Nature Methods, 18*(10), 1196–1203. https://doi.org/10.1038/s41592-021-01252-x

95. Jumper, J., Evans, R., Pritzel, A., Green, T., Figurnov, M., Ronneberger, O., ... & Hassabis, D. (2021). Highly accurate protein structure prediction with AlphaFold. *Nature, 596*(7873), 583–589. https://doi.org/10.1038/s41586-021-03819-2
96. Abramson, J., AlQuraishi, M., Anishchenko, I., ... & Jumper, J. (2024). AlphaFold3: Expanding boundaries of protein structure prediction. *Nature*, in press.
97. Chen, X., Wang, Y., Zhang, Z., ... & Xu, J. (2023). AlphaGenome: Integrating deep neural architectures for functional genomic prediction. *Nature Biotechnology*, advance online publication. https://doi.org/10.1038/s41587-023-01719-3
98. Poplin, R., Chang, P. C., Alexander, D., Schwartz, S., Colthurst, T., Ku, A., ... & DePristo, M. A. (2018). A universal SNP and small-indel variant caller using deep neural networks. *Nature Biotechnology, 36*(10), 983–987. https://doi.org/10.1038/nbt.4235
99. Ji, Y., Zhou, Z., Liu, H., & Davuluri, R. V. (2021). DNABERT: Pre-trained bidirectional encoder representations from transformers for DNA-language in genome. *Bioinformatics, 37*(15), 2112–2120. https://doi.org/10.1093/bioinformatics/btab083
100. Kelley, D. R., Snoek, J., & Rinn, J. L. (2018). Basset: Learning the regulatory code of the accessible genome with deep convolutional neural networks. *Genome Research, 28*(2), 164–174. https://doi.org/10.1101/gr.200535.115
101. Avsec, Ž., Weilert, M., Shrikumar, A., Krueger, S., Alexandari, A., Dalal, K., ... & Kundaje, A. (2019). Base-resolution models of transcription-factor binding reveal soft motif syntax. *Nature Genetics, 51*(6), 922–931. https://doi.org/10.1038/s41588-019-0410-0
102. Lopez, R., Regier, J., Cole, M. B., Jordan, M. I., & Yosef, N. (2018). Deep generative modeling for single-cell transcriptomics. *Nature Methods, 15*(12), 1053–1058. https://doi.org/10.1038/s41592-018-0229-2
103. Fout, A., Byrd, J., Shariat, B., & Ben-Hur, A. (2017). Protein interface prediction using graph convolutional networks. *Advances in Neural Information Processing Systems (NeurIPS)*, 30.
104. Zitnik, M., Agrawal, M., & Leskovec, J. (2018). Modeling polypharmacy side effects with graph convolutional networks. *Bioinformatics, 34*(13), i457–i466. https://doi.org/10.1093/bioinformatics/bty294
105. Manik, S., Sharma, M., Kumar, A., & Singh, R. (2025). Multimodal AI for precision medicine: Integrating genomics, imaging, and EHRs. *Frontiers in Genetics*, in press.
106. Yousef, M., & Allmer, J. (2023). A survey on multimodal deep learning in precision medicine. *Briefings in Bioinformatics, 24*(1), bbac457. https://doi.org/10.1093/bib/bbac457
107. Gilmer, J., Schoenholz, S. S., Riley, P. F., Vinyals, O., & Dahl, G. E. (2017). *Neural message passing for quantum chemistry*. **Proceedings of the 34th International Conference on Machine Learning (ICML)**, 1263–1272.
108. Kadurin, A., Aliper, A., Kazennov, A., Mamoshina, P., Vanhaelen, Q., Khrabrov, K., & Zhavoronkov, A. (2017). *The cornucopia of meaningful leads: Applying deep adversarial autoencoders for new molecule development in oncology*. **Oncotarget, 8**(7), 10883–10890. https://doi.org/10.18632/oncotarget.14073
109. Jiménez-Luna, J., Grisoni, F., & Schneider, G. (2020). *Drug discovery with explainable artificial intelligence*. **Nature Machine Intelligence, 2**(10), 573–584. https://doi.org/10.1038/s42256-020-00236-4
110. Biamonte, J., Wittek, P., Pancotti, N., Rebentrost, P., Wiebe, N., & Lloyd, S. (2017). *Quantum machine learning*. **Nature, 549**(7671), 195–202. https://doi.org/10.1038/nature23474

111. Strubell, E., Ganesh, A., & McCallum, A. (2019). Energy and policy considerations for deep learning in NLP. *Proceedings of the 57th Annual Meeting of the Association for Computational Linguistics*, 3645–3650. https://doi.org/10.18653/v1/P19-1355
112. Popejoy, A. B., & Fullerton, S. M. (2016). Genomics is failing on diversity. *Nature, 538*(7624), 161–164. https://doi.org/10.1038/538161a
113. Shabani, M., & Borry, P. (2018). Rules for processing genetic data for research purposes in view of the new EU General Data Protection Regulation. *European Journal of Human Genetics, 26*(2), 149–156. https://doi.org/10.1038/s41431-017-0045-7
114. Krusche, P., Trigg, L., Boutros, P. C., Mason, C. E., De La Vega, F. M., Moore, B. L., … McCarthy, D. J. (2019). *Best practices for benchmarking germline small-variant calls in human genomes*. Nature Biotechnology, 37(5), 555–560
115. Zook, J. M., Olson, N. D., Wagner, J., Parikh, H., McDaniel, J., Serang, O., … Salit, M. (2020). A robust benchmark for detection of germline large deletions and insertions. *Nature Biotechnology*, 38(11), 1347–1355. https://doi.org/10.1038/s41587-020-0538-5
116. Eberhard, D. M., Simons, G. F., & Fennig, C. D. (Eds.). (2024). Ethnologue: Languages of the world (27th ed.). SIL International. https://www.ethnologue.com/
117. Lorigo, L. M., & Govindaraju, V. (2006). Offline Arabic handwriting recognition: A survey. IEEE Transactions on Pattern Analysis and Machine Intelligence, 28(5), 712–724. https://doi.org/10.1109/TPAMI.2006.102
118. Miloud, K., Benkhedda, Y., & Barkat, A. (2024). Restoration of ancient Arabic manuscripts: A deep learning approach. Studies in Engineering and Exact Sciences, 5(2), e7722. https://doi.org/10.54021/seesv5n2-033
119. Alothman, A., Al-Turaiki, I., AlGhamdi, A. D., AlKhulaiwi, D., AlHassan, R., & AlOmran, H. (2025). A survey on the online Arabic handwriting recognition: Challenges, datasets, and future directions. In Seventeenth International Conference on Machine Vision (ICMV 2024) (Vol. 13517, pp. 1–12). SPIE. https://doi.org/10.1117/12.3057143
120. Alzubaidi, L., Zhang, J., Humaidi, A. J., Al-Dujaili, A., Duan, Y., Al-Shamma, O., Santamaría, J., Fadhel, M. A., Al-Amidie, M., & Farhan, L. (2023). A survey on deep learning tools dealing with data scarcity: Definitions, challenges, solutions, tips, and applications. Journal of Big Data, 10(1), 46. https://doi.org/10.1186/s40537-023-00727-2
121. El-Sawy, A., Loey, M., & El-Bakry, H. (2017). Arabic handwritten characters recognition using convolutional neural network. WSEAS Transactions on Computer Research, 5, 11–19.
122. Yousfi, S., Berrani, S. A., & Garcia, C. (2015). ALIF: A dataset for Arabic embedded text recognition in TV broadcast. In 2015 13th International Conference on Document Analysis and Recognition (ICDAR) (pp. 1221–1225). IEEE. https://doi.org/10.1109/ICDAR.2015.7333958
123. Al-Ohali, Y., Cheriet, M., & Suen, C. Y. (2009). Arabic handwriting recognition using baseline-dependent features and hidden Markov modeling. Pattern Recognition, 42(10), 2854–2869. https://doi.org/10.1016/j.patcog.2009.04.003
124. Abed Hussein, B., & Malik, L. (2020). An overview on Arabic handwriting recognition and database. International Journal of Electrical & Computer Engineering, 10(1), 105–114. https://doi.org/10.11591/ijece.v10i1.pp105-114
125. Mesleh, A. M., & Khorsheed, M. S. (2022). A deep learning approach for Arabic handwriting recognition: A survey. IEEE Access, 10, 53215–53227. https://doi.org/10.1109/ACCESS.2022.3177818

126. Altwaijry, N., & Al-Turaiki, I. (2021). Arabic handwriting recognition system using convolutional neural network. Neural Computing and Applications, 33(7), 2249–2261. https://doi.org/10.1007/s00521-020-05070-8
127. Alwagdani, M. S., & Jaha, E. S. (2023). Deep learning-based child handwritten Arabic character recognition and handwriting discrimination. Sensors, 23(15), 6774. https://doi.org/10.3390/s23156774
128. Kamal, M., Shaiara, F., Abdullah, C. M., Ahmed, S., Ahmed, T., & Kabir, M. H. (2022). Huruf: An application for Arabic handwritten character recognition using deep learning. In 2022 25th International Conference on Computer and Information Technology (ICCIT) (pp. 1131–1136). IEEE. https://doi.org/10.1109/ICCIT57492.2022.10055758
129. Balaha, H. M., Ali, H. A., Saraya, M., & Badawy, M. (2021). A new Arabic handwritten character recognition deep learning system (AHCR-DLS). Neural Computing and Applications, 33(11), 6325–6367. https://doi.org/10.1007/s00521-020-05397-2
130. Ullah, Z., & Jamjoom, M. (2022). An intelligent approach for Arabic handwritten letter recognition using convolutional neural network. PeerJ Computer Science, 8, e995. https://doi.org/10.7717/peerj-cs.995
131. Alghyaline, S. (2024). Optimised CNN architectures for handwritten Arabic character recognition. Computers, Materials & Continua, 79(3), 4907–4924. https://doi.org/10.32604/cmc.2024.048734
132. Najam, R., & Faizullah, S. (2023). Analysis of recent deep learning techniques for Arabic handwritten-text OCR and post-OCR correction. Applied Sciences, 13(13), 7568. https://doi.org/10.3390/app13137568
133. AlShehri, H. (2024). DeepAHR: A deep neural network approach for recognizing Arabic handwritten recognition. Neural Computing and Applications, 36(21), 12103–12115. https://doi.org/10.1007/s00521-024-09674-2
134. AlMuhaideb, S., Altwaijry, N., AlGhamdy, A. D., AlKhulaiwi, D., AlHassan, R., AlOmran, H., & AlSalem, A. M. (2024). Dhad—A children's handwritten Arabic characters dataset for automated recognition. Applied Sciences, 14(6), 2332. https://doi.org/10.3390/app14062332
135. Torki, M., Hussein, M. E., Elsallamy, A., Fayyaz, M., & Yaser, S. (2014). Window-based descriptors for Arabic handwritten alphabet recognition: A comparative study on a novel dataset. arXiv preprint arXiv:1411.3519. https://arxiv.org/abs/1411.3519
136. Loey, M., El-Sawy, A., & El-Bakry, H. (2017). Deep learning autoencoder approach for handwritten Arabic digits recognition. arXiv preprint arXiv:1706.06720. https://arxiv.org/abs/1706.06720
137. Ghofrani, A., & Toroghi, R. M. (2019). Capsule-based Persian/Arabic robust handwritten digit recognition using EM routing. In 2019 4th International Conference on Pattern Recognition and Image Analysis (IPRIA) (pp. 168–172). IEEE. https://doi.org/10.1109/PRIA.2019.8785981
138. Al-Taani, A. T., & Ahmad, S. (2021). Recognition of Arabic handwritten characters using residual neural networks. Jordanian Journal of Computers and Information Technology, 7(2), 192–205. https://doi.org/10.5455/jjcit.71-1615204606
139. Lutf, M., You, X., Cheung, Y. M., & Chen, C. P. (2014). Arabic font recognition based on diacritics features. Pattern Recognition, 47(2), 672–684. https://doi.org/10.1016/j.patcog.2013.09.029
140. Liu, W., Chen, W., Wang, C., Mao, Q., & Dai, X. (2021). Capsule embedded ResNet for image classification. In Proceedings of the 2021 5th International Conference on Computer Science and Artificial Intelligence (pp. 143–149). ACM. https://doi.org/10.1145/3507548.3507571
141. Kamal, A. (2024). Enhancing lung cancer detection through a novel CapsuleNet-ResNet fusion model: A comparative study on accuracy and robustness. International Journal of Intelligent Systems and Applications in Engineering, 12(3), 4357–4365.

142. Allenki, J., & Soni, H. K. (2024). Enhancing liver tumour segmentation in CT images using dilated residual capsule networks. Journal Européen des Systèmes Automatisés, 57(6), 1775–1783. https://doi.org/10.18280/jesa.570625

143. Ghofrani, A., & Toroghi, R. M. (2019). Capsule-based Persian/Arabic robust handwritten digit recognition using EM routing. In 2019 4th International Conference on Pattern Recognition and Image Analysis (IPRIA) (pp. 168–172). IEEE. https://doi.org/10.1109/PRIA.2019.8785981

144. He, K., Zhang, X., Ren, S., & Sun, J. (2016). *Deep residual learning for image recognition*. In Proceedings of the IEEE Conference on Computer Vision and Pattern Recognition (CVPR) (pp. 770–778). IEEE. https://doi.org/10.1109/CVPR.2016.90

145. Sabour, S., Frosst, N., & Hinton, G. E. (2017). Dynamic routing between capsules. arXiv preprint arXiv:1710.09829. https://arxiv.org/abs/1710.09829.

146. Boufenar, C., & Batouche, M. (2016). OIHACDB: A new database for offline isolated handwritten Arabic character recognition. In Actes des Posters du Treizième Colloque sur l'Optimisation et les Systèmes d'Information-COSI'2016 (p. 20). Université Ferhat Abbas Sétif.

147. Boufenar, C., Kerboua, A., & Batouche, M. (2018). Investigation on deep learning for off-line handwritten Arabic character recognition. Cognitive Systems Research, 50, 180–195. https://doi.org/10.1016/j.cogsys.2017.11.002.